

# Karakterizacija interakcije proteina BLNK i receptorne tirozin-kinaze MET uporabom ligacije proteina posredovane pocijepanim inteinom

---

Valla, Robert

Master's thesis / Diplomski rad

2021

Degree Grantor / Ustanova koja je dodijelila akademski / stručni stupanj: **University of Zagreb, Faculty of Science / Sveučilište u Zagrebu, Prirodoslovno-matematički fakultet**

Permanent link / Trajna poveznica: <https://um.nsk.hr/um:nbn:hr:217:560473>

Rights / Prava: [In copyright](#)/[Zaštićeno autorskim pravom.](#)

Download date / Datum preuzimanja: **2024-07-17**



Repository / Repozitorij:

[Repository of the Faculty of Science - University of Zagreb](#)



Sveučilište u Zagrebu  
Prirodoslovno-matematički fakultet  
Biološki odsjek

Robert Valla

**Karakterizacija interakcije proteina BLNK i  
receptorne tirozin-kinaze MET uporabom  
ligacije proteina posredovane pocijepanim  
inteinom**

Diplomski rad

Zagreb, 2021.

University of Zagreb  
Faculty of Science  
Department of Biology

Robert Valla

**Characterization of BLNK protein  
interaction with receptor tyrosine-kinase  
MET using split intein-mediated protein  
ligation**

Master thesis

Zagreb, 2021.

Ovaj rad je izrađen u laboratoriju Igora Štagljara u Donnelly centru za stanična i biomolekularna istraživanja, na zavodu za biokemiju i zavodu za molekularnu genetiku Medicinskog fakulteta sveučilišta u Torontu, Toronto, Kanada, pod voditeljstvom Prof. Dr. Sc. Igora Štagljara, te suvoditeljstvom Izv. Prof. Dr. Sc. Nataše Bauer. Rad je predan na ocjenu Biološkom odsjeku Prirodoslovno-matematičkog fakulteta Sveučilišta u Zagrebu radi stjecanja zvanja magistra molekularne biologije.

This thesis was performed in Igor Štagljar Laboratory, Donnelly Centre for Cellular and Biomolecular Research, Department of Biochemistry and Department of Molecular Genetics, Faculty of Medicine, University of Toronto, Toronto, Canada under supervision of Dr. Igor Štagljar, Prof. and co-supervisor Dr. Nataša Bauer, Assoc. Prof. The thesis is submitted for evaluation to Department of Biology, Faculty of Science, University of Zagreb, Zagreb, Croatia to acquire the academic title of Master of Molecular Biology.

## Acknowledgments

I wish to express my greatest gratitude to Dr. Igor Štagljar for offering me the amazing opportunity to visit his research laboratory in Donnelly Centre for Cellular and Biomolecular Research to do research, gain much-needed experience in a topnotch environment and write a thesis based on that work. I want to thank Jelena Tomić, research manager in Štagljar lab, for providing administrative support with my arrival to Canada, and during my time in Canada. I wish to especially thank my dear colleague Shivanthy Pathmanathan for providing training in various molecular methods, numerous conversations, and support regarding the project and my concerns. I am also grateful to the rest of the team in Štagljar lab for providing a very pleasant and productive working environment and support when needed.

I am appreciative of the effort that Dr. Renata Matoničkin Kepčija made in arranging the scholarship and assisting in my departure from Croatia. I am also very grateful for the efforts of Dr. Nataša Bauer as my home supervisor.

Finally, I wish to thank my parents Sanda and Dominik, and to all my friends, especially Ervin, for providing unconditional support and care during the entire study period and especially during my time in Canada. They made my study period memorable, something I will always be grateful for.

# TEMELJNA DOKUMENTACIJSKA KARTICA

---

Sveučilište u Zagrebu  
Prirodoslovno-matematički fakultet  
Biološki odsjek

Diplomski rad

## **Karakterizacija interakcije proteina BLNK i receptorne tirozin-kinaze MET uporabom ligacije proteina posredovane pocijepanim inteinom**

Robert Valla

Rooseveltov trg 6, 10000 Zagreb, Hrvatska

Receptorna tirozin-kinaza MET je protoonkogen uključen u razne fiziološke procese, sudjeluje u tkivnoj homeostazi i regeneraciji te u brojnim patofiziološkim stanjima, primjerice različitim tipovima raka. Protein BLNK je središnji adaptorni protein nizvodno od signalne kaskade B-staničnog receptora. Protein BLNK omogućuje stvaranje multimolekularnih signalnih kompleksa, što prethodi sazrijevanju limfocita B. Protein BLNK je novo opisani interakcijski partner receptora MET te bi interakcija receptora MET i proteina BLNK mogla imati jedinstvenu biološku značajnost. U ovom istraživanju je u svrhu karakterizacije interakcije receptora MET i proteina BLNK korištena nova metoda istraživanja proteinskih interakcija zvana ligacija proteina posredovana pocijepanim inteinom (engl. *SIMPL*). Interakcija receptora MET i proteina BLNK je potvrđena te je istražena ovisnost interakcije o fosforilaciji. Uspostavljena je i okarakterizirana stanična linija sa stabilnom ekspresijom receptora MET i taj se stabilni sustav MET-SIMPL može upotrijebiti kao platforma za probir lijekova. Identificirane su aminokiseline odgovorne za interakciju receptora MET i proteina BLNK. Metoda SIMPL ELISA također je upotrebljena za određivanje veznih mjesta proteina GRB2 na protein BLNK te za istraživanje uloge proteina GRB2 u interakciji receptora MET i proteina BLNK. Dobiveni rezultati pružaju bolji uvid u funkcionalne i mehanističke značajke interakcije receptora MET i proteina BLNK i proširuju razumijevanje biologije receptorne tirozin-kinaze MET.

(110 stranica, 44 slike, 35 tablica, 71 literaturni navod, jezik izvornika: Engleski).

Rad je pohranjen u Središnjoj biološkoj knjižnici.

Ključne riječi: MET, BLNK, proteinske interakcije, prekrajanje proteina, SIMPL

Voditelj: Prof. Dr. Sc. Igor Štagljar

Suvoditelj: Izv. Prof. Dr. Sc. Nataša Bauer

Ocjenitelji: Izv. Prof. Dr. Sc. Nataša Bauer, Prof. Dr. Sc. Nada Oršolić, Doc. Dr. Sc. Marin Ježić,

Izv. Prof. Dr. Sc. Petra Korać (zamjena)

Rad prihvaćen: 7. 7. 2021.

## BASIC DOCUMENTATION CARD

---

University of Zagreb  
Faculty of Science  
Department of Biology

Master Thesis

### **Characterization of BLNK protein interaction with receptor tyrosine-kinase MET using split intein-mediated protein ligation**

Robert Valla

Rooseveltovej trg 6, 10000 Zagreb, Hrvatska

MET receptor tyrosine-kinase is a proto-oncogene involved in various physiological processes, such as tissue homeostasis and regeneration, as well as numerous pathophysiological conditions, such as different types of cancers. BLNK is a central adaptor protein downstream of the B-cell receptor signaling cascade, which enables the formation of multimolecular signaling complexes preceding the maturation of B lymphocytes. BLNK protein is a newly discovered interaction partner of MET, and MET-BLNK interaction may have a unique biological significance. A novel method to study protein-protein interactions called split intein-mediated protein ligation (SIMPL) was used in this research to characterize MET-BLNK interaction. MET-BLNK interaction was orthogonally confirmed and its phosphorylation-dependent nature was investigated using the SIMPL assay. The stable MET-SIMPL system was generated, characterized, and utilized as a drug screening platform. The amino acid residues on MET and BLNK responsible for MET-BLNK interaction were identified using SIMPL assay. SIMPL ELISA was used to determine the binding sites for GRB2 protein on BLNK and assess the role of GRB2 in MET-BLNK interaction. These results provided insight into functional and mechanistic features of MET-BLNK interaction and have deepened the understanding of MET receptor tyrosine-kinase biology.

(110 Pages, 44 Figures, 35 Tables, 71 References, Original in English)

Thesis is deposited in Central Biological Library.

Keywords: MET, BLNK, PPI, protein splicing, SIMPL

Supervisor: Prof. Dr. Sc. Igor Štagljar

Co-supervisor: Dr. Sc. Nataša Bauer, Assoc. Prof.

Reviewers: Dr. Sc. Nataša Bauer, Assoc. Prof., Dr. Sc. Nada Oršolić, Prof., Dr. Sc. Marin Ježić, Doc, Dr. Sc. Petra Korać, Assoc. Prof. (substitute)

Thesis accepted: 7. 7. 2021.

# Table of Contents

1. INTRODUCTION.....	1
1.1. Receptor Tyrosine-Kinases.....	1
1.1.1. MET Receptor Tyrosine-Kinase .....	2
1.1.2. The Structure of MET .....	2
1.1.3. MET Signaling.....	4
1.1.4. The Physiological Effects of MET Signaling.....	6
1.1.5. The Role of MET in Tumorigenesis.....	6
1.2. Adaptor (Linker) Proteins .....	8
1.2.1. B-Cell Linker Protein (BLNK).....	8
1.3. Protein-Protein Interactions and Methods for their Detection.....	10
1.3.1. The Importance of Protein-Protein Interactions .....	10
1.3.2. Protein-Protein Interaction Detection Methods .....	10
1.3.3. Inteins and SIMPL .....	12
1.4. The Need for MET Protein-Protein Interactome.....	17
2. RESEARCH AIMS.....	19
3. MATERIALS AND METHODS .....	20
3.1. Materials.....	20
3.1.1. Reagents .....	20
3.1.2. Bacteria Strains .....	21
3.1.3. Antibiotics.....	22
3.1.4. Molecular Biology Kits .....	22
3.1.5. Antibodies.....	23
3.2.6. Buffers and Solutions.....	24
3.1.7. Laboratory Equipment .....	26
3.1.8. Vectors.....	26
3.1.9. Gateway Entry Clones .....	27
3.1.10. Primers.....	28
3.1.11. Cell Lines .....	30
3.2.12. Software.....	30
3.2. Methods.....	31
3.2.1. Cell Culture .....	31
3.2.2. Cell Passaging.....	31



3.2.3. Cell Counting .....	32
3.2.4. Cell Freezing .....	32
3.2.5. Cell Thawing .....	32
3.2.6. Generation of Stable Cell Lines .....	32
3.2.7. Preparation of Competent Bacteria Cells (Inoue Method) .....	33
3.2.8. Transformation Using Heat-Shock Method .....	34
3.2.9. Isolation of Plasmid DNA (MiniPrep Method) .....	34
3.2.10. DNA Sequencing .....	34
3.2.11. Site-Directed Mutagenesis .....	35
3.2.12. Gateway Cloning .....	36
3.2.13. Transient SIMPL Assay .....	37
3.2.14. Stable SIMPL Assay .....	38
3.2.15. SIMPL ELISA .....	39
3.2.16. Surface Biotinylation .....	40
3.2.17. Western Blot Analysis .....	41
3.2.18. Generation of Stable Doxycycline-Inducible BLNK shRNA Knock-Down System .....	44
3.2.19. Generation of MET-BLNK Double Stable Construct .....	46
4. RESULTS .....	48
4.1. The Validation of MET-BLNK Interaction Using SIMPL Assay .....	48
4.2. MET Kinase-Dead Mutant Reduced the Interaction with BLNK .....	49
4.3. The Generation and Characterization of the Stable MET-SIMPL System .....	53
4.4. Mapping Residues on MET that Participate in MET-BLNK Interaction .....	60
4.5. MET Mutants Localize to Cell Surface .....	72
4.6. Mapping Residues on BLNK that Participate in MET-BLNK Interaction .....	74
4.7. A Combination of the Alternative SIMPL Format and SIMPL ELISA Uncovers a Dual GRB2-Binding Site on BLNK .....	83
4.8. Creation of Stable Doxycycline-Inducible BLNK shRNA Knock-Down System .....	87
5. DISCUSSION .....	88
5.1. The Validation of MET-BLNK Interaction Using SIMPL Assay .....	88
5.2. MET Kinase Activity is Required for MET-BLNK Interaction .....	89
5.3. The Generation and Characterization of the Stable MET-SIMPL System .....	89
5.4. Mapping Residues on MET that Participate in MET-BLNK Interaction .....	92
5.5. MET Mutants Localize to the Cell Surface .....	95

5.6. Mapping Residues on BLNK that Participate in MET-BLNK Interaction.....	95
5.7. GRB2 Has a Dual Binding Site on BLNK .....	97
6. CONCLUSION.....	99
7. REFERENCES.....	100
8. SUPPLEMENTARY FIGURES & TABLES .....	106
9. CURRICULUM VITAE.....	110

## 1. INTRODUCTION

### 1.1. Receptor Tyrosine-Kinases

Receptor tyrosine-kinases (RTKs) are a subclass of tyrosine-kinases involved in cellular signaling and carry out major cellular functions, such as growth, proliferation, differentiation, cell survival, cell cycle control, and motility (Lemmon & Schlessinger 2010; Organ & Tsao 2011). There is a total of 58 known RTKs encoded by the human genome (Robinson et al. 2000). All share a tripartite molecular architecture, consisting of an extracellular ligand-binding domain, a single transmembrane  $\alpha$ -helix, and an intracellular part that includes a juxtamembrane regulatory domain, a tyrosine-kinase domain, and a C-terminal docking domain (Hubbard 1999).

Another common feature of receptor tyrosine-kinases is their mechanism of activation (Lemmon & Schlessinger 2010). Upon ligand binding, conformational changes in the extracellular domain occur that enable dimerization/oligomerization of receptor tyrosine-kinase monomers (Lemmon & Schlessinger 2010), triggering the activation of the tyrosine-kinase domain and trans-autophosphorylation of receptors on tyrosine residues located in intracellular domains (Lemmon & Schlessinger 2010). The resulting phosphorylated tyrosine residues create specific motifs for the binding of specific proteins that will relay the signal. These proteins include enzymes, regulatory molecules, and adaptors that predominantly contain Src homology-2 (SH2) or a phosphotyrosine-binding (PTB) domain (Lemmon & Schlessinger 2010; Du & Lovly 2018).

The elucidation of functions and mechanisms of activation of receptor tyrosine-kinases is of great importance since numerous human diseases are associated with genetic alterations that affect RTK activation, expression, regulation of activity, and subcellular localization (Du & Lovly 2018). Genetic aberrations of these proteins have been associated with various cancers, developmental malformations, diabetes, inflammation disorders, and other diseases (Robertson et al. 2000; McDonnell et al. 2015). Cancer cells in particular use gain-of-function mutations, chromosome translocations, amplification, and overexpression of RTKs to promote their proliferation, growth, and ultimately migration (Robertson et al. 2000). Therefore, targeting receptor tyrosine-kinases represents a promising approach in developing novel therapeutics, especially anti-cancer drugs, for the last couple of decades.

### 1.1.1. MET Receptor Tyrosine-Kinase

MET, also known as c-MET or hepatocyte growth factor receptor is a membrane protein that belongs to the receptor tyrosine-kinase family (Segaliny et al. 2015; Koch et al. 2020). It is a proto-oncogene that binds the hepatocyte growth factor (HGF), also known as the scatter factor (Koch et al. 2020). MET is extensively involved in embryogenic development and tissue regeneration throughout life (Petrini 2015), as well as tumorigenesis of numerous cancer types (Trusolino et al. 2010). The gene encoding MET is located on chromosome 7, transcribed into a 6637 nucleotide long mRNA containing 24 exons, translated into a 1390 amino acid long protein that has a molecular weight of around 170 kDa (Koch et al. 2020).

### 1.1.2. The Structure of MET

MET has a structure shared by all receptor tyrosine-kinases, whereby it consists of an extracellular moiety, a single-pass transmembrane  $\alpha$ -helix, and an intracellular moiety (Figure 1). MET consists of an  $\alpha$ -subunit, which is localized on the extracellular side of the membrane, and a transmembrane  $\beta$ -subunit (Koch et al. 2020). The extracellular portion of the MET receptor consists of a SEMA domain, a PSI domain, and four IPT domains (Koch et al. 2020). SEMA (semaphorin-homology) domain consists of  $\alpha$ -subunit and N-terminal portion of  $\beta$ -subunit; this domain is essential for binding of HGF, as well as MET homodimerization and activation (Gherardi et al. 2003; Kong-Beltran et al. 2004). PSI (plexin-semaphorin-integrin) domain contains several disulfide bonds that ensure the proper conformation necessary for the binding of HGF (Koch et al. 2020). The four IPT (immunoglobulin-plexin-transcription factor) domains exhibit a strong affinity towards HGF (Koch et al. 2020). The intracellular section of the MET receptor consists of a juxtamembrane (JM) domain, a tyrosine-kinase (TK) domain, and a C-terminal docking domain (Gherardi et al. 2003). The juxtamembrane domain contains two phosphorylation sites (S985, Y1003), which regulate MET degradation through a negative feedback loop (Jeffers et al. 1997; Koch et al. 2020). The tyrosine-kinase domain contains two tyrosine residues (Y1234, Y1235); the phosphorylation of these residues is crucial for the activation of the MET receptor (Koch et al. 2020). The C-terminal domain represents a docking site for adaptor proteins and downstream signaling partners of MET receptor (Koch et al. 2020).

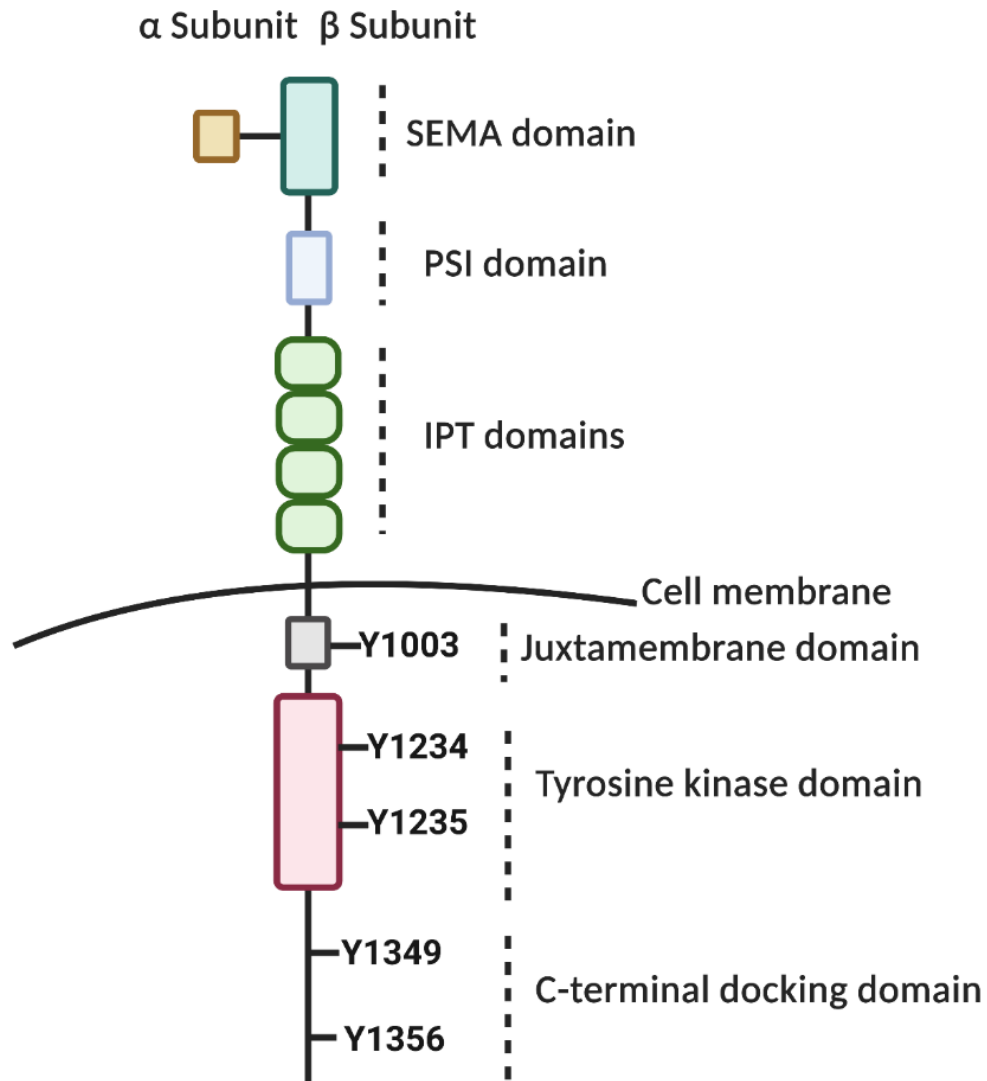


**Figure 1:** Structure of MET receptor. MET consists of an extracellular moiety, a single-pass transmembrane  $\alpha$ -helix, and an intracellular moiety. The extracellular moiety of the MET receptor consists of a SEMA domain (comprised of an  $\alpha$  subunit and an N-terminal portion of  $\beta$  subunit), a PSI domain, and four IPT domains. The  $\beta$  subunit of MET passes through the cell membrane by a single transmembrane  $\alpha$ -helix. The intracellular moiety of MET consists of a juxtamembrane domain, a kinase domain, and a C-terminal docking domain. The juxtamembrane domain contains tyrosine residue Y1003, essential in the regulation of MET degradation. The tyrosine-kinase domain of MET contains tyrosine residues Y1234 and Y1235, essential in the activation of MET. The C-terminal docking domain of MET contains tyrosine residues Y1349 and Y1356. Once phosphorylated, these tyrosine residues create the binding sites for adaptor proteins and downstream signaling partners of MET. Created with BioRender.com.

### 1.1.3. MET Signaling

MET receptor undergoes a conformational change upon HGF binding that enables its homodimerization (Lemmon & Schlessinger 2010), which results in transphosphorylation of tyrosine residues Y1234 and Y1235 in the kinase domain. This event leads to phosphorylation of tyrosine residues Y1349 and Y1356 in the C-terminal docking domain (Ponzetto et al 1994). The phosphorylated C-terminal domain turns into an SH2 recognition site and enables the recruitment of adaptor and effector proteins, such as GRB2, GAB1, SHC1, PI3K, PLC $\gamma$ , and STAT3 (Koch et al. 2020). These adaptors cause the activation of downstream signaling pathways essential for growth, proliferation, cell cycle progression, and cell migration (Koch et al. 2020). These signaling pathways are summarized in Figure 2. Through recruitment of SHC1 and GRB2 proteins activated MET activates RAS proteins (Koch et al. 2020). Activated RAS proteins cause the subsequent activation of MAPK signaling cascade which ultimately activates extracellular-signal-regulated kinases (ERK) 1, 2 and enables their translocation to the nucleus, where they enable the expression of genes necessary for cell motility and cell cycle progression (Johnson et al. 2002). Through activation of the p85 subunit of PI3K, MET activates kinase AKT. AKT has a plethora of activities, the most impactful being the activation of mTOR and MDM2, and inactivation of GSK 3 $\beta$  (Koch et al. 2020). Active mTOR leads to the induction of cellular growth and protein synthesis (Ponzetto et al. 1994). Activation of MDM2 leads to the inactivation of protein p53, which enables the cells to avoid apoptosis (Johnson et al. 2002). Inactivation of GSK 3 $\beta$  enables the activation of mitogens cyclin D1 and MYC, both of which exhibit positive effects on cell cycle progression. The aforementioned signaling pathways are not the only ones activated by MET. STAT3 protein is phosphorylated by active MET, triggering its translocation to the nucleus to act as a transcription factor for several genes associated with proliferation and differentiation (Koch et al. 2020). Active MET also leads to activation of the kinase IKK, which ultimately leads to activation of NF- $\kappa$ B (Fan et al. 2005). Like STAT3, active NF- $\kappa$ B translocates into the nucleus, where it upregulates several genes responsible for cell cycle progression and cell survival. Active MET is known to activate Src kinase, which in turn enables activation of FAK kinase (Hui et al. 2009). Active FAK kinase mediates resistance to anoikis and promotes invasiveness of the cells by triggering cytoskeleton reorganization (Hui et al. 2009; Koch et al. 2020).

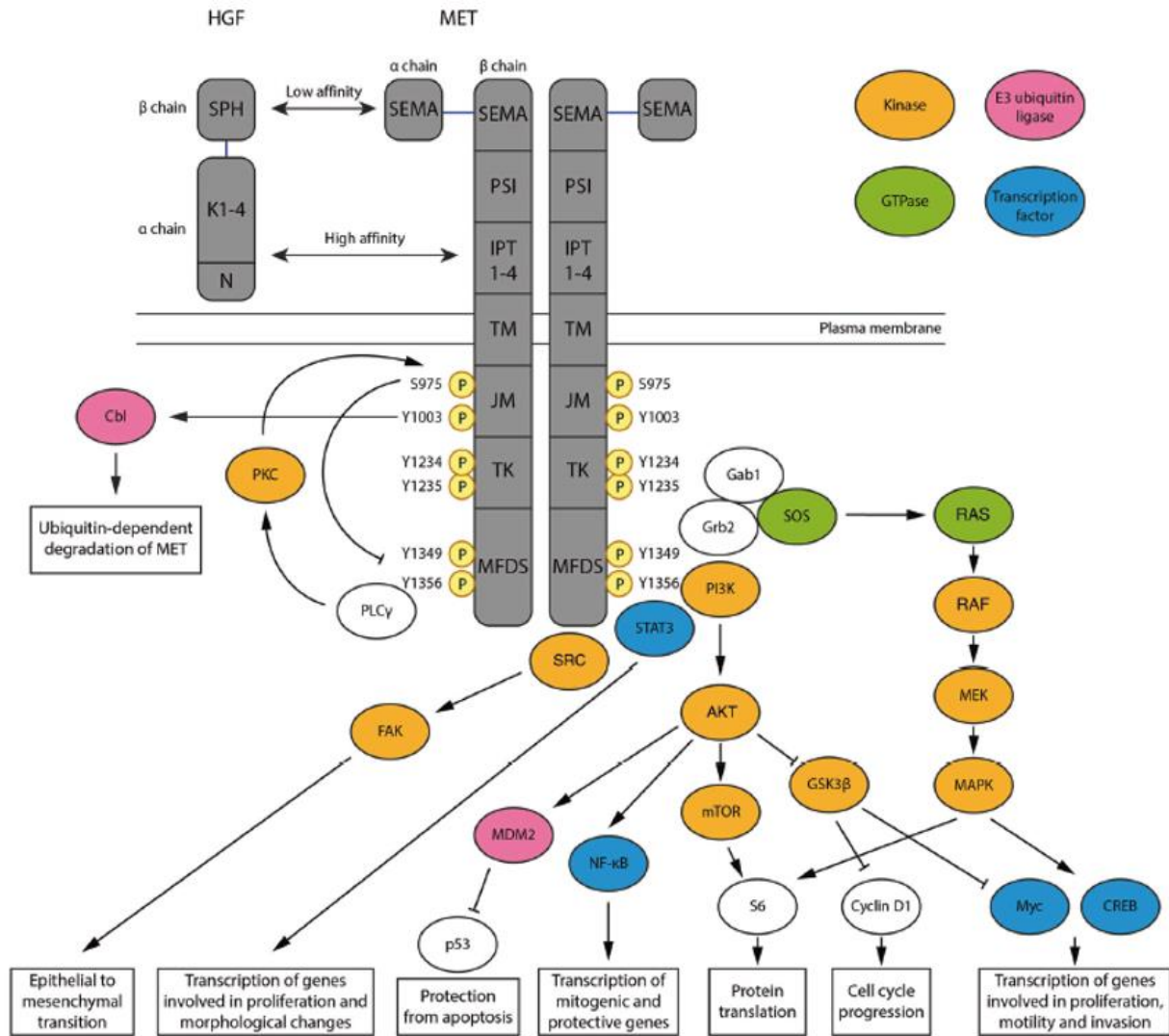


**Figure 2:** Summary of major signaling pathways activated by MET. Active MET recruits SHC1 and GRB2 proteins subsequently activates RAS proteins, which ultimately leads to activation of MAPK signaling cascade, enabling transcription of genes involved in proliferation, motility, invasion, and protein translation. Active MET activates kinase AKT by activating PI3K, which leads to activation of mTOR and MDM2, and inactivation of GSK 3 $\beta$ . Activation of mTOR leads to induction of cellular growth and protein translation. Activation of MDM-2 leads to the inactivation of p53 protein, which enables cells to avoid apoptosis. Inactivation of GSK 3 $\beta$  leads to activation of mitogens cyclin D1 and MYC, thus enhancing cell cycle progression. By phosphorylating STAT3 active MET enables the transcription of genes involved in cell proliferation and morphological changes. Active MET also activates NF- $\kappa$ B, which upregulates genes responsible for cell cycle progression and cell survival. Active MET activates Src kinase, which activates FAK kinase, leading to invasiveness and resistance to anoikis (adapted from Koch et al. 2020).

#### **1.1.4. The Physiological Effects of MET Signaling**

MET is mostly expressed by epithelial cells of various tissues and organs (including the gastrointestinal tract, lung, liver, kidney, thyroid, and skin) as well as some endothelial cells, cells in the hematopoietic lineage, B-cells, and in neurons of various brains structures (Koch et al. 2020). During development, MET acts as the main coordinator of a complex program that involves proliferation, matrix degradation, survival, and migration of various cell types (Koch et al. 2020). MET contributes to the growth and survival of hepatocytes and placental trophoblast cells, growth of neuronal axons, and proliferation of muscle progenitors (Koch et al. 2020). MET is also responsible for the promotion of angiogenesis (Koch et al. 2020). Throughout life, MET is responsible for tissue regeneration and repair, especially of the liver and kidneys (Koch et al. 2020). Active MET enables the cells to migrate to the damaged tissues and reconstitute them while avoiding anoikis (Trusolino et al. 2010; Koch et al. 2020). MET signaling also mediates bone remodeling (Koch et al. 2020).

#### **1.1.5. The Role of MET in Tumorigenesis**

Although MET signaling mediates several essential physiological functions, mentioned above, MET signaling is often appropriated by cancers to promote various stages of their development (Birchmeier et al. 2003; Koch et al. 2020). MET enhances cell proliferation and cell growth, allows the cells to evade growth inhibitors (such as p53), promotes cell motility and cell survival, all of which represent standard hallmarks of cancer (Hanahan & Weinberg 2011). MET signaling in cancer can occur in either HGF-dependent or HGF-independent manner (Koch et al. 2020). The HGF-dependent activation of MET occurs through excess secretion of HGF by stromal cells surrounding the tumor mass (Matsumoto & Nakamura 2006). HGF can also activate MET in an autocrine manner, in addition to paracrine (Park et al 2005). The most common HGF-independent mechanism of MET activation in tumors is overexpression of wild-type MET via transcriptional upregulation (Koch et al. 2020). Overexpression of MET increases the local concentration of MET receptors on the cell surface, resulting in its constitutive activation (Koch et al. 2020). This occurrence has been reported in a variety of cancers of different origins, such as thyroid, colorectal, ovarian, pancreatic, lung, and breast cancers (Koch et al. 2020). MET overexpression



can be the result of hypoxia (HIF-1 $\alpha$  is known to upregulate MET expression) and activation of other oncogenes, such as Ras and NF- $\kappa$ B (Koch et al. 2020). MET activity can also be enhanced by point mutations (Di Renzo et al. 2000), MET gene amplification (Houldsworth et al. 1990), exon deletions (Heist et al. 2016), and by stimulation of other oncogenes, such as EGFR (Brindel et al. 2013). The most notable oncogenic MET variant is the exon 14 skipping mutation, which lacks a part of the juxtamembrane domain that contains amino acids S985 and Y1003, essential for downregulation of MET through ubiquitin-proteasome system (Jeffers et al. 1997; Heist et al. 2016). Therefore, MET exon 14 skipping mutants are constitutively active (Frampton et al. 2015; Koch et al. 2020). Moreover, exon 14 skipping mutations, as well as MET locus amplifications have been uncovered as mechanisms of acquired resistance to EGFR-targeted therapy of NSCLC (Bean et al. 2007; Frampton et al. 2015).

Any of the aforementioned mechanisms by which MET is transformed from a proto-oncogene to an oncogene can occur at any point of tumorigenesis, meaning that oncogenic MET has the potential to promote any stage of primary tumor formation, as well as the dissemination of cancer cells during metastasis (Di Renzo et al. 1995; Koch et al. 2020). The research of MET is paramount since several studies show a link between high MET expression and poor clinical outcomes of some cancers, mainly cancers of the lung and gastrointestinal origin (Birchmeier et al. 2003). High MET activity is a particularly negative clinical marker for NSCLC as it confers the acquired resistance to EGFR-targeted therapy in this cancer type (Kong-Beltran et al. 2006; Reis et al. 2018). In summary, MET is an important oncogene and a major clinical target as its activity contributes to the tumorigenesis of numerous cancer types.

## **1.2. Adaptor (Linker) Proteins**

Adaptor proteins have an important role in signal transduction carried out by receptor tyrosine-kinases and other signaling receptor proteins, such as receptors that contain immunoreceptor tyrosine-based activation motifs (Koretzky et al. 2006; Luo & Hahn 2015). Adaptor proteins lack intrinsic enzymatic activity (Koretzky et al. 2006; Luo & Hahn 2015). Therefore, their function is the regulation of assembly and proper localization of multimolecular signaling complexes (Koretzky et al. 2006). This function is derived from their ability to temporally and spatially regulate the availability of a substrate to an enzyme and/or to serve as protein scaffolds to facilitate key signaling transduction events downstream of receptor proteins (Koretzky et al. 2006; Luo & Hahn 2015). One of the best-known adaptor proteins is growth-factor-receptor-bound protein 2 (GRB2), the first adaptor protein ever discovered (Clark et al. 1992; Koretzky et al. 2006). Activation of various RTKs results in the formation of binding sites for GRB2 and enables its recruitment, along with its constitutively bound interaction partner son of sevenless (SOS), to the cell membrane. Consequently, SOS mediates the activation of membrane-localized RAS and thus relays the signal from the activated RTKs to the downstream effectors of signaling cascades (Koretzky et al. 2006).

### **1.2.1. B-Cell Linker Protein (BLNK)**

BLNK (also known as SLP65, BCA, or BASH) is a central adaptor protein downstream of the B-cell receptor signaling cascade (Fu et al. 1998; Koretzky et al. 2006). The gene locus for BLNK is located on chromosome 10 and encodes a 456 amino acid protein (Koretzky et al. 2006). BLNK is mainly expressed in the cells of the B-cell lineage and to an extent in macrophages (Koretzky et al. 2006). The structure of BLNK is represented in Figure 3. BLNK consists of an N-terminal leucine zipper (LZ) motif, an N-terminal acidic domain that contains five tyrosine residue phosphorylation motifs, a central proline-rich domain, and a C-terminal SH2 domain (Koretzky et al. 2006). The leucine zipper motif has been shown to mediate the association of BLNK to the plasma membrane (Kohler et al. 2005). The structure of BLNK bears a striking resemblance to protein SLP76, another adaptor protein that has a very similar function in a plethora of blood cells (Koretzky et al. 2006).

BLNK is a tyrosine phosphoprotein that, once phosphorylated by kinase Syk, enables the recruitment of numerous BCR signaling pathways components, such as GRB2, NCK, VAV, BTK, and PLC $\gamma$ 2 to relay the signal from activated B-cell receptor to its downstream effectors, which ultimately leads to the activation of MAPK, NK- $\kappa$ B, NFAT, PI3K, and PLC $\gamma$ 2 signaling cascades in pre-B lymphocytes (Fu et al. 1998; Koretzky et al. 2006). Therefore, BLNK acts as a central protein that mediates B-cell development, maturation, and differentiation (Fu et al. 1998; Flemming et al. 2002; Koretzky et al. 2006). Consequently, loss of function of BLNK causes a partial block of B-cell maturation, which causes the accumulation of immature pre-B lymphocytes (Kohler et al. 2005). Moreover, BLNK deficiency seems to be a major contributor to the occurrence of pre-B cell leukemia as BLNK acts as a tumor suppressor in those cells, promoting their differentiation and limiting their proliferation capability (Flemming et al. 2002, Kohler et al. 2005).

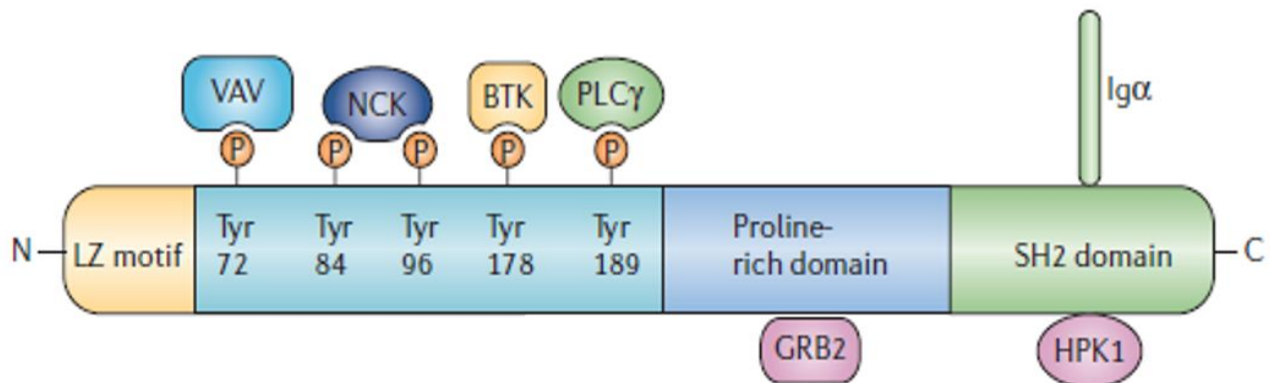


**Figure 3:** The structure of BLNK protein. BLNK consists of an N-terminal leucine zipper (LZ) motif, an N-terminal acidic domain that contains five tyrosine phosphorylation motifs, a central proline-rich domain, and a C-terminal SH2 domain. Once phosphorylated, the tyrosine residues in the N-terminal acidic domain create the binding sites for various interaction partners of BLNK. Proteins of the VAV family bind to BLNK via a phosphorylated tyrosine residue Y72, NCK protein binds to BLNK via phosphorylated tyrosine residues Y84 and Y96, BTK protein binds to BLNK via its phosphorylated tyrosine residue Y178, and PLC $\gamma$  interacts with BLNK via its phosphorylated tyrosine residue Y189. The central proline-rich domain of BLNK allows its interaction with GRB2 protein. The C-terminal SH2 domain of BLNK is responsible for the interaction of BLNK with HPK1 protein, as well as B-cell receptor through its component CD79 $\alpha$ , also known as Ig $\alpha$  (adapted from Koretzky et al. 2006).

## **1.3. Protein-Protein Interactions and Methods for their Detection**

### **1.3.1. The Importance of Protein-Protein Interactions**

Each cell represents a complex biological system, comprised of numerous components that work together, thus enabling the proper function of the cell as a whole. Proteins represent a major fraction of these cellular components. As proteins have a multitude of cellular functions (sensors of the cellular environment, structural units of cells, molecular machines, enzymes, transporters, etc.), no cell can function without them (Snider et al. 2015). Proteins seldom perform any of their functions alone. Therefore, understanding how proteins work together (i.e. protein-protein interactions, PPIs) is of vital importance in uncovering the physiological foundations of cellular functions, and consequently the pathophysiological conditions that arise from the dysregulation or dysfunction of certain protein-protein interactions. Understanding the vast networks of protein-protein interactions in the cells (interactomics) has thus become highly attractive research of interest in modern biomedicine as mapping out the interactome of the cells has great potential of providing answers on the treatment of numerous diseases.

### **1.3.2. Protein-Protein Interaction Detection Methods**

There are many classical methods available to characterize and investigate protein-protein interactions (Snider et al. 2015). They are divided into two major groups according to the approach underlying them: biochemical and genetic methods (Petshcnigg et al. 2011). Biochemical methods entail a direct approach to study PPIs as they investigate protein interactions by working with proteins themselves (for example co-immunoprecipitation or affinity purification), whereas genetic methods entail an indirect approach in determining PPIs based on the reconstitution of a reporter molecule upon interaction (Petshcnigg et al. 2011). Each method has its strengths and weaknesses, hence the selection of the appropriate PPI detection method is no easy task and depends on several parameters, such as the system to study PPIs, cellular localization of proteins in question (this is especially important for the study of membrane protein interaction partners), binding affinity, transient vs stable interactions, and the

requirement of certain post-translational modifications (i.e. proper phosphorylation or glycosylation), co-factors or additional interaction partners (Snider et al. 2015; Valla 2018). Genetic methods are limited mainly by the system used to study PPIs (Petshcnigg et al. 2011; Snider et al. 2015). For example, yeast two-hybrid is a traditional, but widely popular PPI detection method, although one of its main limitations is the proper expression and localization of exogenous proteins in yeast cells (Snider et al. 2015). Biochemical methods are often hindered by the lack of a natural cellular environment and the involvement of harsh experimental conditions during processing that often leads to the inability to detect weak and transient PPIs. Therefore, the selection of an appropriate method to validate protein-protein interaction of interest and its confirmation using at least one other unrelated method is of utmost importance to ensure the validity and biological relevance of newly discovered PPIs. Another major problem is the study of interaction partners of membrane proteins. Methods like co-immunoprecipitation are not suitable to study PPIs of membrane proteins for one simple reason: membrane proteins are unstable outside of the context of the cellular membrane (Snider & Štagljar 2016).

To address the issues regarding the study of PPIs in their native environment, the study of transient PPIs without the involvement of harsh experimental conditions, and to facilitate the research of PPIs involving membrane proteins, has been the mission of the team in Igor Štagljar laboratory to develop novel technologies which can overcome those issues. These methods are: membrane yeast two-hybrid, MYTH (Snider & Štagljar 2016), mammalian membrane two-hybrid, MaMTH (Petshcnigg et al. 2014), and split intein-mediated protein ligation, SIMPL (Yao et al. 2020). MYTH and MaMTH are both based on a split ubiquitin principle, wherein the integral membrane bait protein is fused with a C-terminal ubiquitin moiety (Cub), followed by an artificial transcription factor (TF), whereas the prey protein is fused with an N-terminal ubiquitin (Nub) moiety (Petshcnigg et al. 2011; Snider & Štagljar 2016). Upon the interaction of bait and prey, Nub and Cub reconstitute a pseudo-ubiquitin, which is then recognized by deubiquitinating enzymes (DUBs), following the proteolytic release of the TF which translocates to the nucleus and enables the expression of a stably integrated reporter gene, typically GFP or luciferase. Measurement of the reporter gene activity gives the readout for the PPIs. The features of MaMTH technology are summarized in Figure 4.

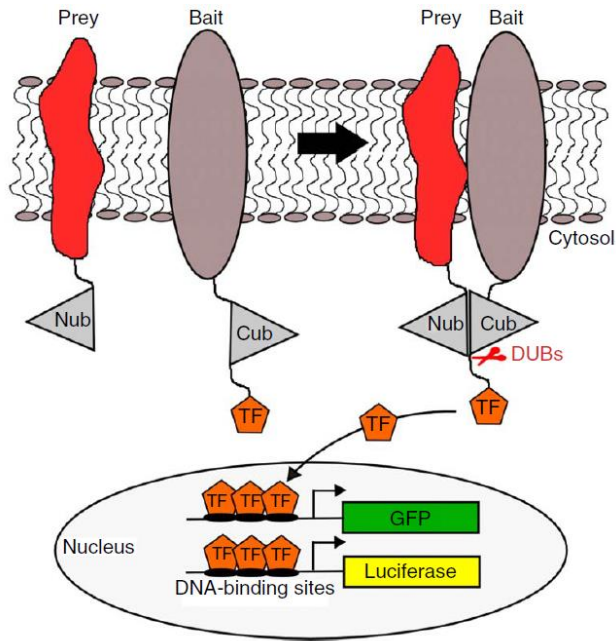


**Figure 4:** Schematic representation of mammalian membrane two-hybrid (MaMTH) technology. MaMTH detects transcriptional activation of luciferase or GFP reporter genes located downstream of 5×GAL4UAS or 8×lexAops DNA-binding sites. The bait protein, fused with Cub-TF, and the prey protein, fused with Nub are co-expressed in HEK293 cells stably expressing the reporter genes. Upon bait and prey interaction, ubiquitin reconstitution occurs, which leads to proteolytic cleavage by deubiquitinating enzymes (DUBs) and subsequent release of the transcription factor (TF). The TF enters the nucleus and activates the reporter gene (adapted from Petshcnigg et al. 2014).

### 1.3.3. Inteins and SIMPL

An intein (intervening protein) is a segment of a protein that can excise itself from the protein and join the flanking segments of the protein, called the exteins (external proteins) with a peptide bond in a process called protein splicing (Shah & Muir 2014). Inteins represent an equivalent of introns and are thus called protein introns (Shah & Muir 2014). Therefore, protein splicing bears a striking resemblance to mRNA splicing during pre-mRNA processing. Protein splicing represents another post-translational modification as it occurs after the protein has been synthesized, which broadens the functional complexity of cellular proteins (Shah & Muir 2014). Inteins are auto-processing domains found in unicellular organisms in all three domains of life (Archaea, Bacteria, Eukaryota), as well as some viruses (Shah & Muir 2014). The fact that inteins are auto-processing

domains implies that no enzyme is required to perform the protein splicing, as opposed to enzymatic proteolysis (Shah & Muir 2014). Another feature of inteins is the spontaneity of action, meaning no external (co)factor or energy source is required to carry out the protein splicing (Shah & Muir 2014). The only prerequisite for the protein splicing to occur is the proper folding of the intein domain (Aranko et al. 2014; Shah & Muir 2014). There are at least 70 different intein alleles known, dispersed across a wide range of host genomes in all three domains of life (Shah & Muir 2014). Inteins are typically embedded within essential proteins, such as DNA and RNA polymerase subunits, DNA helicases, DNA gyrases, and metabolic enzymes, which indicates that intein excision might be required for the proper function of these proteins (Shah & Muir 2014). However, no regulatory role of any intein has thus far been distinguished (Shah & Muir 2014). Since inteins appear to be present throughout all domains of life and share a common biochemical mechanism for protein splicing, they are considered to have an ancient origin, but their biological role (if any) is yet to be discovered (Shah & Muir 2014).

Split inteins are a small fraction of intein genes that, unlike most other inteins (called contiguous inteins) exist as two separate polypeptides (N-intein and C-intein), each fused to one extein (Aranko et al. 2014; Shah & Muir 2014). As opposed to contiguous inteins, which perform the protein cis-splicing, split inteins need to reconstitute the functional intein structure to carry out the protein trans-splicing, as represented in Figure 5 (Aranko et al. 2014). This feature of inteins, along with spontaneity of action, auto-catalytical activity, and complete absence from multicellular organisms makes split inteins attractive tools in biotechnology (Aranko et al. 2014; Shah & Muir 2014). Some of the applications of split inteins are tagless protein purification, a platform for protein evolution through combinatorial domain swapping, protein cyclization, and a platform for the investigation of protein-protein interactions (Aranko et al. 2014; Shah & Muir 2014; Yao et al. 2020).

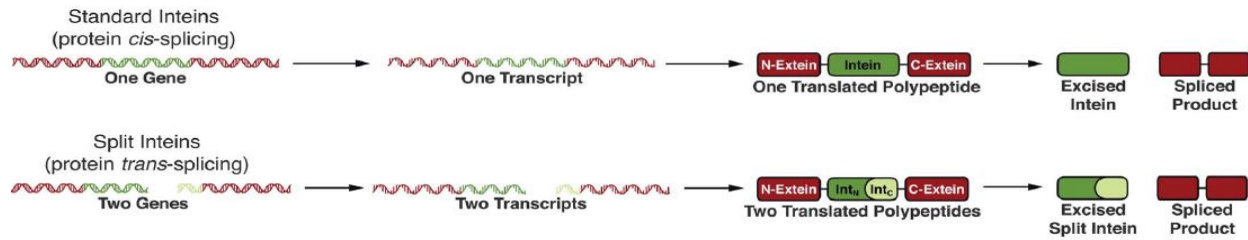


**Figure 5:** Comparison of standard contiguous and uncommon split inteins. Contiguous inteins carry out the protein cis-splicing, resulting in the joining of flanking exteins (N-extein and C-extein), whereas split inteins carry out protein trans-splicing upon reconstitution, resulting in a fusion of two separate exteins (adapted from Shah & Muir 2014).

The platform for the research of protein-protein interactions based on split inteins is conceptualized in Štagljar lab under the name split intein-mediated protein ligation, SIMPL (Yao et al. 2020). SIMPL elegantly utilizes split inteins as sensors for the detection of protein-protein interactions (Yao et al. 2020). In the original SIMPL format bait and prey proteins are fused to N-terminal intein (IN) and C-terminal intein (IC), respectively (Yao et al. 2020). Moreover, bait protein is tagged with a V5 tag, whereas prey protein is tagged with a FLAG tag (Figure 6). Once bait and prey proteins interact, both intein moieties are brought in close proximity and thus allow the reconstitution of a functional intein, following its excision and subsequent ligation of bait and prey proteins, as well as V5 and FLAG tags (Yao et al. 2020). The resulting spliced protein can then be visualized by Western Blot or purified and analyzed by regular biochemical techniques due to the presence of V5 and FLAG tags in the spliced protein (Yao et al. 2020).

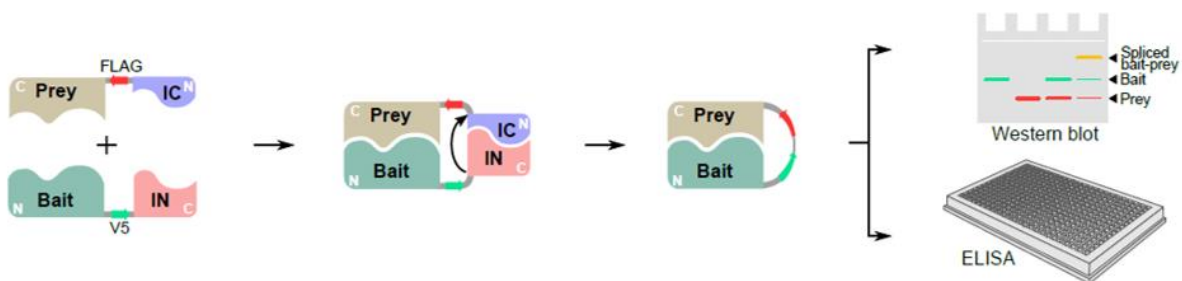


**Figure 6:** The original SIMPL format. The bait protein is fused at its C-terminus to a V5 tag and IN fragment, while the prey protein is fused at its N-terminus to a FLAG tag and IC fragment. The interaction of bait and prey allows the reconstitution of a functional intein and protein splicing of bait and prey occurs. The presence of V5 and FLAG tags allows detection of spliced products by Western Blot or biochemical methods (adapted from Yao et al. 2020).



The original SIMPL format entails fusing the prey protein with appropriate tags at its N-terminus and the bait protein with appropriate tags at its C-terminus (Yao et al. 2020). The presence of tags at specific termini has the potential to disrupt the proper folding and function of some proteins, or the tags may be inaccessible to each other (Yao et al. 2020). Therefore, a few more SIMPL formats were designed to extend the detection capability of SIMPL (Yao et al. 2020). In the CIC format, the IC moiety is fused to the C-terminus of prey while keeping the FLAG tag downstream (Yao et al. 2020). Its interaction with a molecule in IN format leads to splicing between the bait (as well as the V5 tag) and the FLAG tag, which produces a bait-V5-FLAG peptide (Yao et al. 2020). In the NIN format, the bait is N-terminally tagged with the IN fragment and an upstream V5 tag (Yao et al. 2020). The interaction between a bait in NIN format with prey in IC format produces a V5-FLAG-prey peptide (Yao et al. 2020). The CIC-GFP format entails the prey-IC-FLAG-GFP construct which can react with NIN bait to produce V5-FLAG-GFP peptide (Yao et al. 2020).

The detection of the spliced products using Western blot is limited to low-throughput experiments and is at best semi-quantitative (Yao et al. 2020). An ELISA-coupled SIMPL platform overcomes both issues. For this purpose, hemagglutinin (HA) and MYC tags are introduced into the bait and prey constructs alongside V5 and FLAG tags, respectively (Yao et al. 2020). These tags allow the capture of protein expression, as well as protein splicing by performing an appropriate sandwich ELISA (Yao et al. 2020). Furthermore, the capture of protein expression allows for the spliced signal to be normalized to either the bait or the prey expression. The ELISA-coupled SIMPL platform is applicable to all four SIMPL formats (Yao et al. 2020). The alternative SIMPL formats and the set-up of SIMPL ELISA are summarized in Figure 7.

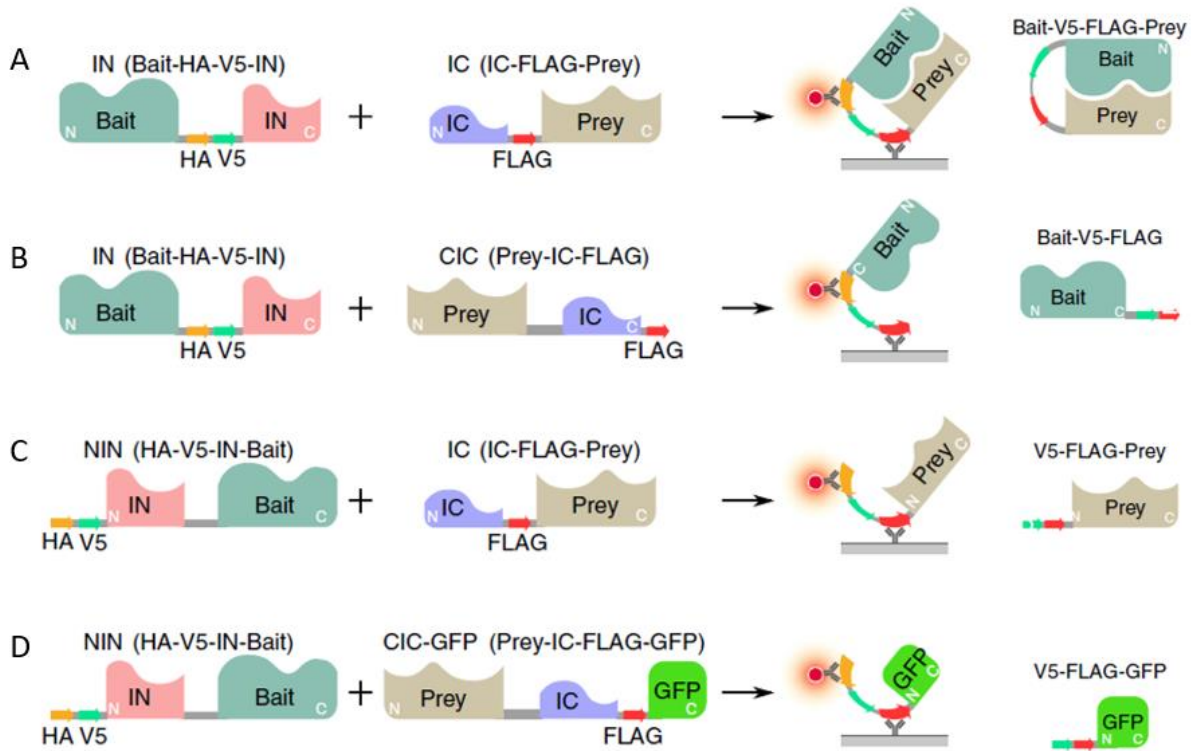


**Figure 7:** Summary of the SIMPL formats and the set-up of SIMPL ELISA. **(A)** IN/IC (original) SIMPL format. The bait protein is fused with V5 and HA tags and IN moiety at its C-terminus, whereas the prey protein is fused with FLAG and MYC tags and IC moiety at its N-terminus. Upon bait-prey interaction, protein splicing occurs that results in the fusion of bait and prey proteins, along with the tags. **(B)** IN/CIC SIMPL format. The bait protein is fused at its N-terminus with HA and V5 tags and IN moiety, whereas the prey protein is fused at its N-terminus with FLAG and MYC tags and IC moiety. Upon bait-prey interaction, the transfer of FLAG and MYC tags to bait protein occurs. **(C)** NIN/IC SIMPL format. The bait protein is fused at its N-terminus with V5 and HA tags, and IN moiety, whereas the prey protein is fused at its N-terminus with FLAG and MYC tags and IC moiety. Upon bait-prey interaction, the transfer of V5 and MYC tags to prey protein occurs. **(D)** CIC/NIN SIMPL format. The bait protein is fused at its N-terminus with V5 and HA tags, and IN moiety, whereas prey protein is fused at its C-terminus with FLAG and MYC tags, IC moiety, and GFP. Upon bait-prey interaction, the transfer of V5 and FLAG tags to GFP occurs. The presence of HA and MYC tags makes all four SIMPL formats compatible to use with ELISA (adapted from Yao et al. 2020).

## 1.4. The Need for MET Protein-Protein Interactome

To deepen the understanding of the biological significance, signaling cascades, and regulatory mechanisms of MET, it is necessary to study its interactome (Stelzl et al. 2005). However, known and validated interacting partners of MET are not only scarce, but have also been discovered using traditional methods that are low-throughput, involve harsh experimental conditions, and cannot effectively detect transient interactions. Therefore, a targeted interactome mapping of MET has been performed using the MET-MaMTH system involving two prey libraries: SH2/PTB domain-containing protein library and FpClass predicted interactions library. SH2/PTB domains preferentially interact with phosphotyrosine-containing motifs (Wagner et al. 2013), while FpClass is a PPI predictive algorithm that uses feature sets to generate the probability of interaction scores to a given query protein (Kotlyar et al. 2015). A prey library of 100 SH2/PTB domain-containing proteins and a prey library of 67 predicted FpClass proteins were screened against MET. Combined, the screens identified 36 interactors of MET, 28 of which appeared to be previously unknown (unpublished data, Štagljar lab). Out of 36 uncovered interaction partners of MET, 15 belong to adaptor proteins, 8 to kinases, 3 to chaperons, 1 to phosphatases, and 8 to other proteins. These interactors are summarized in Figure 8. One of the newly discovered interaction partners is the BLNK protein. Based on previous data from the Štagljar lab, BLNK is not an interactor of ErBB family members, FGFR family members, or ALK kinase, indicating that MET-BLNK interaction could have a unique functional relevance and biological significance. Therefore, the investigation of functional and mechanistic features of this interaction is chosen as a research topic for this thesis.

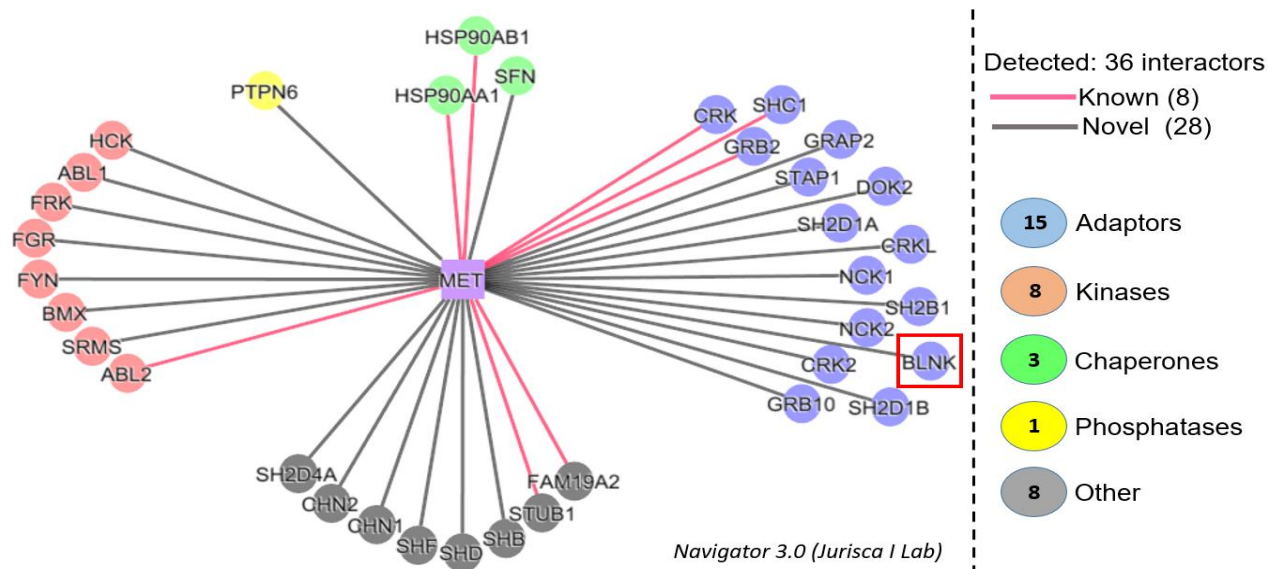


**Figure 8:** Summary of targeted interactome mapping of MET receptor using MET-MaMTH system. A prey library of 100 SH2/PTB domain-containing proteins and a prey library of 67 predicted FpClass proteins were screened against MET. The screens identified 36 interactors of MET, 28 of which appear to be newly discovered. 15 interaction partners are adaptor proteins, 8 interaction partners are kinases, 3 are chaperones, 1 is a phosphatase, and 8 belong to other protein classes. Adaptor protein BLNK is highlighted as the characterization of MET-BLNK interaction was chosen as a research topic for this thesis. Unpublished data generated by Shivanthy Pathmanathan (Štagljar lab).

## 2. RESEARCH AIMS

This research aims will be to:

- 1) Confirm and characterize MET-BLNK interaction by using SIMPL assay.
- 2) Investigate the phosphorylation dependency of MET-BLNK interaction and determine the responsiveness of MET-BLNK interaction to known MET inhibitors.
- 3) Generate and characterize a stable MET-SIMPL system.
- 4) Use site-directed mutagenesis to generate a series of mutated *MET* and *BLNK* genes and use them in a SIMPL assay to uncover the amino acids responsible for MET-BLNK interaction, as well as for detection of GRB2-binding site on BLNK.
- 5) Analyze the proper localization of MET mutants.

### 3. MATERIALS AND METHODS

#### 3.1. Materials

##### 3.1.1. Reagents

The reagents used throughout the research and their origin are summarized in Table 1.

**Table 1:** List of reagents and manufacturers.

<b>Reagent</b>	<b>Company</b>
1,4-Piperazinediethanesulfonic acid (PIPES)	BioShop
1 Kb Plus DNA Ladder RTU	GeneDireX
Acetic Acid	BioShop
Acrylamide Mix (30 %)	BioRad
Agar	BioShop
Albumin	BioShop
Ammonium Persulfate (APS)	Thermo Fisher Scientific
Aprotinin	BioShop
Benzaminidine	BioShop
Bovine Serum Albumin Standard	Thermo Fisher Scientific
Calcium Chloride (CaCl <sub>2</sub> x 2H <sub>2</sub> O)	BioShop
Crizotinib	Sigma Aldrich
Dithiothreitol	BioShop
Dulbecco's Modified Eagle Medium (DMEM)	Gibco
Dulbecco's Phosphate Buffered Saline (PBS)	Gibco
Dulbecco's Phosphate Buffered Saline + CaCl <sub>2</sub> and MgCl <sub>2</sub> (PBS +)	Gibco
Dimethyl Sulfoxide (DMSO)	BioShop
<i>DpnI</i>	New England Biolabs
Ethanol	Commercial Alcohols
Ethylenediaminetetraacetic Acid (EDTA)	BioShop
Egtazic Acid (EGTA)	BioShop
EZ-Link Sulfo-NHS-SS-Biotin	Thermo Fisher Scientific
Fetal Bovine Serum (FBS)	MultiCan
Gateway BP Clonase II Enzyme Mix	Invitrogen
Gateway LR Clonase II Enzyme Mix	Invitrogen
Gel Loading Dye Purple (6x)	New England Biolabs
Gibson Assembly Master Mix (2x)	New England Biolabs
Glycerol	BioShop
Glycine	BioShop
Hepatocyte Growth Factor (HGF)	Sigma Aldrich

Human ORFeome v8.1	AddGene
Hydrochloric Acid	BioShop
Hydrogen Peroxide (30 %)	BioShop
KAPA HiFi Hot St. Ready Mix (2x)	New England BioLabs
Lennox Broth (LB) Medium	BioShop
Leupeptin	BioShop
Luminol	Sigma Aldrich
Manganese (II) Chloride (MnCl <sub>2</sub> x 4H <sub>2</sub> O)	BioShop
Opti-MEM Reduced Serum Medium (1x)	Gibco
p-Coumaric Acid	Sigma Aldrich
Page Ruler Plus Prestained Protein Ladder	Thermo Fisher Scientific
Pepstatin A	BioShop
Polyethylenimine (PEI)	Sigma Aldrich
Ponceau S	BioShop
Potassium Chloride (KCl)	BioShop
Proteinase K	Invitrogen
Sodium Chloride (NaCl)	BioShop
Sodium Dodecyl Sulfate (20 %)	BioShop
Sodium Orthovanadate (Na <sub>3</sub> VO <sub>4</sub> )	NEB
Streptavidin, Agarose Conjugate	Milipore
SYBR Safe DNA Gel Stain	Invitrogen
TAE (50x)	Fisher Bioreagents
TE (Tris/HCl, EDTA) Buffer (10x)	Teknova
Tetramethylethylenediamine (TEMED)	Invitrogen
Triton X-100	Sigma Aldrich
Tris	BioShop
Trypan Blue Stain (0.4 %)	Invitrogen
TrypLE Express	Gibco
Tween 20	VWR
UltraPure Agarose	Invitrogen
X-tremeGENE 9 DNA Transfection Reagent	Roche
β-Glycerophosphate Disodium Salt Hydrate	Sigma Aldrich

### 3.1.2. Bacteria Strains

I used *Escherichia coli* strain DH5α for the amplification of any Gateway expression clone, whereas I used *Escherichia coli* strain DB3.1 to amplify any Gateway donor or destination vector. I obtained both strains by performing the Inoue method, as described below.

### 3.1.3. Antibiotics

I used spectinomycin as a selection marker to obtain any Gateway entry clone, carbenicillin as a selection marker to generate any Gateway expression clone, and to amplify plasmids pOG44 and pA1128 (Thermo Fisher Scientific). I used kanamycin to amplify plasmid pEGFPN1 (Thermo Fisher Scientific). I used penicillin/streptomycin as supplements to the cell culture medium to disenable contamination of animal cells with bacteria and fungi. I used hygromycin B as a selection marker during the generation of the MET-SIMPL system. I used tetracycline to induce expression of proteins cloned in SIMPL bait and prey expression vectors (Figure S1), as well as to induce the expression of MET stably integrated into the genome of the MET-SIMPL system. Table 2 summarizes the antibiotics I used throughout the research and their origin.

**Table 2:** List of antibiotics with working concentrations and manufacturers.

<b>Antibiotic</b>	<b>Working Concentration</b>	<b>Company</b>
Carbenicillin	1000 µg/ml	BioShop
Hygromycin B	100 mg/ml	BioShop
Kanamycin	50 µg/ml	BioShop
Penicillin/Streptomycin	(10000 U/ml)/(10000 µg/ml)	Sigma Aldrich
Spectinomycin	50 µg/ml	BioBasic Canada
Tetracycline	1 mg/ml	BioShop

### 3.1.4. Molecular Biology Kits

I used Presto mini plasmid kit to isolate any plasmid DNA of interest from bacteria. I used Monarch PCR and DNA cleanup kit to isolate PCR products from agarose gel during generation of MET-BLNK double stable construct and generation of constructs for the stable doxycycline-inducible BLNK shRNA knock-down system. I used the Pierce BCA protein assay kit to determine the protein concentration of lysates when performing Western blot analysis. I used Amersham ECL selected Western blotting detection reagent, SuperSignal west pico PLUS chemiluminescent substrate, and UltraScence Western substrate when developing the films for Western blot analysis. I used SuperSignal West pico PLUS chemiluminescent substrate to detect luminescence when performing the ELISA analysis. Table 3 summarizes the molecular biology kits used in the research and their origin.



**Table 3:** List of molecular biological kits and manufacturers.

<b>Commercial Kit</b>	<b>Company</b>
Amersham ECL Selected Western Blotting Detection Reagent	GE Healthcare
Monarch PCR and DNA Cleanup Kit	New England Biolabs
Pierce BCA Protein Assay Kit	Thermo Fisher Scientific
Presto Mini Plasmid Kit	Geneaid
SuperSignal ELISA Pico Reagents	Thermo Fisher Scientific
SuperSignal West Pico PLUS Chemiluminescent Substrate	Thermo Fisher Scientific
UltraScience Western Substrate	FroggaBio

### 3.1.5. Antibodies

I used anti-FLAG antibody (Sigma Aldrich, F1804-1MG), and anti-V5 (Cell Signaling Technology #13202S) in the SIMPL assay. I used an anti-tubulin antibody to measure the loading control. I used an anti-pY99 antibody to detect phosphorylated tyrosine residues of proteins in Western blot analysis. I used HRP-conjugated anti-IgG mouse and rabbit as secondary antibodies in Western blot analysis. I used anti-FLAG (Sigma Aldrich M2 F1804-5MG), anti-V5 (BioRad MCA1360G), anti-HA (GeneTex #115044-01), and anti-MYC (Santa Cruz Biotechnology #J1014) antibodies in ELISA analysis. Table 4 summarizes the antibodies used in Western blot and ELISA analysis and their origin.

**Table 4:** List of antibodies with manufacturers.

<b>Antibody</b>	<b>Company</b>
$\alpha$ -FLAG	Sigma Aldrich, F1804-1MG
$\alpha$ -FLAG	Sigma Aldrich M2 F1804-5MG
$\alpha$ -HA	GeneTex #115044-01
$\alpha$ -IgG Mouse	Cell Signaling Technology #97166S
$\alpha$ -IgG Rabbit	Cell Signaling Technology #7074S
$\alpha$ -MYC	Santa Cruz Biotechnology #J1014
$\alpha$ -pY99	Santa Cruz Biotechnology, sc-7020
$\alpha$ -TUBULIN	Cell Signaling Technology #3873S
$\alpha$ -V5	Cell Signaling Technology #13202S
$\alpha$ -V5	BioRad MCA1360G

### 3.2.6. Buffers and Solutions

Table 5 summarizes buffers and solutions used in the research and their composition.

**Table 5:** List of buffers/solutions and their composition.

<b>Buffer/Solution</b>	<b>Final Concentration</b>
Biotin Solution	0.5 mg/ml Sulfo-NHS-SS Biotin PBS + CaCl <sub>2</sub> + MgCl <sub>2</sub> (PBS +)
Biotin Quenching Solution	0.1 % (w/v) Albumin DMEM
Cell Culture Medium	10 % (v/v) FBS 1 % (v/v) Penicillin/Streptomycin DMEM
Cell Lysis Buffer H	50 mM β-Glycerophosphate (pH = 7.3) 1.5 mM EGTA 1.0 mM EDTA 1.0 mM DTT 0.1 mM Sodium Orthovanadate 1 % (v/v) Triton X-100 1 mM Benzaminidine (1 M in ddH <sub>2</sub> O) 10 μg/ml Aprotinin (10 mg/ml in ddH <sub>2</sub> O) 10 μg/ml Leupeptin (10 mg/ml in ddH <sub>2</sub> O) 1 μg/ml Pepstatin A (1 mg/ml in EtOH)
Crizotinib Solution	10 mM Crizotinib 100 % DMSO
ELISA Blocking Buffer	2 % (w/v) Albumin PBST
Inoue Buffer	55 mM MnCl <sub>2</sub> x 4 H <sub>2</sub> O 15 mM CaCl <sub>2</sub> x 2H <sub>2</sub> O 250 mM KCl 0.5 M PIPES (pH = 6.7) ddH <sub>2</sub> O
Laemmli Sample Buffer (4x)	40 % (v/v) glycerol 0.2 M Tris (pH=6.8) 0.4 % (w/v) Bromophenol Blue 8 % (v/v) SDS 0.1 M DTT
LB Agar Medium	20 g LB 20 g Agar ddH <sub>2</sub> O to 1L
LB Medium	20 g LB ddH <sub>2</sub> O
PBST Buffer	0.05 % (v/v) Tween 20 PBS

Running Buffer (10x)	250 mM Tris 960 mM glycine 1 % (v/v) SDS ddH <sub>2</sub> O
Surface Biotinylation Lysis Buffer	50 mM Tris (pH = 7.5) 1 mM EDTA 1.5 mM EGTA 0.1 mM Sodium Orthovandate 150 mM NaCl 1 % (v/v) Triton X-100 1 mM Benzaminidine (1M in ddH <sub>2</sub> O) 10 µg/ml Aprotinin (10mg/ml in ddH <sub>2</sub> O) 10 µg/ml Leupeptin (10mg/ml in ddH <sub>2</sub> O) 1 µg/ml Pepstatin A (1mg/ml in EtOH)
Surface Biotinylation Wash Buffer 1	50 mM Tris (pH = 7.5) 1 mM EDTA 1.5 mM EGTA 0.1 mM Sodium Orthovandate 50 mM NaCl
Surface Biotinylation Wash Buffer 2	0.1 M Tris (pH = 8.0) 0.5 M LiCl
TBST Buffer (10x)	0.2 M Tris (pH = 7.5) 1.5 M NaCl 0.5 % (v/v) Tween 20 ddH <sub>2</sub> O
TNEG Lysis Buffer	20 mM Tris (pH = 7.5) 150 mM NaCl 2 mM EDTA 0.5 % (v/v) Triton X-100 1 mM Benzaminidine (1 M in ddH <sub>2</sub> O) 10 µg/ml Aprotinin (10 mg/ml in ddH <sub>2</sub> O) 10 µg/ml Leupeptin (10 mg/ml in ddH <sub>2</sub> O) 1 µg/ml Pepstatin A (1 mg/ml in EtOH)
Transfer Buffer (10x)	150 mM Tris 1.2 M Glycine ddH <sub>2</sub> O
Western Blot Blocking Buffer	2 % (w/v) Albumin 1x TBST
Western Blot Developing Reagent	90 mM p-Coumaric Acid 250 mM Luminol 0.0162 % (v/v) Hydrogen Peroxide 0.1 M Tris (pH = 8.5)

### 3.1.7. Laboratory Equipment

Table 6 summarizes the laboratory equipment used in the research.

**Table 6:** List of laboratory equipment with specifications and manufacturers.

Equipment	Specification	Manufacturer
Bacteria Incubator	/	VWR
Bacteria Incubator Shaker	Minitron	Infors HT
Bath Sonicator	8510	Branson
Biological Safety Cabinet	CLASS II Type A2	Microzone Corporation
BlooK LED Transilluminator	BK001	Gene DireX
Cell Culture Incubator	Hera Cell 150i	Thermo Fisher Scientific
Centrifuge	Microfuge 18	Beckman Coulter
Centrifuge	5810R	Eppendorf
Countess 3	/	Thermo Fisher Scientific
DNA Gel Electrophoresis Apparatus	Mini-Sub Cell GT Cell	BioRad
Dry Baths	Precision GD 20	Thermo Fisher Scientific
Greiner Bio-One ELISA Plate	White 384-well Polystyrene Plates, #781074	Lumitrec
Microscope	Vista Vision	VWR
Nitrocellulose Membrane	/	Pall Corporation
Protein Gel Electrophoresis Apparatus	Mini-PROTEAN Tetra Cell	BioRad
Spectrophotometer	ClarioStar	BMG Labtech
Thermal Cycler	Mastercycler Epigradient	Eppendorf
Water Bath	/	Thermo Fisher Scientific
Western Blotting Apparatus	Criterion™ Blotter	BioRad
X-ray Developer	SRX-101A	Konica Minolta

### 3.1.8. Vectors

I used vectors pA1127, pA1128, and pOG44 (Thermo Fisher Scientific) to generate the stable MET-SIMPL system. I used Gateway donor vector pDONR223 to generate Gateway entry clones containing BLNK shRNA cassettes and pLV709G vector to clone BLNK shRNA cassettes. I used SIMPL destination vectors IN4B to generate Gateway expression clone containing wild-type *MET* gene and Gateway expression clones containing mutants of *MET* gene. I used SIMPL prey destination vector IC2 to generate Gateway expression clones containing *PEX7*, *SHC1*, *GRB2*, and

*BLNK*, genes and to generate Gateway expression clones containing mutants of the *BLNK* gene. I used SIMPL bait destination vector IN4B\_FRT to create Gateway expression clone containing wild-type *MET* gene compatible to use with the Flp-In system to generate the stable MET-SIMPL system. I used SIMPL bait destination vector NIN4 to generate Gateway expression clone containing the *GRB2* gene. Vectors used in the research are summarized in Table 7. Vector maps of SIMPL destination vectors, MET and BLNK entry clones, and lentivirus transfer vector pLV709G are summarized in chapter Supplementary Figures & Tables.

**Table 7:** List of vectors and their origin.

Vector	Origin
C-terminal SIMPL Bait Destination Vector (IN4B)	Designed by Zhong Yao
Flp-In Recombinase Expression Vector (pOG44)	Thermo Fisher Scientific
FRT/C-terminal SIMPL Bait Destination Vector (IN4B_FRT)	Designed by Zhong Yao
Gateway Donor Vector (pDONR223)	AddGene
pA1127 (pEGFPN1)	Thermo Fisher Scientific
pA1128 (CAT Positive Control Vector)	Thermo Fisher Scientific
pLV709G	OriGene
N-terminal SIMPL Prey Destination Vector (IC2)	Designed by Zhong Yao
N-terminal SIMPL Bait Destination Vector (NIN4)	Designed by Zhong Yao

### 3.1.9. Gateway Entry Clones

Tables 8 and 9 summarize Gateway entry clones used in the research and their origin.

**Table 8:** Gateway entry clones containing wild-type genes used in the research and their origin.

Gateway Entry Clone	Origin
pDONR223-MET	AddGene
pDONR223-PEX7	Human ORFeome collection v8.1 (Štagljar lab)
pDONR223-SHC1	Human ORFeome collection v8.1 (Štagljar lab)
pDONR223-GRB2	Human ORFeome collection v8.1 (Štagljar lab)
pDONR223-BLNK	Human ORFeome collection v8.1 (Štagljar lab)

**Table 9:** List of Gateway entry clones containing mutants of *MET* or *BLNK* genes and their origin.

Gateway Entry Clone	Origin
pDONR223-MET K1110A	Created by Shivanthy Pathmanathan (Štagljar lab)
pDONR223-MET D1204A	Created by Shivanthy Pathmanathan (Štagljar lab)
pDONR223-MET Exon14Δ	Created by Shivanthy Pathmanathan (Štagljar lab)
pDONR223-BLNK Y72F	Created by Shivanthy Pathmanathan (Štagljar lab)
pDONR223-BLNK Y84F	Created by Shivanthy Pathmanathan (Štagljar lab)
pDONR223-BLNK Y96F	Created by Shivanthy Pathmanathan (Štagljar lab)
pDONR223-BLNK Y84F Y96F	Created by Shivanthy Pathmanathan (Štagljar lab)
pDONR223-BLNK Y72F Y84F Y96F	Created by Shivanthy Pathmanathan (Štagljar lab)
pDONR223-BLNK Y178F	Created by Shivanthy Pathmanathan (Štagljar lab)
pDONR223-BLNK Y189F	Created by Shivanthy Pathmanathan (Štagljar lab)
pDONR223-BLNK P204A	Created by Shivanthy Pathmanathan (Štagljar lab)
pDONR223-BLNK P212A	Created by Shivanthy Pathmanathan (Štagljar lab)
pDONR223-BLNK P204A P212A	Created by Shivanthy Pathmanathan (Štagljar lab)
pDONR223-BLNK P204A P212A Y72F	Created by Shivanthy Pathmanathan (Štagljar lab)
pDONR223-BLNK L18E	Created by Shivanthy Pathmanathan (Štagljar lab)
pDONR223-BLNK I25E	Created by Shivanthy Pathmanathan (Štagljar lab)
pDONR223-BLNK SH2Δ	Created by Shivanthy Pathmanathan (Štagljar lab)
pDONR223-BLNK SH2Δ L18E	Created by Shivanthy Pathmanathan (Štagljar lab)
pDONR223-BLNK SH2Δ Y72F	Created by Shivanthy Pathmanathan (Štagljar lab)
pDONR223-BLNK SH2Δ L18E Y72F	Created by Shivanthy Pathmanathan (Štagljar lab)
pDONR223-BLNK R372A	Created by Shivanthy Pathmanathan (Štagljar lab)
pDONR223-BLNK R372A L18E	Created by Shivanthy Pathmanathan (Štagljar lab)
pDONR223-BLNK R372A I25E	Created by Shivanthy Pathmanathan (Štagljar lab)

### 3.1.10. Primers

All primers I used in the research are summarized in Table 10. I used BLNK shRNA primers to generate constructs for BLNK shRNA knock-down system. I used BLNK shRNA seq primer to verify the presence of BLNK shRNA cassettes cloned in Gateway vector pLV709G. I used MET primers to generate mutants of the *MET* gene. I used the MET Y1003 seq primer to verify the presence of Y1003F mutation in the *MET* gene. I used primers ZY1446, ZY1447, ZY1569, ZY1570, ZY1571, and ZY1572 to generate PCR products for the MET-BLNK double stable construct. I used MET seq and BLNK seq primers to verify the presence of *MET* and *BLNK* genes in the MET-BLNK double stable construct. All primers were obtained as lyophilized powders. I added the appropriate amount of ddH<sub>2</sub>O to each primer, as specified by the manufacturer to prepare the 100 μM stocks.

**Table 10:** List of primers with sequences. Synthesized by Eurofins Genomics.

<b>Primer</b>	<b>Sequence (5' -&gt; 3')</b>
BLNK shRNA attB1	GGGGACAAGTTTGTACAAAAAAGCAGGCTTAGATCTGAATTCAAG
BLNK shRNA attB2	GGGGACCACTTTGTACAAGAAAGCTGGGTCTCTGCATGCAACCC
BLNK shRNA 1 Fw	GTTTCATGAGAATGACTATATACTCGCCTCTGGCGAATTTTTGGGTTGCATGCAGAG
BLNK shRNA 1 Rev	GTCATTCTCATGAACATATACTCGCAGCTGGCGAAGATCTCTATCACTGA
BLNK shRNA 2 Fw	GTTTCATGAGAATGACTAATATGCACTGGCCCTGAACTTTTTGGGTTGCATGCAGAG
BLNK shRNA 2 Rev	GTCATTCTCATGAACATAATATGCACTTTCCTGAACGATCTCTATCACTGA
BLNK shRNA 3 Fw	GTTTCATGAGAATGACCATAATCAGCCTCATCCTCAATTTTTGGGTTGCATGCAGAG
BLNK shRNA 3 Rev	GTCATTCTCATGAACCATAATCAGCCGAATCCTCAAGATCTCTATCACTGA
BLNK shRNA 4 Fw	GTTTCATGAGAATGACTATTAAGCTTGTCCATTCTGTTTTTGGGTTGCATGCAGAG
BLNK shRNA 4 Rev	GTCATTCTCATGAACATTAAGCTTGGACATTCTGTGATCTCTATCACTGA
BLNK shRNA 5 Fw	GTTTCATGAGAATGACATTTATTAACACAGTAGGGATTTTTGGGTTGCATGCAGAG
BLNK shRNA 5 Rev	GTCATTCTCATGAACATTTATTAACCAAGTAGGGAGATCTCTATCACTGA
BLNK shRNA 6 Fw	GTTTCATGAGAATGACAAATCTTGGCAGAGGTATGGGTTTTGGGTTGCATGCAGAG
BLNK shRNA 6 Rev	GTCATTCTCATGAACAAATCTTGGCATCGGTATGGGGATCTCTATCACTGA
BLNK shRNA 7 Fw	GTTTCATGAGAATGACGTATATGGTTGTTTGGAAATCATTTTTGGGTTGCATGCAGAG
BLNK shRNA 7 Rev	GTCATTCTCATGAACGTATATGGTTGGGTGGAATCAGATCTCTATCACTGA
BLNK shRNA 8 Fw	GTTTCATGAGAATGACTTTATTCATTATCCACCTTCTTTTTGGGTTGCATGCAGAG
BLNK shRNA 8 Rev	GTCATTCTCATGAACTTTATTCATTAGGCCACCTTCGATCTCTATCACTGA
BLNK Seq	ATGGACAAGCTTAATAAAAATAACC
BLNK shRNA Seq	GACAAGATAGAGGAGCAAAACAAAAG
MET Seq	ATGAAGGCCCCCGCTGTGC
MET Y1003F Fw	GAATCTGTAGACTAGCTACTTTTCCA
MET Y1003F Rev	TGGAAAAGTAGCTAGTCTACATTC
MET Y1003 Seq	TTAAAAGTTGGAAATAAGAGCTG
MET Y1284F Fw	GGAGCCCCACCTTTGACGTAAACACC
MET Y1284F Rev	GGTGTTTACGTCAAAGGTGGGGCTCC
MET Y1349F Fw	AGCGTTCACATGGAGTGCTCCCAAT
MET Y1349F Rev	ATTGGGGAGCACTCCATGTGAACGCT
MET Y1356F Fw	GTGAACGCTACTTGAACGTAATAATGT
MET Y1356F Rev	ACATTTTACGTTCAAGTAGCGTTCAC
MET Y1356F N1358A Fw	CATGTGAACGCTAAAAATGTGTCGCT
MET Y1356F N1358A Rev	AGCGACACATTTTTAGCGTTCACATG
MET N1358A Fw	AACGCTACTTATGCGTAAAATGTGTC
MET N1358A Rev	GACACATTTTACGCATAAGTAGCGTT
MET Y1365F Fw	TGTGTCGCTCCGTTTCTCTGTTGTCA
MET Y1365F Rev	TGACAACAGAGAAACGGAGCGACACA
ZY1446	CGGCAACAATTAATAGACTG
ZY1447	TATCCGCTCCATCCAGTC
ZY1569	TCCAGACACAGCATACAAACAACAGATGGCTG
ZY1570	GCCATCTGTTGTTTGTATGCTGTGTCTGGACG
ZY1571	CAGAAGCCATAGAGCTCATGTCCAATATGACC
ZY1572	TCATATTGGACATGAGCTCTATGGCTTCTGAG

### 3.1.11. Cell Lines

I used the T-REx HEK293 cell line to perform any transient SIMPL assay, the surface biotinylation experiments, and the SIMPL ELISA experiment. I created the RV001 cell line (MET-SIMPL T-REx HEK293), characterized it, and used it to determine the responsiveness of MET-BLNK interaction to known MET inhibitors.

### 3.2.12. Software

I used the program ApE for in silico analysis of DNA sequences and Finch TV for viewing chromatograms generated by Sanger sequencing. I used NCBI BLAST and ApE to analyze the sequences generated by Sanger sequencing. I generated the shRNA sequences targeting BLNK mRNA in the program GPP Portal. I used the program HPRD to detect potential phosphotyrosine-binding motifs of BLNK protein. I used BioRender to create Figures for this thesis. The programs used in this research are summarized in Table 11.

**Table 11:** List of software.

Software	Company	Web Address
ApE	University of California	<a href="http://biologylabs.utah.edu/jorgensen/wayned/ape/">http://biologylabs.utah.edu/jorgensen/wayned/ape/</a>
BioRender	BioRender	<a href="https://biorender.com/">https://biorender.com/</a>
FinchTV	Geospiza Inc.	<a href="https://digitalworldbiology.com/FinchTV">https://digitalworldbiology.com/FinchTV</a>
GPP Portal	Broad Institute	<a href="https://portals.broadinstitute.org/gpp/public/">https://portals.broadinstitute.org/gpp/public/</a>
HPRD	Johns Hopkins University	<a href="http://www.hprd.org/">http://www.hprd.org/</a>
NCBI BLAST	NCBI	<a href="https://blast.ncbi.nlm.nih.gov/Blast.cgi">https://blast.ncbi.nlm.nih.gov/Blast.cgi</a>



## 3.2. Methods

### 3.2.1. Cell Culture

I handled all cell culture handling according to appropriate cell culture practices. I used T-REx (Tetracycline-Regulated Expression) HEK293 cell line, engineered to stably express Tet repressor from the pcDNA™6/TR plasmid to perform all transient expression experiments (Thermo Fisher Scientific). To design the MET-SIMPL system, I stably integrated the MET-IN-V5 expression cassette into the genome of T-REx cells using Flp-In System, as described below. All cell lines were grown in Dulbecco's Modified Eagle Medium (DMEM) with 4.5 g/L D-glucose, L-glutamine, and sodium pyruvate, supplemented with 10 % (v/v) FBS and 1 % (v/v) penicillin/streptomycin in cell culture incubators at 37 °C with an atmosphere saturated with 5 % CO<sub>2</sub>. I passaged cells after reaching 90-100 % confluency.

### 3.2.2. Cell Passaging

I assessed cell morphology using a light microscope before passaging. I aspirated the existing medium with a glass pipette attached to the suction tip. I washed cells with 4 ml of PBS to remove any leftover medium and dead cells. I incubated cells in 1 ml TrypLE for at least 5 minutes at 37 °C to detach cells from the plate surface. I added 1 ml of pre-warmed cell culture medium to cells to completely detach cells and inactivate the detaching reagent. I resuspended cells in a pre-warmed cell culture medium. I added 1 ml of the cell suspension to a new cell plate that contained 9 ml of freshly added pre-warmed cell culture medium and tilted the plate to disperse cells throughout the plate. I distributed the rest of the cell suspension to well plates according to Table 12. Cells were grown at 37 °C in a cell culture incubator with an atmosphere saturated with 5 % CO<sub>2</sub>. I replaced the old cell culture medium with a fresh cell culture medium every three days until cells were ready for passaging.

**Table 12:** The volume of cell suspension added per well of the appropriate plates.

Number of Wells per Plate	Volume of Cells per Plate (ml)
6	2.0
12	1.0
24	0.5
96	0.1

### **3.2.3. Cell Counting**

For some experiments, the number of cells seeded per plate had to be regulated. After I detached the cells, I mixed 10  $\mu$ l of cell suspension with 10  $\mu$ l of Trypan Blue, added that mix to a chamber slide, and inserted the slide into Countess 3 Automatic Cell Counter. The instrument automatically provided cell concentration and the percentage of viable cells in the suspension.

### **3.2.4. Cell Freezing**

I aspirated the existing cell culture medium with the glass pipette attached to the suction tip. I washed cells with 1 ml of PBS to remove any leftover medium and dead cells. I incubated cells in 1 ml TrypLE for 5 minutes at 37 °C to detach cells from the plate surface. I added 1 ml of pre-warmed cell culture medium to completely detach cells and inactivate the detaching reagent. I prepared and properly labeled the appropriate number of cryovials. I mixed 500  $\mu$ l of the appropriate cell resuspension, 100  $\mu$ l of DMSO, and 400  $\mu$ l of FBS per cryovial. I immediately froze the cryovials at -80 °C and kept them for 1-2 days, following their transfer to a liquid nitrogen tank for long-term storage.

### **3.2.5. Cell Thawing**

I took cells from -80 °C storage and thawed them in a 37 °C dry bath. I transferred the content of the cryovial into 10 ml of the cell culture medium in a Falcon tube and centrifuged them at 1000 rpm for 3 minutes. I resuspended the pellet in 1 ml of cell culture medium and transferred cell resuspension to a 10 cm plastic plate containing 9 ml of the appropriate medium. Cells were grown at 37 °C in a cell culture incubator with an atmosphere containing 5 % CO<sub>2</sub>.

### **3.2.6. Generation of Stable Cell Lines**

I generated an isogenic SIMPL reporter cell line stably expressing MET using Flp-In Technology (Thermo Fisher Scientific). I grew T-REx cells at 37 °C in a cell culture incubator to 50 % confluency. I prepared the transfection mix as follows. In each of the 3 micro-centrifuge tubes, I mixed 97  $\mu$ l of Opti-MEM Reduced Serum Medium with 3  $\mu$ l of transfection reagent X-tremeGene 9 and vortexed the mixture. I added 900 ng of pOG44 vector + 100 ng of MET-IN4B\_FRT construct to

one tube, 900 ng of pOG44 vector + 100 ng of vector pA1128 to the second tube, and 1 µg of pEGFPN1 to the third tube. I vortexed the mixtures, incubated them at room temperature for 30 minutes, and added them dropwise to cells. After 5 hours, I removed the medium and replaced it with a fresh culture medium. Cells were grown for 48 hours. I estimated transfection efficiency by detecting fluorescence emitted by GFP. I passaged cells into a new 6-well plate in 2 ml of the medium using DMEM medium + 10 % (v/v) FBS + 1 % (v/v) penicillin/streptomycin with 100 µg/ml hygromycin until individual foci appeared. I isolated individual foci using cloning cylinders. I added 20 µl of TripLE per cylinder and incubated it for 3 minutes at room temperature. I added 50 µl of pre-warmed cell culture medium per cylinder to deactivate the detaching reagent and resuspend cells. I added each cell suspension to a different well on a 48-well plate containing 250 µl of pre-warmed cell culture medium with 100 µg/ml hygromycin. I expanded each focus into a cell line and verified tetracycline-induced MET expression by Western blot, as described below.

### **3.2.7. Preparation of Competent Bacteria Cells (Inoue Method)**

A plate of *E. coli* strain DH5α was grown on a plate containing solid LB medium overnight in an incubator at 37 °C. The next day I inoculated a single colony into 25 ml of LB medium. It was grown at 37 °C at 200 rpm in a shaking bacteria incubator for approximately 6 hours. I measured OD<sub>600</sub> of culture and calculated the volume of cells necessary to achieve the initial OD<sub>600</sub> of 0.025. I inoculated the determined volume of cells in a total of 250 ml of LB medium and cells were grown overnight at 18 °C at 200 rpm in a shaking bacterial incubator until the OD<sub>600</sub> of 0.4 was reached. After I removed the flask from the incubator, cells had to be kept on ice at all times during the following steps to avoid a dramatic decrease of final competency. I chilled the flask on ice for 10 minutes. I transferred cells into 50 ml Falcon tubes and centrifuged them at 4000 rpm for 5 minutes at 4 °C. I resuspended the pellet in Falcon tubes with 16 ml of pre-chilled Inoue buffer without introducing bubbles and incubated the suspension on ice for 5 minutes. I centrifuged the cells at 4000 rpm for 5 minutes at 4 °C and gently resuspended the pellets in 4 ml of Inoue Buffer (Table 5) per Falcon tube. I pooled the suspensions in a single 50 ml Falcon tube and added DMSO to a final concentration of 7 % while swirling cells (1.5 ml to 20 ml of cell suspension). I incubated the cells on ice for 10 minutes, aliquoted them in 1.5 ml tubes (500 µl per tube), and flash-froze them in liquid nitrogen. I stored the cells to -80 °C for long-term storage.

### **3.2.8. Transformation Using Heat-Shock Method**

I thawed an aliquot of competent *E. coli* strain DH5 $\alpha$  or DB3.1 on ice. I pipetted 30  $\mu$ l of cells to a 1.5 ml tube, added 3  $\mu$ l of plasmid DNA to bacteria, and mixed by flicking the tube. I incubated cells for 30 minutes on ice, following by a heat shock for 45 seconds at 42 °C in a water bath. I incubated cells on ice for 2 minutes and added 1 ml of LB medium to cells. The cells were incubated for 1 hour at 37 °C in a shaking bacteria incubator at 200 rpm. I pre-warmed a plate containing solid LB medium with an appropriate antibiotic. I centrifuged the cells at 7000 rpm for 2 minutes at room temperature. All but 50  $\mu$ l of supernatant was discarded. I resuspended the pellet in the remaining LB medium and plated the suspension on the plate containing solid LB medium with an appropriate antibiotic. Cells were grown overnight at 37 °C in bacteria incubator.

### **3.2.9. Isolation of Plasmid DNA (MiniPrep Method)**

I picked a single bacteria colony from the solid LB medium and inoculated it in 3 ml of LB medium with 3  $\mu$ l of an appropriate antibiotic (1:1000 dilution) overnight at 37 °C in a shaking bacteria incubator at 200 rpm. To increase the plasmid yield, 10 ml of LB medium with 10  $\mu$ l of an appropriate antibiotic can be used to inoculate single bacteria colonies. I used the molecular biology kit Presto Mini Plasmid Kit (Geneaid) to isolate plasmid DNA, as per the manufacturer's instructions. I determined the mass concentration and purity ( $A_{260}/A_{280}$  and  $A_{260}/A_{230}$  ratios) of DNA using the Microplate Reader ClarioStar. I stored the tubes containing isolated DNA at -20 °C.

### **3.2.10. DNA Sequencing**

Sequencing was carried out at The Centre for Applied Genomics, Hospital for Sick Children, Toronto. I analyzed the results using the software ApE, Finch TV, and NCBI BLAST. I sent 250-350 ng of each sample for sequencing. If I used custom primers, I added 0.7  $\mu$ l of the appropriate primer (Table 10) of concentration 5  $\mu$ M to each tube. The personnel that conducted the sequencing added the custom primers (M13 forward, CMV forward, T7 reverse).

### 3.2.11. Site-Directed Mutagenesis

I performed site-directed mutagenesis using KAPA quick-change protocol to create mutations of the *MET* gene. I created the following *MET* mutants using *MET* entry clone (Figure S2, A) as a template: *MET* Y1349F, *MET* Y1356F, *MET* Y1365F, *MET* Y1284F, *MET* Y1003F, *MET* Y1356F N1358A, and *MET* N1358A. I used mutagenic primers designed by Shivanthy Pathmanathan (Štagljar lab) to create specific point mutations on *MET* with the specific mutation located in the center of the primer (Table 10). I created double mutants of the *MET* gene (*MET* Y1349F Y1356F, *MET* Y1349F Y1365F, and *MET* Y1356F Y1365F) using *MET* Y1349F entry clone and *MET* Y1356F entry clone as a template with mutagenic primers from Table 10. I created a triple *MET* mutant (*MET* Y1349F Y1356F Y1365F) using *MET* Y1349F Y1356F entry clone as a template and mutagenic primers from Table 10. I mixed the PCR reactions according to Table 13. I added ddH<sub>2</sub>O to the reaction instead of the DNA template in the negative control. I performed the PCR reactions according to the program in Table 14.

**Table 13:** The composition of a single PCR reaction for KAPA Quick-Change Protocol used for site-directed mutagenesis of *MET* gene.

Reagent	Volume [μL]
KAPA HiFi Hot St. Ready Mix (2x)	12.5
Forward Primer (20.0 μM)	0.5
Reverse Primer (20.0 μM)	0.5
Template (100.0 ng)	0.5
ddH <sub>2</sub> O	11.0

**Table 14:** PCR program for performing KAPA Quick-Change Protocol used for site-directed mutagenesis of *MET* gene.

Step	Time [min]	Temperature [°C]
Initial Denaturation	0.5	95.0
Denaturation x 18	0.5	95.0
Annealing x 18	0.5	63.0
Extension x 18	7.0	72.0
Final Extension	7.0	72.0

After I performed the PCR reaction, I added 0.5  $\mu\text{l}$  of restriction enzyme *DpnI* to the reaction and incubated it for 1 hour at 37 °C to digest methylated parental DNA. I mixed a 5  $\mu\text{l}$  aliquot of the reaction with 1  $\mu\text{l}$  of 6x DNA Gel Loading Dye Purple and loaded it on 1 % agarose gel prepared with 1x TAE buffer and 0.005 % SYBR Safe dye. I run the gel electrophoresis in 1x TAE Buffer for 30 minutes at 100 V. I visualized the DNA using a Blook LED transilluminator. I used 1  $\mu\text{l}$  of the PCR product treated with *DpnI* to transform *E. coli* strain DH5 $\alpha$  and plated them on an LB agar plate containing spectinomycin. I cultured individual colonies that grew on the plate. I isolated plasmid DNA using MiniPrep protocol and determined the entry clones containing *MET* genes with the appropriate point mutations by sending aliquots of each plasmid DNA to Sanger sequencing using T7 reverse primer.

### 3.2.12. Gateway Cloning

#### 3.2.12.1 Generation of Entry Clones

I used Gateway BP reaction to clone the created constructs for the generation of a stable doxycycline-induced BLNK shRNA knock-down system into Gateway donor vector pDONR223. I mixed the reaction for BP cloning according to Table 15 and incubated it at room temperature overnight. After incubation, I added 0.5  $\mu\text{l}$  of Proteinase K and incubated the mixture at 37 °C for 20 minutes. I used 3  $\mu\text{l}$  of the reaction to transform *E. coli* strain DH5 $\alpha$  and amplify plasmid DNA, as described above. I isolated plasmid DNA from overnight bacterial cultures using MiniPrep protocol, and DNA sequences were confirmed by Sanger sequencing using M13 forward primer.

**Table 15:** The composition of a single reaction mix for the Gateway BP reaction.

Component	Volume [ $\mu\text{l}$ ]
Vector (150.0 ng/ $\mu\text{l}$ )	0.5
Insert (100.0 ng/ $\mu\text{l}$ )	0.5
1x TE Buffer	3.0
BP Clonase Enzyme Mix	0.5

### 3.2.12.2. Generation of SIMPL Expression Clones

I performed Gateway LR cloning to transfer all genes from Gateway entry clones (Table 8, Table 9) into SIMPL destination vectors (Figure S1), to transfer all the mutants of MET gene I generated using site-directed mutagenesis into SIMPL bait destination vector (Figure S1), and to transfer all the BLNK shRNA constructs for generation of stable doxycycline-inducible BLNK shRNA knock-down system into Gateway lentivirus vector pLV-709G (Figure S4). I mixed the LR reaction according to Table 16 and incubated it overnight at room temperature. The insert represented the Gateway entry clone. After incubation, I added 0.5  $\mu$ l of Proteinase K and incubated at 37 °C for 20 minutes. I used 3  $\mu$ l of the reaction to transform *E. coli* strain DH5 $\alpha$  and amplify plasmid DNA as described above. I verified DNA sequences by Sanger sequencing using a CMV forward primer.

**Table 16:** The composition of a single reaction mix for the Gateway LR reaction.

Component	Volume [ $\mu$ l]
Vector (150 ng/ $\mu$ l)	0.5
Insert (100 ng/ $\mu$ l)	0.5
1x TE Buffer	3.0
LR Clonase Enzyme Mix	0.5

### 3.2.13. Transient SIMPL Assay

The SIMPL assay required co-transfection of bait and prey genes, cloned into SIMPL bait and prey destination vectors, respectively, into T-REx cells. I prepared the transfection mix for each bait-prey pair according to Table 17. DNA mass represents both bait and prey constructs and I added them in a 1:1 ratio to the mix. After adding all components (Table 17) to a 1.5 ml tube, I mixed the content of the tube by gently pipetting up and down 5 times and incubated for 30 minutes in a BSC at room temperature. After incubation, I added 55  $\mu$ l of transfection mix dropwise into pre-labeled wells on a 12-well plate containing T-Rex cells at 50-60 % confluency. Cells were incubated overnight in a tissue culture incubator with an atmosphere containing 5 % CO<sub>2</sub> at 37 °C. I induced the expression of bait and prey proteins 24 hours after co-transfection by adding tetracycline to a final concentration of 1  $\mu$ g/ml. I lysed cells 24 hours after the addition of tetracycline and subjected the lysates to Western blot analysis using anti-FLAG and anti-V5

antibodies by a standard procedure, as described below. An entire membrane was incubated with an anti-FLAG antibody, whereas the other membrane was cut in half (around 100 kDa) to incubate the upper half with an anti-V5 antibody and the lower half with an anti-tubulin antibody.

**Table 17:** Composition of a single transfection mix prepared for the transient SIMPL assay. DNA mass represents both bait and prey constructs and was added to the mix in a 1:1 ratio.

Component	Volume per well [ $\mu$ l]
DNA (0.5 $\mu$ g)	5.0
PBS	50.0
PEI (1.0 mg/ml)	1.5

### 3.2.14. Stable SIMPL Assay

I performed the stable SIMPL assay using MET-SIMPL cells. Therefore, only the prey proteins needed to be transfected into cells. I prepared the transfection mix according to Table 18. To keep the amount of prey proteins the same as in the transient SIMPL assay, I mixed the appropriate SIMPL expression clones containing the prey gene and the empty SIMPL bait destination vector in a 1:1 ratio. After adding all components (Table 18) to a 1.5 ml tube, I mixed the content of the tube by gently pipetting up and down 5 times and incubated it for 30 minutes in a biosafety cabinet at room temperature. After incubation, I added 55  $\mu$ l of transfection mix dropwise into pre-labeled wells on a 12-well plate containing MET-SIMPL cells at 50-60 % confluency. Cells were incubated overnight in a tissue culture incubator with an atmosphere containing 5 % CO<sub>2</sub> at 37 °C. I induced the expression of bait and prey proteins 24 hours after co-transfection by adding tetracycline to a final concentration of 0.5  $\mu$ g/ml. If I investigated the effect of crizotinib on the interaction of MET with its interaction partners, I added crizotinib in increasing concentrations (the range from 0.5 nM to 25 nM) to different wells containing cells. I lysed cells 24 hours after the addition of tetracycline and subjected the lysates to Western blot analysis using anti-FLAG and anti-V5 antibodies by a standard procedure, as described below. An entire membrane was incubated with an anti-FLAG antibody, whereas the other membrane was cut in half (around 100 kDa) to incubate the upper half with an anti-V5 antibody and the lower half with an anti-tubulin antibody.



**Table 18:** Composition of a single transfection mix prepared for the stable SIMPL assay. DNA mass represents prey construct and IN4B vector, which were added to the mix in a 1:1 ratio.

Component	Volume per well [ $\mu$ l]
DNA (0.5 $\mu$ g)	5.0
PBS	50.0
PEI (1.0 mg/ml)	1.5

### 3.2.15. SIMPL ELISA

I seeded T-REx cells on a 96-well plate at 15000 cells/well and transfected them 4 hours after seeding. I prepared the transfection mix for each bait-prey pair according to Table 19. After adding all components (Table 19) to a 1.5 ml tube, I mixed the content of the tube by gently pipetting up and down 5 times and incubated for 30 minutes in a BSC at room temperature. I added 5  $\mu$ l of each mix in triplicates to cells. I induced protein expression 24 hours after transfecting cells by adding 50  $\mu$ l of DMEM medium with 1.5  $\mu$ g/ml tetracycline per well (the final concentration of tetracycline was 0.5  $\mu$ g/ml). On the same day, I coated an ELISA plate. I diluted the antibodies ( $\alpha$ -FLAG, Sigma M2 and  $\alpha$ -V5, Bio-Rad) 1:100 in PBS. I added 20  $\mu$ l of the antibody per well in a 384-well plate, sealed it with a plastic adhesive PCR foil, and incubated it for 1 hour at 37  $^{\circ}$ C, with occasional shaking. I removed the antibodies from the plate and added 80  $\mu$ l of ELISA blocking buffer (Table 5) to each well. I sealed the plate. The plate was rocked overnight at 4  $^{\circ}$ C. I lysed the cells the next day by adding 90  $\mu$ l of TNEG buffer (Table 5) per well. I sealed the plate and sonicated it for 1 minute at 4  $^{\circ}$ C. I removed ELISA blocking buffer from the antibody-coated plate and added 20  $\mu$ l of lysates per well. I sealed the plate and it was rocked for 3 hours at 4  $^{\circ}$ C. I removed the lysates from the wells of the plate and washed each well with 60  $\mu$ l of PBST (Table 5) per well three times. I diluted the secondary antibodies in ELISA blocking buffer (1:2000 for  $\alpha$ -HA, GeneTex 115044 or 1:5000 for  $\alpha$ -Myc, Santa Cruz Biotechnology). I added 30  $\mu$ l of the appropriate antibody dilution per well, sealed the plate, and rocked it at room temperature for 1 hour. I removed the secondary antibodies and washed each well with 60  $\mu$ l of PBST per well three times. I prepared an ELISA substrate buffer by mixing the two reagents with ddH<sub>2</sub>O in a 1:1:8 ratio. I added 30  $\mu$ l of the ELISA substrate buffer per well and measured the luminescence using Microplate Reader ClarioStar, for integration time 0.2 seconds/well.

**Table 19:** Composition of a single transfection mix prepared for the SIMPL ELISA assay. DNA mass represents both bait and prey constructs and was added to the mix in a 1:1 ratio.

Component	Volume per well [ $\mu$ l]
DNA (0.2 $\mu$ g)	2.0
PBS	20.0
PEI (1.0 mg/ml)	0.6

### 3.2.16. Surface Biotinylation

I seeded T-REx cells on a 6-well plate at 50 % confluency and transfected them 4 hours after seeding. I prepared the transfection mix for each well according to Table 20. After I added all the components (Table 20) in a 1.5 ml tube, I mixed them by gently pipetting up and down 5 times and incubated them for 30 minutes in a biosafety cabinet at room temperature. After incubation, I added the transfection mixes dropwise to pre-labeled cells. Cells were incubated overnight in a cell culture incubator with an atmosphere containing 5 % CO<sub>2</sub> at 37 °C. I induced protein expression 24 hours after transfection by adding tetracycline to a final concentration of 1  $\mu$ g/ml. 24 hours after the addition of tetracycline, I washed cells with ice-cold PBS supplemented with CaCl<sub>2</sub> and MgCl<sub>2</sub> to remove the leftover media and dead cells. I added 1 ml of freshly made biotin solution (Table 5) to each well and incubated the cells for 30 minutes at 4 °C. During incubation, I prepared the biotin quenching solution (Table 5) and kept it on ice. I aspirated the biotin solution and washed the cells three times with biotin quenching solution, and once with ice-cold PBS supplemented with CaCl<sub>2</sub> and MgCl<sub>2</sub>. I lysed the cells with 0.5 ml of surface biotinylation lysis buffer (Table 5) per well and scraped them off the plate using a pipette tip. I collected the lysates in 1.5 micro-centrifuge tubes and centrifuged them at 14000 rpm for 10 minutes at 4 °C. I added a 45  $\mu$ l aliquot from the supernatant of each sample to a new 1.5 micro-centrifuge tube, mixed each aliquot with 15  $\mu$ l of 4x sample buffer (Table 5), and boiled them at 95 °C for 5 minutes. This fraction represented the input. I transferred 400  $\mu$ l of each supernatant to a new 1.5 ml micro-centrifuge tube and kept them on ice. The preparation of the streptavidin beads conjugate followed. 25  $\mu$ l of beads was necessary for each sample. I calculated the appropriate amount of beads slurry for the entire experiment, pipetted the equivalent volume of ddH<sub>2</sub>O into a 1.5 micro-centrifuge tube, and labeled the volume line on the tube. I removed ddH<sub>2</sub>O, added the beads-slurry, and centrifuged it at 2000 rpm until the beads precipitate reached the labeled line. I

washed the beads two times with ice-cold PBS and two times with surface biotinylation wash buffer 1 (Table 5). I mixed the beads precipitate with surface biotinylation wash buffer 1 in a 1:1 ratio and resuspended the beads by pipetting up and down with a tip that was cut. I added 50  $\mu$ l of beads to each sample. The samples were nutated for 2 hours at 4 °C. I centrifuged the samples at 2000 rpm for 1 minute at 4 °C. I added a 45  $\mu$ l aliquot from the supernatant of each sample to a new 1.5 micro-centrifuge tube, mixed it with 15  $\mu$ l of 4x sample buffer (Table 5), and boiled them at 95 °C for 5 minutes. This fraction represented the intracellular fraction. I aspirated the rest of the supernatant. I washed the beads two times with surface biotinylation wash buffer 2 (Table 5) and two times with surface biotinylation wash buffer 1 (Table 5). I aspirated the buffer, added 40  $\mu$ l of 2x sample buffer to every sample, and boiled them at 95 °C for 5 minutes. This fraction represented the surface fraction.

**Table 20:** Composition of a single transfection mix prepared for the surface biotinylation assay.

<b>Component</b>	<b>Volume per Well [<math>\mu</math>l]</b>
DNA (1 $\mu$ g)	10.0
PBS	100.0
PEI (1.0 mg/ml)	3.0

### **3.2.17. Western Blot Analysis**

#### **3.2.17.1. Sample Preparation**

I pre-cooled two 1.5 ml micro-centrifuge tubes on ice for each sample. I moved the cells to ice and aspirated the cell culture medium. I washed the cells with ice-cold PBS to remove any leftover medium and dead cells. I added cell lysis buffer H (Table 5) to each well according to the size of the wells of the plate (90  $\mu$ l for 12-well plates, 150  $\mu$ l for 6-well plates). While on ice, I scraped the cells off with the back of a pipette tip. I transferred the lysates to pre-cooled 1.5 ml micro-centrifuge tubes and centrifuged them at 14000 rpm for 10 minutes at 4 °C. I transferred 65  $\mu$ l of each supernatant to new pre-cooled 1.5 ml micro-centrifuge tubes. I added 2  $\mu$ l of each lysate in duplicates to wells of a 96-well plate to perform the BCA assay. I added 15  $\mu$ l of 4x sample buffer to each sample and mixed them by inverting. I boiled the samples at 95 °C for 5 minutes and stored them at 4 °C.

### **3.2.17.2. BCA Assay**

I determined the protein concentration of each sample using the Pierce BCA Protein Assay kit (Thermo Fisher Scientific). I prepared the BCA reagent by mixing 9.9 ml of Reagent A with 100  $\mu$ l of Reagent B. I pipetted 2  $\mu$ l of standards (BSA of the following concentrations: 0 mg/ml, 31.25 mg/ml, 62.5 mg/ml, 125.0 mg/ml, 250.0 mg/ml, 500.0 mg/ml, and 1000.0 mg/ml) in duplicates in wells of 96-well plate that also contained the duplicates of each lysate. I pipetted 100  $\mu$ l of BCA reagent to each lysate and standard. The plate was incubated for 30 minutes at 37 °C. I measured the absorbance using Microplate Reader ClarioStar at a wavelength of 562 nm. I generated a calibration graph using the absorbance of the standards. I extrapolated the protein concentration of each sample using the calibration graph. I determined the volume of each sample to load 15 ng of proteins for each sample in each well of the polyacrylamide gel.

### **3.2.17.3. SDS PAGE and Protein Transfer**

I prepared the polyacrylamide gels with appropriate acrylamide percentages according to ROTH and Table 21. I mixed the separating gel and cast it between two electrophoresis glass plates in the casting apparatus, followed by polymerization of the gel. I added ddH<sub>2</sub>O over the mix to even the gel surface and to disenable inhibition of acrylamide/bisacrylamide polymerization by atmospheric O<sub>2</sub>. I removed ddH<sub>2</sub>O from the polymerized gel, mixed the stacking gel (Table 21), cast it over the polymerized separating gel, and inserted the comb. I assembled the gasket using two gels and placed it into the electrophoresis apparatus. I removed the combs from the gels and filled the space between two gels with 1x running buffer (Table 5). I loaded 3  $\mu$ l of Page Ruler plus Prestained Protein Ladder into the first well, following the appropriate volume of each sample in the desired order. I filled the apparatus with 1x running buffer to submerge the gels. Gels were run at 150 V until the dye front reached the bottom of gel. I used a wet transfer approach to prepare protein transfer. I wet 1 nitrocellulose membrane, 2 filter papers, and 4 sponges in 1x transfer buffer (Table 5). I assembled the transfer sandwich in the transfer cassette in the following order: black side of the cassette, 2 sponges, 1 filter paper, the gel, the membrane, 1 filter paper, 2 sponges, and the red side of the cassette. I closed the cassette under the buffer to remove any leftover bubbles between the gel and the membrane and placed the cassette into the transfer apparatus, along with an ice pack. I added 1x transfer

buffer to the apparatus to submerge the cassette. The transfer was run at 0.3 A for 110 minutes. I stained the membrane in 1 % Ponceau S for 1 minute and washed it with 1 % acetic acid to determine the transfer quality. I cut the membrane if I used more than 1 antibody. I labeled each membrane, completely de-stained them using 1x TBST (Table 5), and incubated them in Western blot blocking buffer (Table 5) for 1 hour at room temperature. I rinsed the membrane in 1x TBST.

**Table 21:** Recipe for preparing a single polyacrylamide gel. Stacking gel always had 4% acrylamide/bisacrylamide solution added, whereas separating gel had either 6 %, 8 % or 10 % of 30 % acrylamide/bisacrylamide solution added.

Component	Stacking Gel	Separating Gel		
	Volume - 4 % (μl)	Volume - 6 % (μl)	Volume - 8 % (μl)	Volume - 10% (μl)
ddH <sub>2</sub> O	680	2650	2.325	1975
30 % Acrylamide Mix	170	1000	1325	1.675
Tris (1.0 M, pH 6.8)	130	1250	1250	
SDS (20 % Solution)	5	25	25	25
APS (10 % Solution)	10	50	50	50
TEMED	1	5	5	5

#### 3.2.17.4. Antibody Binding and Protein Detection

I prepared the appropriate primary antibody in 1x TBST (usually 1:5000). I incubated the membrane overnight in 10 ml of the primary antibody dilution on a rocker at 4 °C. The next day I washed the membrane with 1x TBST 3 times for 10 minutes at room temperature to remove excess primary antibody. I prepared the appropriate secondary antibody in 1x TBST (1:10000). I incubated the membrane in 10 ml of the secondary antibody dilution for 1 hour on a rocker at room temperature. I washed the membrane with 1x TBST for 10 minutes 3 times. I prepared the enhanced chemiluminescent (ECL) substrate by mixing the solutions from the appropriate molecular biology kits (Table 3) in a 1:1 ratio or I made it (Table 5). I incubated the membrane in the ECL substrate for 1 minute at room temperature, transferred it to the developing cassette, and slid the cover over to remove any leftover bubbles. In the darkroom, I inserted the X-ray film in the developing cassette, exposed it to the membrane, and developed it in an X-ray developer.

### 3.2.18. Generation of Stable Doxycycline-Inducible BLNK shRNA Knock-Down System

I designed 8 different BLNK shRNA sequences, including 2 located within 3' UTR using GPP Portal (Table 22). I chose the sequences with the least off-targeting (Table 22). I designed the primers for the generation of shRNAs using the shRNA barcode primer designer (Štagljar lab). I generated the cassettes containing the shRNAs by PCR reaction, using the pBS-tH1 construct as a template. The pBS-tH1 construct contains an H1 promoter for Tet-On expression, di-TT nucleotide sequence transcribed to di-UU-recognition site for RNA Polymerase III to terminate transcription, and attB1 and attB2 sites for Gateway cloning. I mixed the PCR reactions according to Table 23 and performed the PCR reaction according to the program in Table 24. I added 1  $\mu$ l of 6x DNA Gel Loading Dye Purple to each PCR product and loaded them on 1 % agarose gel prepared with 1x TAE Buffer and 0.005 % SYBR Safe dye. Gel electrophoresis was run in 1x TAE Buffer for 30 minutes at 100 V. I visualized the DNA using a Blook LED transilluminator. I excised the PCR products of the appropriate size (350 bp) from the gel and purified them using Monarch PCR and DNA Cleanup Kit (New England Biolabs), as per the manufacturer's instructions. I determined the concentration of purified PCR products using Microplate Reader ClarioStar. I cloned the PCR products into a Gateway donor vector pDONR223 using Gateway Cloning BP reaction, as described above. I isolated the plasmid DNA using MiniPrep protocol, as described above, and verified the constructs by Sanger sequencing using M13 primer. I cloned the constructs into a lentiviral transfer vector pLV709G (Figure S4) using Gateway cloning LR reaction. I isolated the plasmid DNA using MiniPrep protocol and verified the constructs by Sanger sequencing using BLNK shRNA seq primer (Table 10).

**Table 22:** The features of the chosen BLNK shRNA sequences. Designed in GPP Portal.

Name	Start Position	Intrinsic Score	Target sequence	Location	Existing
shRNA1	511	15.000	TTCGCCAGAGGCGAGTATATA	Coding	+
shRNA2	3607	15.000	GTTCAGGGCCAGTGCATATTA	3' UTR	+
shRNA3	686	13.200	TTGAGGATGAGGCTGATTATG	Coding	+
shRNA4	167	15.000	ACAGAATGGACAAGCTTAATA	Coding	-
shRNA5	4254	15.000	TCCCTACTGTGTTTAATAAAT	3' UTR	-
shRNA6	1090	13.200	CCCATACCTCTGCCAAGATTT	Coding	+
shRNA7	256	15.000	GAAGGTGGAATAATGAATAAA	Coding	-
shRNA8	1302	13.200	TGATTCCAAACAACCATATAC	Coding	+

**Table 23:** The composition of a single PCR reaction mixed to create BLNK shRNA constructs.

Reagent	Volume [ $\mu$ L]
KAPA HiFi Hot St. Ready Mix (2x)	5.0
pBS-tH1 (150.0 ng/ $\mu$ l)	1.0
attB1 Primer (5.0 $\mu$ M)	1.0
attB2 Primer (5.0 $\mu$ M)	1.0
shRNA Fw Primer (0.1 $\mu$ M)	0.5
shRNA Rev Primer (0.1 $\mu$ M)	0.5
ddH <sub>2</sub> O	1.0

**Table 24:** PCR Program used for generating BLNK shRNA constructs.

Step	Time [min]	Temperature [ $^{\circ}$ C]
Initial Denaturation	5.0	95.0
Denaturation x20	0.75	95.0
Annealing x20	0.75	50.0
Extension x20	0.75	72.0

### 3.2.19. Generation of MET-BLNK Double Stable Construct

I mixed the PCR reactions for the generation of MET-BLNK double stable construct according to Table 25. I added ddH<sub>2</sub>O to the reaction instead of the DNA template in the negative control. I performed the PCR reaction according to the program in Table 26. I generated three constructs: MET cassette (using primers ZY1447 and ZY1569 and *MET* gene cloned into IN4B\_FRT vector as a template), BLNK cassette (using primers ZY1570 + ZY1571 and *BLNK* gene cloned into IC2 vector as a template), and IN4B\_FRT vector backbone (using primers ZY1572 + ZY1446 and IN4B\_FRT as a template). I added 0.5 µl of *DpnI* restriction enzyme to each PCR product and incubated them for 1 hour at 37 °C to digest the parental templates. I mixed the PCR products with 1 µl of 6x DNA Gel Loading Dye Purple and loaded them on 1 % agarose gel prepared with 1x TAE Buffer and 0.005 % SYBR Safe dye. Gel electrophoresis was run in 1x TAE Buffer for at least 45 minutes at 100 V until the loading dye front reached the bottom of the gel. I visualized the DNA using a Blook LED transilluminator, cut each PCR product out of the gel using a scalpel, and purified them using Monarch PCR and DNA Cleanup Kit (New England Biolabs), as per the manufacturer's instructions. I measured the mass concentration and purity of PCR products using Microplate Reader ClarioStar. I used the PCR products in a Gibson Assembly reaction (New England Biolabs), as per the manufacturer's instructions. I treated MET cassette as the vector in calculations for preparing Gibson Assembly reaction. I incubated the reaction for 4 hours at 50 °C. I diluted the reaction 4-fold with ddH<sub>2</sub>O. I used 2 µl of the diluted Gibson Assembly reaction to transform the *E. coli* DH5α strain and plated them on an LB agar plate containing carbenicillin. I cultured individual colonies, isolated plasmid DNA using MiniPrep protocol, and verified the presence of *MET* and *BLNK* genes in the construct (Figure S6) by Sanger sequencing using MET seq and BLNK seq primers, respectively (Table 10).



**Table 25:** The composition of a single PCR reaction mixed for the generation of constructs necessary for creating the MET-BLNK double stable construct.

<b>Component</b>	<b>Volume [<math>\mu</math>L]</b>
KAPA HiFi Hot St. Ready Mix (2x)	10.0
Forward Primer (12.0 $\mu$ M)	0.5
Reverse Primer (12.0 $\mu$ M)	0.5
DMSO	0.6
Template (50.0 ng)	0.5
ddH <sub>2</sub> O	8.4

**Table 26:** PCR program used for the generation of constructs necessary for creating the MET-BLNK double stable construct.

<b>Step</b>	<b>Time [min]</b>	<b>Temperature [<math>^{\circ}</math>C]</b>
Initial Denaturation	0.5	95.0
Denaturation x18	0.5	95.0
Annealing x18	0.5	63.0
Extension x18	8.0	72.0
Final Extension	8.0	72.0

## 4. RESULTS

### 4.1. The Validation of MET-BLNK Interaction Using SIMPL Assay

To validate MET-BLNK interaction, the transient SIMPL assay was performed. PEX7 was chosen as a negative control as it is known not to interact with MET (unpublished data, Štagljar lab), whereas SHC1 and GRB2 were chosen as positive controls, as they are both known interactors of MET (Koch et al. 2020). *MET* gene was cloned into SIMPL bait destination vector IN4B (Figure S1, A), while *PEX7*, *SHC1*, *GRB2*, and *BLNK* genes were cloned in SIMPL prey destination vector IC2 (Figure S1, B) using Gateway Technology. The generated expression clones were verified by Sanger sequencing. Table 27 summarizes SIMPL expression clones generated for this experiment.

**Table 27:** List of SIMPL expression clones generated for validation of MET-BLNK interaction using Gateway technology.

Gene	Expression Clone
<i>MET</i>	IN4B-MET
<i>PEX7</i>	IC2-PEX7
<i>SHC1</i>	IC2-SHC1
<i>GRB2</i>	IC2-GRB2
<i>BLNK</i>	IC2-BLNK

MET-prey combinations were co-transfected in T-REx cells in duplicates. Protein expression was induced by the addition of tetracycline (1 µg/ml) 24 hours after transfection in one replica. Cells were lysed 24 hours after the addition of tetracycline and lysates were subjected to Western blot analysis using anti-V5 and anti-FLAG antibodies to detect bait and prey expression, respectively, as well as the spliced proteins if the interaction occurred (Figure 9). Due to a similar size of mature MET, precursor MET, and spliced proteins involving MET, gel electrophoresis using 6 % polyacrylamide gel was performed for Western blot using an anti-V5 antibody to provide sufficient separation (Figure S3). No interaction was observed upon co-expressing MET-PEX7, whereas spliced signals of the appropriate sizes (Table S1) were observed upon co-expressing MET with SHC1 and GRB2, as well as BLNK, both in the presence and absence of tetracycline, indicating the leakiness of the system. The interaction of SHC1 and GRB2 with both precursor MET and mature MET was observed, whereas BLNK interacted with only one form of MET.  $\alpha$ -tubulin was used as a loading control.

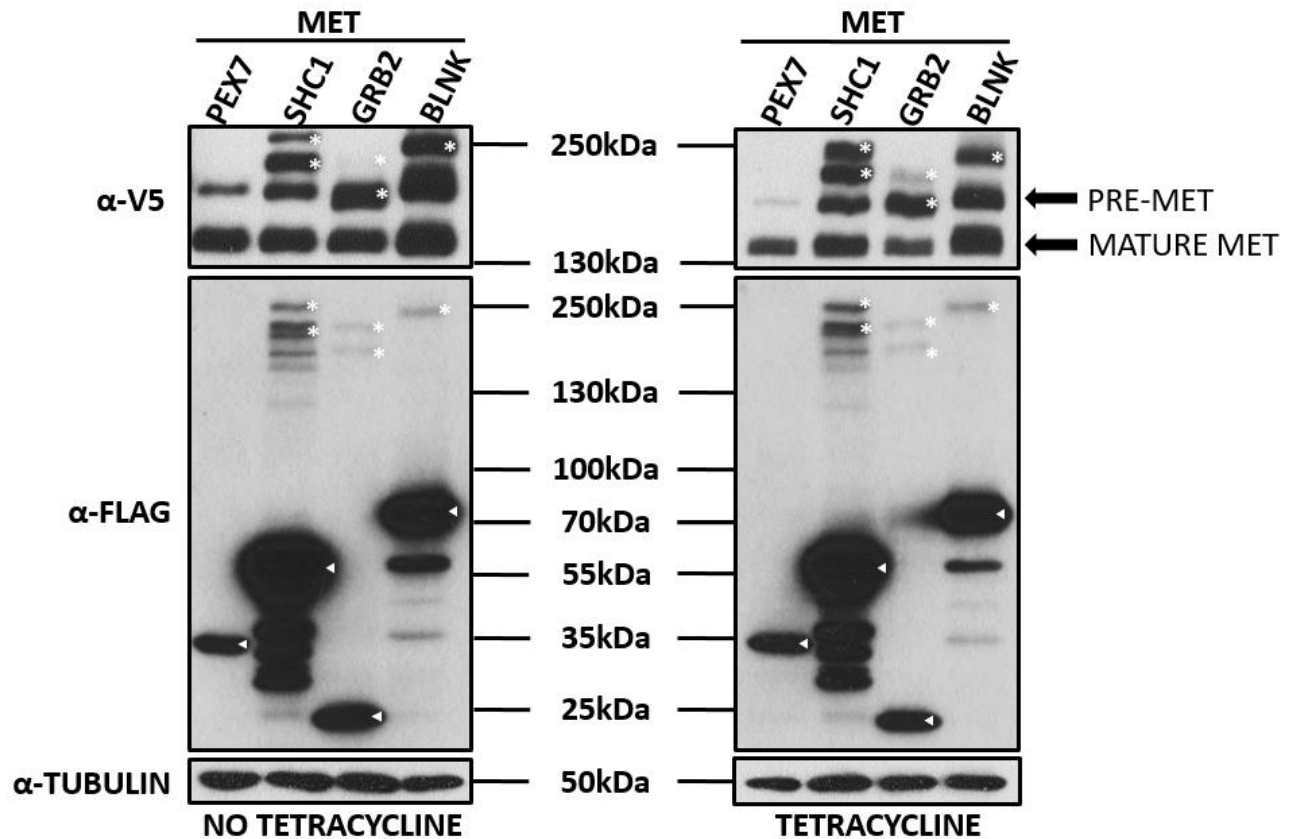


**Figure 9:** Validation of MET-BLNK interaction in the absence (left panel) and presence (right panel) of tetracycline (1  $\mu\text{g/ml}$ ) was analyzed by Western blot using anti-V5 and anti-FLAG antibodies to detect bait and prey expression, respectively, as well as spliced proteins if the interaction occurred. The precursor MET (PRE-MET) and mature MET are denoted with arrows.  $\alpha$ -tubulin was used as a loading control. Parental prey proteins are highlighted by triangles, while spliced proteins are highlighted by asterisks. Note that the spliced band of MET-GRB2 is the same size as pre-MET. Sizes of proteins detected by Western blot when performing a SIMPL assay involving MET are summarized in Table S1.

#### 4.2. MET Kinase-Dead Mutant Reduced the Interaction with BLNK

To test the effects of abolishing the kinase activity of MET on the interaction with BLNK, two kinase-dead mutants of MET gene MET K1110A and MET D1204A were cloned into SIMPL bait destination vector IN4B (Figure S1, A) using Gateway Technology. The generated expression clones were verified by Sanger sequencing. To determine whether the introduction of these mutations affected expression and phosphorylation of MET, their expression and phosphorylation profiles were compared to the expression and phosphorylation profile of wild-

type MET by expressing them in T-REx cells. To keep the amount of MET transfected in T-REx cells the same as in the SIMPL assay, the constructs were co-transfected into T-REx cells alongside the empty SIMPL prey vector in a 1:1 ratio. Protein expression was induced by the addition of tetracycline (1 µg/ml) 24 hours after transfection. Cells were lysed 24 hours after the addition of tetracycline and lysates were subjected to Western blot analysis using anti-V5 and anti-pTyr antibodies to detect MET expression and phosphorylation, respectively (Figure 10). Both precursor and mature forms of MET K1110A demonstrated reduced expression, compared to wild-type MET. Expression of MET D1204A was not detected. K1110A point mutation abolished the phosphorylation of MET.  $\alpha$ -tubulin was used as a loading control.

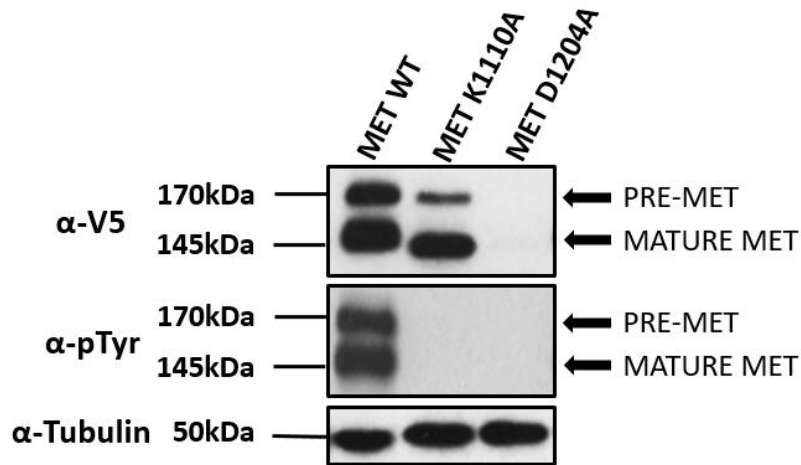


**Figure 10:** Expression and phosphorylation profiles of wild-type MET, and mutated MET K1110A and MET D1204A were analyzed by Western blot using anti-V5 and anti-pTyr antibodies, respectively. The precursor MET (PRE-MET) and mature MET are denoted with arrows.  $\alpha$ -tubulin was used as a loading control.

To test the effect of abolishing phosphorylation of MET on the interaction with BLNK, the transient SIMPL assay was performed in T-REx cells. BLNK was co-transfected with MET K1110A and MET D1204A. PEX7 was used as a negative control, whereas SHC1 and BLNK were used as positive controls. Protein expression was induced by the addition of tetracycline (1 µg/ml) 24 hours after transfection. Cells were lysed 24 hours after the addition of tetracycline and lysates were subjected to Western blot analysis using anti-V5 and anti-FLAG antibodies to detect bait and prey expression, respectively, as well as spliced proteins if the interaction occurred. No

interaction was detected upon co-expressing MET-PEX7, whereas spliced proteins of the appropriate sizes (Table S1) were detected upon co-expressing MET with SHC1 and BLNK (Figure 11). The interaction of MET kinase-dead mutant MET K1110A with BLNK was reduced, as compared to the interaction of wild-type MET and BLNK, although reduced expression of MET kinase-dead mutant MET K1110A was also observed. Expression of MET D1204A was not detected.  $\alpha$ -tubulin was used as a loading control.

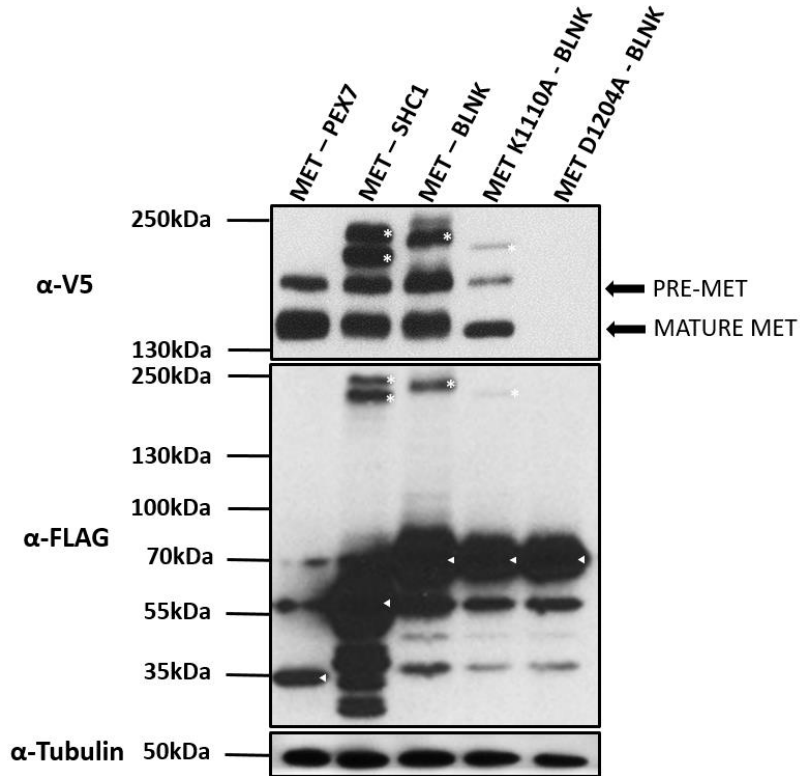


**Figure 11:** The effects of MET kinase-dead mutants on MET-BLNK interaction were analyzed by Western blot using anti-V5 and anti-FLAG antibodies to detect bait and prey expression, respectively, as well as spliced proteins if the interaction occurred.  $\alpha$ -tubulin was used as a loading control. Precursor (PRE-MET) and mature MET are denoted with arrows. Parental prey proteins are highlighted by triangles, while spliced proteins are highlighted by asterisks. Sizes of proteins detected by Western blot when performing a SIMPL assay involving MET are summarized in Table S1. Note that the  $\alpha$ -FLAG panel of the figure needed to be overexposed to capture the interaction of MET K1110A and BLNK.

To validate that BLNK interacts with MET in the same fashion as other known interactors that contain an SH2 domain, the transient SIMPL assay was performed. SHC1 and BLNK were co-transfected with wild-type MET and MET kinase-dead mutant MET K1110A in T-REx cells. PEX7 was used as a negative control for both MET variants. Protein expression was induced by the addition of tetracycline (1 µg/ml) 24 hours after co-transfection. Cells were lysed 24 hours after the addition of tetracycline and lysates were subjected to Western blot analysis using anti-V5 and anti-FLAG antibodies to detect bait and prey expression, respectively, as well as spliced proteins if the interaction occurred. No interaction was observed upon co-expressing PEX7 with any MET variant. The interaction of both SHC1 and BLNK with MET kinase-dead mutant MET K1110A was markedly reduced, as compared to wild-type MET (Figure 12), although expression of MET K1110A was also reduced, compared to wild-type MET.  $\alpha$ -tubulin was used as a loading control.

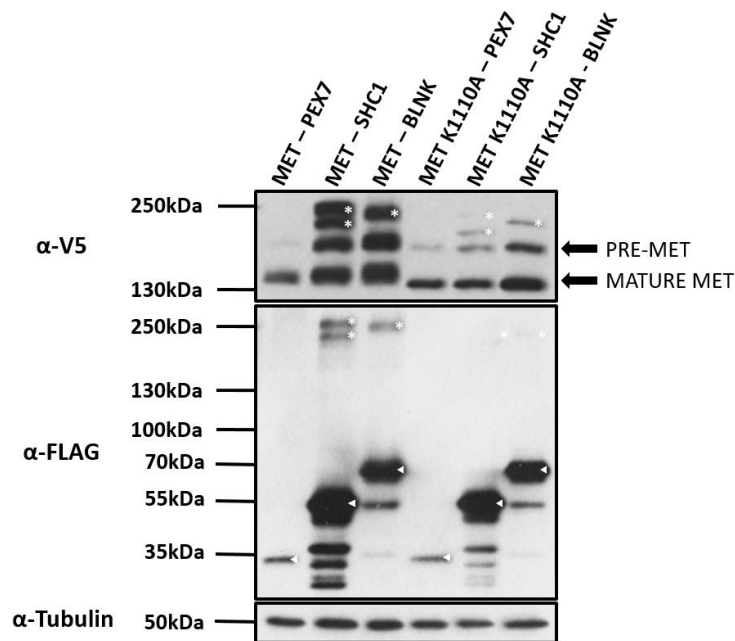


**Figure 12:** Interaction of SHC1 and BLNK with wild-type MET and MET kinase-dead mutant MET K1110A was analyzed by Western blot using anti-V5 and anti-FLAG antibodies to detect bait and prey expression, respectively, as well as spliced proteins if the interaction occurred. Precursor (PRE-MET) and mature MET are denoted with arrows.  $\alpha$ -tubulin was used as a loading control. Parental prey proteins are highlighted by triangles, while spliced proteins are highlighted by asterisks. Sizes of proteins detected by Western blot when performing a SIMPL assay involving MET are summarized in Table S1.

### 4.3. The Generation and Characterization of the Stable MET-SIMPL System

To circumvent the lack of tetracycline-inducible control over the expression of MET in the transient SIMPL system, a stable MET-SIMPL system was generated. *MET* gene was cloned into Flp-In SIMPL bait destination vector, which contains an FRT site (Figure S1, C). The generated construct was verified by Sanger sequencing. T-REx HEK293 cells were stably transfected with MET-IN-V5 construct using Flp-In Technology, as described above. After the expansion of several clones MET expression was verified. Each clone was seeded in two replicas. Protein expression was induced by the addition of tetracycline (1  $\mu\text{g}/\text{ml}$ ) in one replica 24 hours after seeding. Cells were lysed 24 hours after the addition of tetracycline and lysates were subjected to Western blot analysis using an anti-V5 antibody to detect MET expression. Expression of precursor and mature MET was detected in all clones only in presence of tetracycline (Figure 13).  $\alpha$ -tubulin was used as a loading control. Clone 2 was chosen for further validation as it demonstrated the highest expression of MET.

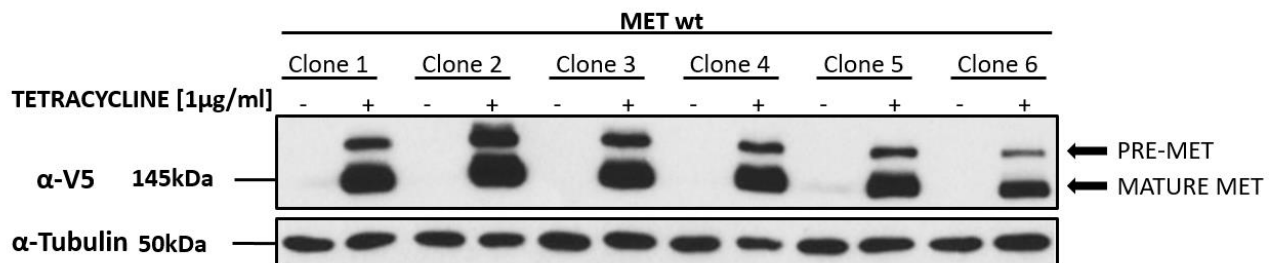


**Figure 13:** MET expression in the MET-SIMPL system was analyzed in the presence and absence of tetracycline by Western blot using an anti-V5 antibody. Both precursor (pre-MET) and mature MET (arrows) expressed in all checked clones only upon the addition of tetracycline.  $\alpha$ -tubulin was used as a loading control.

To characterize the MET-SIMPL system further, the localization of MET bait was assessed. To verify the proper localization of mature MET in the MET-SIMPL system, a surface biotinylation assay was performed. Cells were seeded to 50 % confluency in a 6-well plate. Expression of MET was induced by the addition of tetracycline (1  $\mu\text{g}/\text{ml}$ ) 24 hours after seeding. Cells were subjected to surface biotinylation assay 24 hours after the addition of tetracycline. Three different conditions were analyzed: no tetracycline with biotin, tetracycline with biotin, and tetracycline

with no biotin. The fractions representing the input, the supernatant (i.e. intracellular proteins), and the pull-down (i.e. surface proteins) were subjected to Western blot analysis using an anti-V5 antibody. Expression of both precursor and mature MET was observed in the input only with the addition of tetracycline (Figure 14). Both precursor and mature MET were observed in the intracellular fraction, regardless of the biotin addition. Mature MET was observed in the pull-down fraction only in the presence of tetracycline and biotin. Precursor MET was observed at the surface at a markedly lower level than in the intracellular fraction, as well as compared to mature MET.  $\alpha$ -tubulin was used as a loading control. No loading control was observed in the pull-down samples.

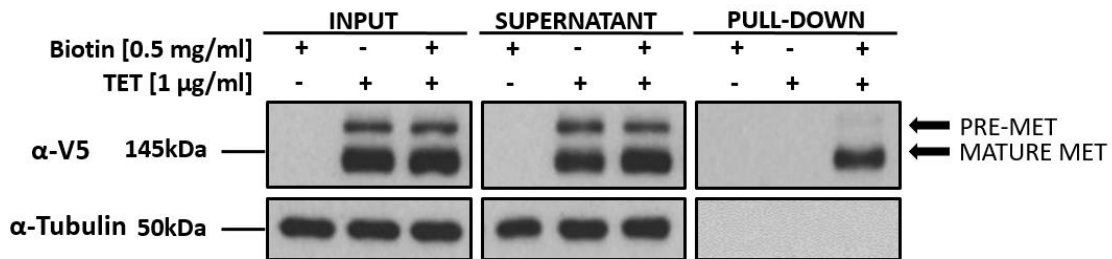


**Figure 14:** Localization of precursor (PRE-MET) and mature MET in the MET-SIMPL system was analyzed by performing surface biotinylation experiment and Western blot analysis using an anti-V5 antibody. The supernatant represents an intracellular fraction of proteins, whereas the pull-down represents a surface fraction of proteins. Precursor (PRE-MET) and mature MET are denoted with arrows.  $\alpha$ -tubulin was used as a loading control and to mark intracellular fraction.

Next, the ability of the MET-SIMPL system to detect known interactors of MET was assessed by performing the SIMPL assay. PEX7 was chosen as a negative control, whereas SHC1, GRB2, and BLNK were chosen as positive controls. MET-SIMPL cells were co-transfected with prey constructs and the empty SIMPL bait vector in a 1:1 ratio. Protein expression was induced by the addition of tetracycline (1  $\mu$ g/ml) 24 hours after transfection. Cells were lysed 24 hours after the addition of tetracycline and lysates were subjected to Western blot analysis using anti-V5 and anti-FLAG antibodies to detect bait and prey expression, respectively, as well as spliced proteins if the interaction occurred (Figure 15). No interaction was observed when co-expressing MET-PEX7, whereas the interaction of SHC1, GRB2, and BLNK with MET was observed.  $\alpha$ -tubulin was used as a loading control.



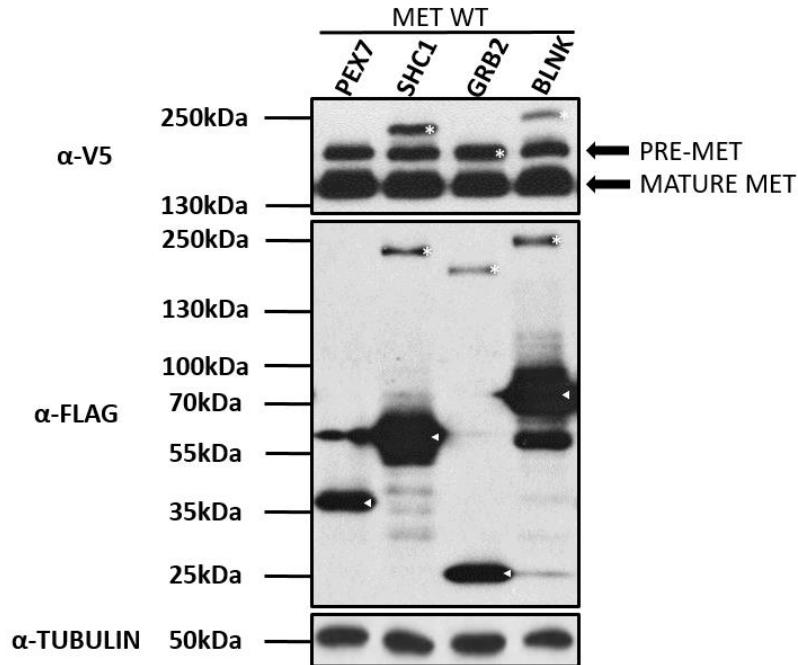


**Figure 15:** The ability of the MET-SIMPL system to detect known interaction partners of MET was analyzed with Western blot using anti-V5 and anti-FLAG antibodies to detect bait and prey expression, respectively, as well as spliced proteins if the interaction occurred. Precursor (PRE-MET) and mature MET are denoted with arrows.  $\alpha$ -tubulin was used as a loading control. Parental prey proteins are highlighted by triangles, while spliced proteins are highlighted by asterisks. Note that the spliced band of MET-GRB2 is the same size as pre-MET. Sizes of proteins detected by Western blot when performing a SIMPL assay involving MET are summarized in Table S1.

Then the capacity of a single Tet repressor, stably integrated into the genome of T-REx HEK293 cells, to repress MET expression in addition to prey expression was examined. MET-SIMPL cells were seeded on a 12-well plate. Two wells were transfected with an empty SIMPL prey vector and four wells were transfected with BLNK. Additionally, two mock controls (no transfection) were used. Protein expression was induced after 24 hours by the addition of tetracycline (1  $\mu$ g/ml) in one mock control replica and one replica transfected with an empty SIMPL prey vector. Protein expression was also induced in cells transfected with BLNK by addition of tetracycline in increasing concentrations (0  $\mu$ g/ml, 0.25  $\mu$ g/ml, 0.5  $\mu$ g/ml, and 1.0  $\mu$ g/ml). Cells were lysed 24 hours after the addition of tetracycline and lysates were subjected to Western blot analysis using anti-V5 and anti-FLAG antibodies to detect bait and prey expression, respectively, as well as spliced proteins if the interaction occurred (Figure 16). Expression of precursor and mature MET

was detected in mock control only with the addition of tetracycline. Correspondingly, MET expression was detected in the empty vector transfection control only in the addition of tetracycline. No MET expression and basal BLNK expression were observed by co-expressing MET and BLNK without the addition of tetracycline. The addition of 0.25  $\mu\text{g/ml}$  tetracycline to cells co-expressing MET and BLNK induced expression of both MET and BLNK, as well as MET-BLNK interaction. Both the expression of MET and BLNK and their interaction were saturated by the addition of tetracycline in a concentration of 0.5  $\mu\text{g/ml}$ .  $\alpha$ -tubulin was used as a loading control.

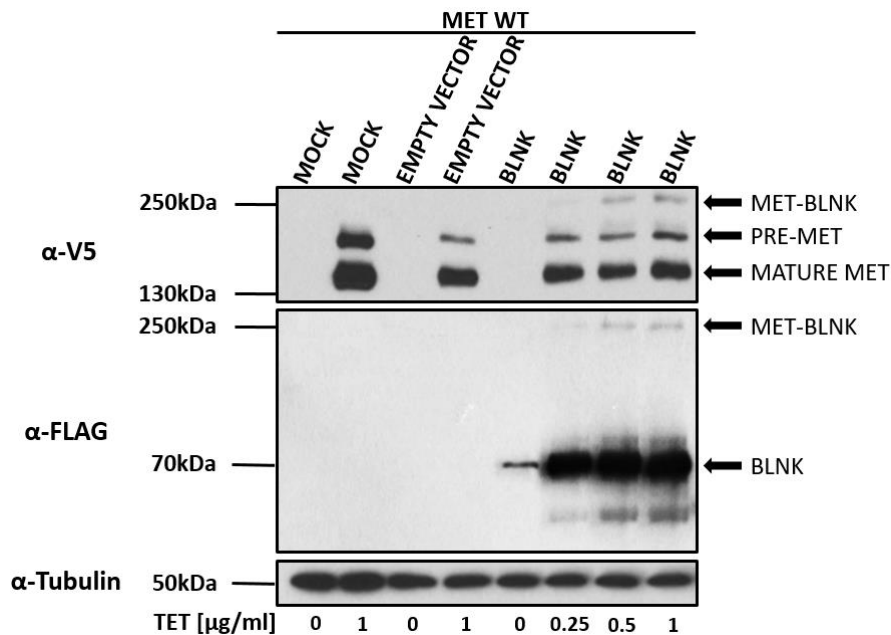


**Figure 16:** The capacity of a single Tet repressor, stably integrated into the genome of the MET-SIMPL system, to repress bait and prey expression was assessed by Western blot using anti-V5 and anti-FLAG antibodies to detect bait and prey expression, respectively, as well as spliced protein (MET-BLNK) if the interaction occurred. The expression of precursor and mature MET was detected only with the addition of tetracycline both in mock control (no transfection) and cells transfected with an empty SIMPL prey vector. Precursor (PRE-MET), mature MET, and MET-BLNK are denoted with arrows.  $\alpha$ -tubulin was used as a loading control. Sizes of proteins detected by Western blot when performing a SIMPL assay involving MET are summarized in Table S1.

Next, the ability of the MET-SIMPL system to respond to known MET tyrosine-kinase inhibitors was assessed. The effect of crizotinib on MET expression and phosphorylation profile was determined in the MET-SIMPL system. MET-SIMPL cells were seeded to 50 % confluency. Expression of MET was induced after 24 hours by the addition of tetracycline (0.5  $\mu\text{g/ml}$ ). Simultaneously, cells were treated with increasing concentrations of crizotinib. DMSO was used as solvent control. Cells were lysed 24 hours after the addition of tetracycline and crizotinib and lysates were subjected to Western blot analysis using anti-V5 and anti-pTyr antibodies to detect MET expression and phosphorylation, respectively (Figure 17). No MET expression was observed in the no tetracycline sample. DMSO did not affect the expression and phosphorylation of MET. The expression of precursor and mature MET expression decreased upon treatment with the increasing concentrations of crizotinib, starting at a concentration of 10 nM. A steep dose-dependent decrease of MET phosphorylation upon the addition of crizotinib was observed, wherein crizotinib in the concentration of 25 nM and higher abolished MET phosphorylation.  $\alpha$ -tubulin was used as a loading control.

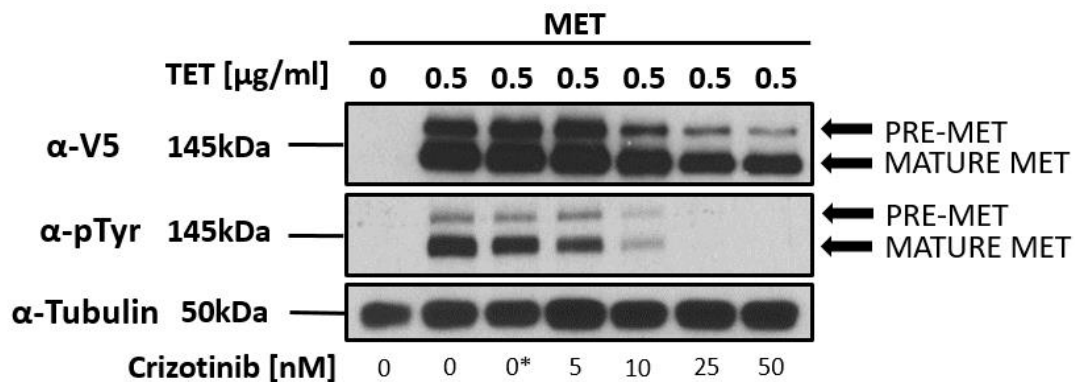


**Figure 17:** The effect of crizotinib on MET expression and phosphorylation in the MET-SIMPL system was analyzed by Western blot using anti-V5 and anti-pTyr antibodies to detect precursor (PRE-MET) and mature MET expression and phosphorylation, respectively. 0\* corresponds to treatment with DMSO. Precursor (PRE-MET) and mature MET are denoted with arrows.  $\alpha$ -tubulin was used as a loading control.

The ability of crizotinib to modulate the interaction of MET with a known phosphorylation-dependent interaction partner SHC1 in the MET-SIMPL system was assessed next. MET-SIMPL cells were seeded and transfected with SHC1. Protein expression was induced by the addition of tetracycline (0.5  $\mu\text{g}/\text{ml}$ ) 24 hours after transfection. Simultaneously, crizotinib in increasing concentrations was administered to cells. DMSO was used as solvent control. Cells were lysed 24 hours after the addition of tetracycline and crizotinib. The lysates were subjected to Western blot analysis using anti-V5 and anti-FLAG antibodies to detect bait and prey expression, respectively, as well as spliced proteins if the interaction occurred (Figure 18). DMSO did not affect MET-SHC1 interaction. MET-SHC1 interaction diminished with increasing crizotinib concentrations, starting with 5 nM. The expression of both MET and SHC1 was reduced upon the treatment of cells with crizotinib at concentration of 10 nM and higher.  $\alpha$ -tubulin was used as a loading control.

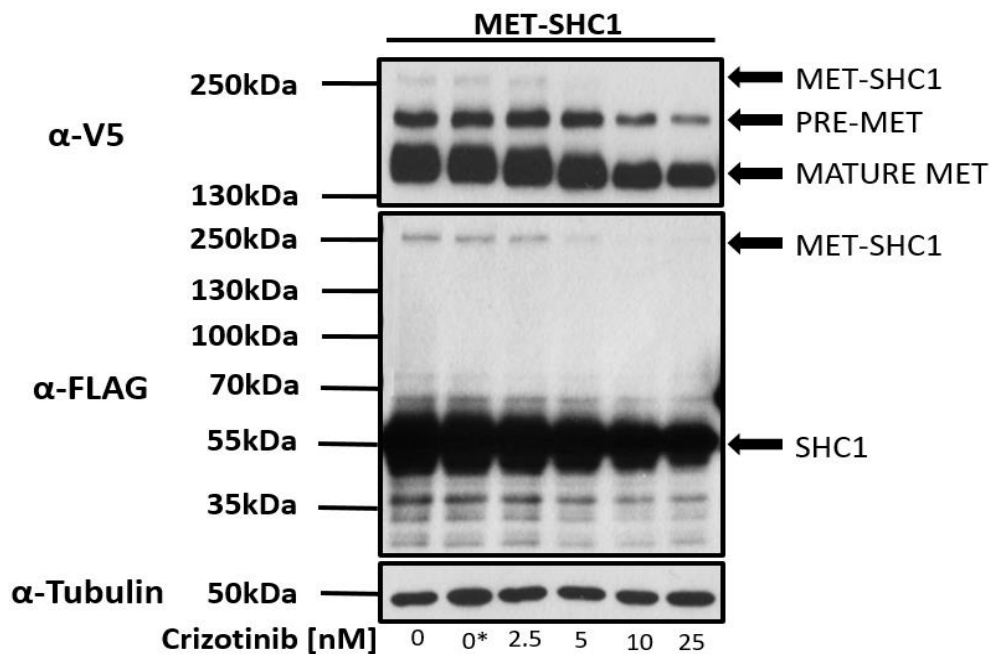


**Figure 18:** Modulation of MET-SHC1 interaction using crizotinib was analyzed by Western blot using anti-V5 and anti-FLAG antibodies to detect bait (PRE-MET and mature MET) and prey (SHC1) expression, respectively, as well as spliced proteins if the interaction occurred. 0\* corresponds to treatment with DMSO. Precursor (PRE-MET), mature MET, SHC1, and MET-SHC1 are denoted with arrows.  $\alpha$ -tubulin was used as a loading control. Sizes of proteins detected by Western blot when performing a SIMPL assay involving MET are summarized in Table S1.

Finally, the ability of crizotinib to modulate MET-BLNK interaction in the MET-SIMPL system was assessed. MET-SIMPL cells were seeded and transfected with BLNK. Protein expression was induced by the addition of tetracycline (0.5 µg/ml) 24 hours after transfection. Simultaneously, crizotinib in the increasing concentrations was administered to cells. DMSO was used as solvent control. Cells were lysed 24 hours after the addition of tetracycline and crizotinib and lysates were subjected to Western blot analysis using anti-V5 and anti-FLAG antibodies to detect bait and prey expression, respectively, as well as spliced proteins if the interaction occurred (Figure 19). DMSO did not affect MET-BLNK interaction. Like SHC1, MET-BLNK interaction diminished with increasing crizotinib concentrations, with complete loss of interaction observed at the concentration of crizotinib of 10 nM.  $\alpha$ -tubulin was used as a loading control.

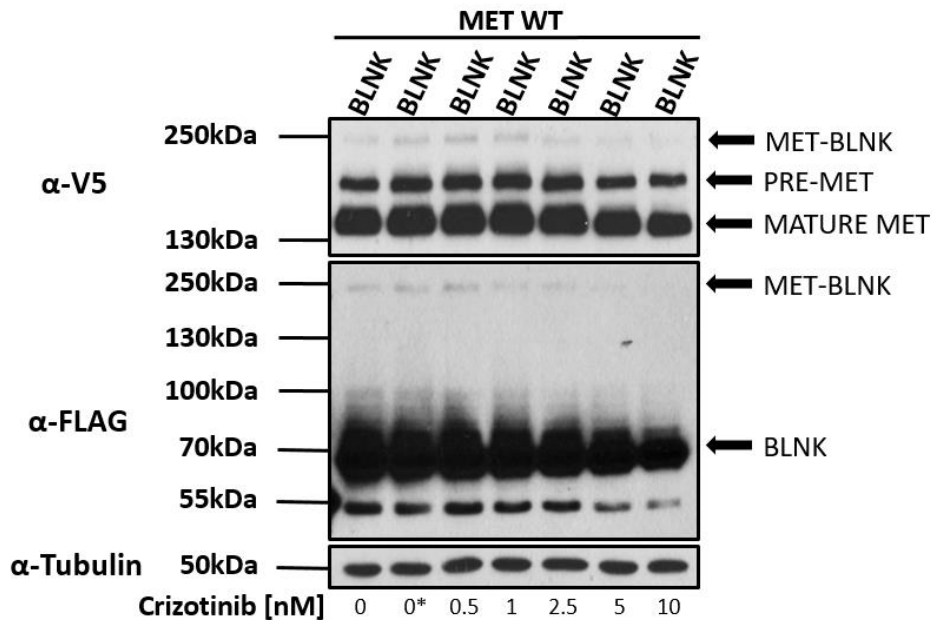


**Figure 19:** Modulation of MET-SHC1 interaction using crizotinib was analyzed by Western blot using anti-V5 and anti-FLAG antibodies to detect bait (PRE-MET and mature MET) and prey (BLNK) expression, respectively, as well as spliced proteins if the interaction occurred. 0\* corresponds to treatment with DMSO. Precursor (PRE-MET), mature MET, BLNK, and MET-BLNK are denoted with arrows.  $\alpha$ -tubulin was used as a loading control. Sizes of proteins detected by Western blot when performing a SIMPL assay involving MET are summarized in Table S1.

#### 4.4. Mapping Residues on MET that Participate in MET-BLNK Interaction

The experiments performed thus far demonstrated the phosphorylation-dependency of MET-BLNK interaction. The next step in the characterization of MET-BLNK interaction was to map the amino acid residues on MET and BLNK responsible for this interaction. The phosphorylation dependency of this interaction indicated that a certain tyrosine once phosphorylated upon MET activation, created a binding site for BLNK on MET.

To determine which tyrosine created a binding site for BLNK on MET, a series of MET phospho-null mutants, namely MET Y1349F, MET Y1356F, MET Y1365F, MET Y1284F, MET Y1003F, and MET Y1356F N1358A were generated by site-directed mutagenesis, using MET entry clone (Figure S2, A) as a template, and verified by Sanger sequencing. Table 28 contains the list of generated mutants of the *MET* gene.

**Table 28:** List of Gateway entry vectors containing mutants of *MET* gene generated by site-directed mutagenesis.

<b><i>MET</i> Mutant</b>	<b>Entry Clone</b>
<i>MET</i> Y1003F	pDONR223-MET Y1003F
<i>MET</i> Y1349F	pDONR223-MET Y1349F
<i>MET</i> Y1356F	pDONR223-MET Y1356F
<i>MET</i> Y1365F	pDONR223-MET Y1365F
<i>MET</i> Y1284F	pDONR223-MET Y1284F
<i>MET</i> Y1356F N1358A	pDONR223-MET Y1356F N1358A
<i>MET</i> N1358A	pDONR223-MET N1358A

The oncogenic variant of MET, MET exon 14 skipping mutant (Frampton et al. 2015; Koch et al. 2020) was also included in the screening as it is a mutant that exhibits the same phenotype as MET Y1003F. MET exon 14 skipping mutant was previously created in Štagljar lab using Gibson Assembly. All *MET* mutant genes were cloned into SIMPL bait destination vector (Figure S1, A) using Gateway Technology. The generated expression clones were verified by Sanger sequencing. Table 29 contains the list of SIMPL expression clones containing mutants of the *MET* gene.

**Table 29:** The list of SIMPL expression clones that contain mutants of the *MET* gene. All mutants of the *MET* gene were cloned into SIMPL Gateway destination vector IN4B.

<b><i>MET</i> Mutant</b>	<b>Expression Clone</b>
<i>MET</i> Exon 14Δ	IN4B-MET Exon 14Δ
<i>MET</i> Y1003F	IN4B-MET Y1003F
<i>MET</i> Y1349F	IN4B-MET Y1349F
<i>MET</i> Y1356F	IN4B-MET Y1356F
<i>MET</i> Y1265F	IN4B-MET Y1365F
<i>MET</i> Y1284F	IN4B-MET Y1284F
<i>MET</i> Y1356F N1358A	IN4B-MET Y1356F N1358A
<i>MET</i> N1358A	IN4B-MET N1358A

To determine whether the introduction of these mutations affected the expression and phosphorylation of MET, the expression and phosphorylation profile of these mutants were compared to the expression and phosphorylation profile of wild-type MET by expressing them in T-REx HEK293 cells. To keep the amount of MET transfected in T-REx HEK293 cells the same as in the SIMPL assay, the constructs were co-transfected alongside the empty SIMPL prey vector in a 1:1 ratio. Protein expression was induced by the addition of tetracycline (1 μg/ml) 24 hours after transfection. Cells were lysed 24 hours after the addition of tetracycline and lysates were subjected to Western blot analysis using anti-V5 and anti-pTyr antibodies to detect MET expression and phosphorylation, respectively (Figure 20). MET Y1349F, MET Y1356F, and MET Y1356F N1358A exhibited expression comparable to wild-type MET, whereas the expression of MET Y1365F, as well as the equivalent mutants, MET Y1003F and MET exon 14 skipping mutant increased. The expression of MET Y1284F decreased. A band shift for both mature and precursor MET for MET exon 14 skipping mutant was observed compared to wild-type MET, indicating the truncation. The phosphorylation profiles of these mutants demonstrated that none of these mutants were kinase-dead as a result of introducing these mutations. α-tubulin was used as a loading control.

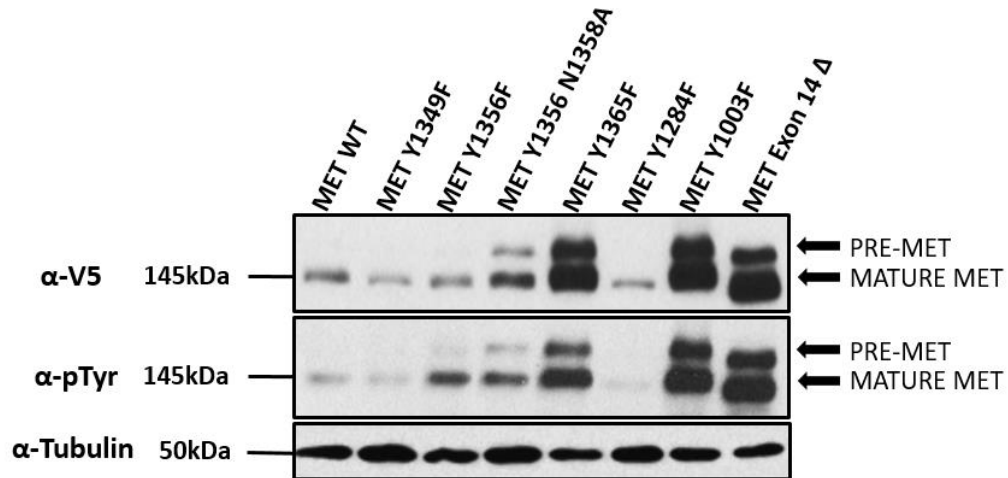


**Figure 20:** Expression and phosphorylation profile of MET mutants was analyzed by Western blot using anti-V5 and anti-pTyr antibodies, respectively. Precursor (PRE-MET) and mature MET are denoted with arrows.  $\alpha$ -tubulin was used as a loading control.

The generated MET mutants were used in screening to determine the tyrosine responsible for the interaction of MET with BLNK. Firstly, MET Y1003F and MET exon 14 skipping mutant were tested for their interaction with BLNK. A transient SIMPL assay was performed. MET-prey combinations were co-transfected into T-REx HEK293 cells. PEX7 was used as a negative control, whereas SHC1 and GRB2 were used as positive controls. Protein expression was induced by the addition of tetracycline (1  $\mu$ g/ml) 24 hours after transfection. Cells were lysed 24 hours after the addition of tetracycline and lysates were subjected to Western blot analysis using anti-V5 and anti-FLAG antibodies to detect bait and prey expression, respectively, as well as spliced proteins if the interaction occurred (Figure 21). No interaction was observed upon co-expressing PEX7 with any MET variant. Spliced proteins of the appropriate sizes (Table S1) were observed upon co-expression of all MET variants with SHC1 and GRB2, as well as BLNK. The interaction between SHC1, GRB2, and BLNK with MET Y1003F and MET exon 14 skipping mutant was increased, as compared to wild-type MET.  $\alpha$ -tubulin was used as a loading control.



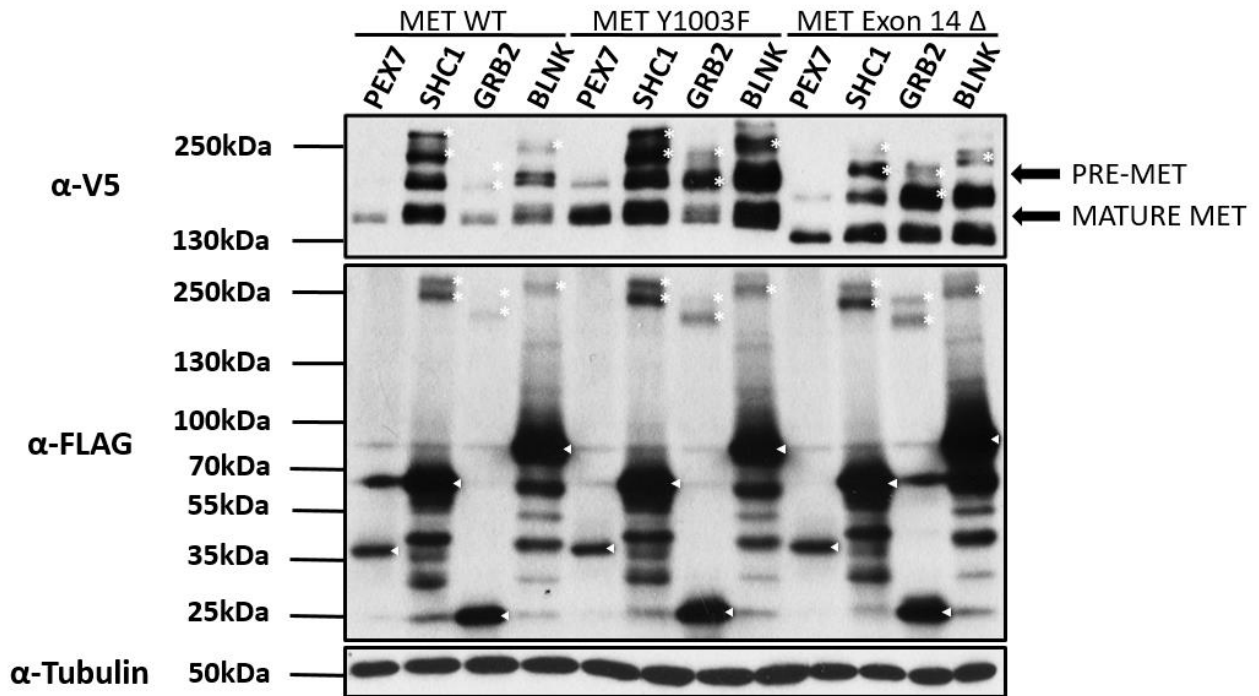


**Figure 21:** The ability of MET Y1003F and MET exon 14 skipping mutant to interact with PEX7, SHC1, GRB2, and BLNK, as compared to wild-type MET, was assessed by Western blot analysis using anti-V5 and anti-FLAG antibodies to detect bait and prey expression, respectively, as well as spliced proteins if the interaction occurred. Precursor MET (PRE-MET) and mature MET are denoted with arrows.  $\alpha$ -tubulin was used as a loading control. Parental prey proteins are highlighted by triangles, while spliced proteins are highlighted by asterisks. Note that the spliced band of MET-GRB2 is the same size as pre-MET. Sizes of proteins detected by Western blot when performing a SIMPL assay involving MET are summarized in Table S1.

MET Y1349F and MET Y1356F were tested next for their interaction with BLNK. The transient SIMPL assay was performed. MET-prey combinations were co-transfected into T-REx HEK293 cells. PEX7 was used as a negative control, whereas SHC1 and GRB2 were used as positive controls. Protein expression was induced by the addition of tetracycline (1  $\mu$ g/ml) 24 hours after transfection. Cells were lysed 24 hours after the addition of tetracycline and lysates were subjected to Western blot analysis using anti-V5 and anti-FLAG antibodies to detect bait and prey expression, respectively, as well as spliced proteins if the interaction occurred (Figure 22). No interaction was observed upon co-expressing PEX7 with any MET variant. Spliced proteins of the appropriate sizes (Table S1) were observed upon co-expressing MET variants with SHC1 and

GRB2, as well as BLNK. Interaction of MET Y1349F and SHC1 was increased as compared to wild-type MET. Interaction of MET Y1349F and Y1356F with BLNK was reduced, as compared to wild-type MET. MET Y1356F reduced the interaction with BLNK more than MET Y1349F.  $\alpha$ -tubulin was used as a loading control.

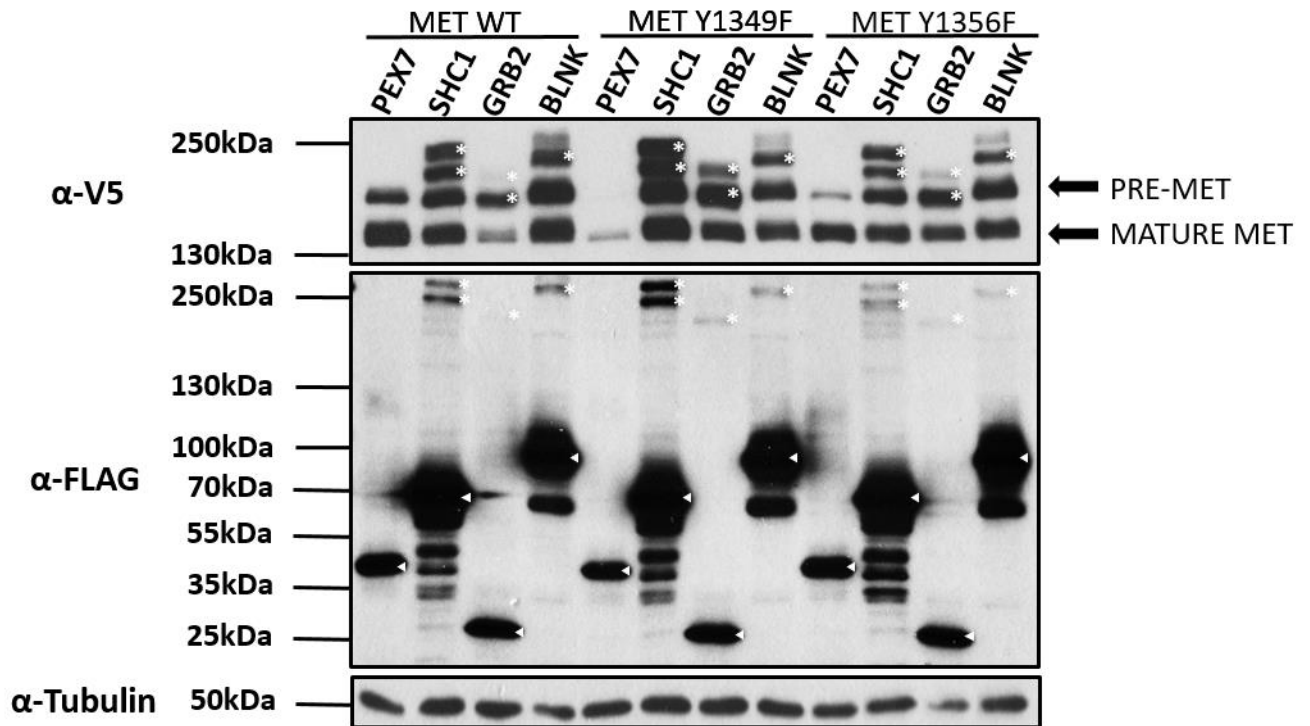


**Figure 22:** The ability of MET Y1349F and MET Y1356F to interact with PEX7, SHC1, GRB2, and BLNK, as compared to wild-type MET was assessed by Western blot analysis using anti-V5 and anti-FLAG antibodies to detect bait and prey expression, respectively, as well as spliced proteins if the interaction occurred. Precursor MET (PRE-MET) and mature MET are denoted with arrows.  $\alpha$ -tubulin was used as a loading control. Parental prey proteins are highlighted by triangles, while spliced proteins are highlighted by asterisks. Note that the spliced band of MET-GRB2 is the same size as pre-MET. Sizes of proteins detected by Western blot when performing a SIMPL assay involving MET are summarized in Table S1.

Next, MET Y1365F and MET Y1284F were tested for their ability to interact with BLNK. The transient SIMPL assay was performed. MET-prey combinations were co-transfected into T-REx HEK293 cells. PEX7 was used as a negative control, whereas SHC1 and GRB2 were used as positive controls. Protein expression was induced by the addition of tetracycline (1  $\mu\text{g}/\text{ml}$ ) 24 hours after transfection. Cells were lysed 24 hours after the addition of tetracycline and lysates were subjected to Western blot analysis using anti-V5 and anti-FLAG antibodies to detect bait and prey expression, respectively, as well as spliced proteins if the interaction occurred (Figure 23). No interaction was observed upon co-expressing PEX7 and any MET variant. Spliced proteins of the appropriate sizes (Table S1) were observed upon co-expression of all MET variants with SHC1 and GRB2, as well as BLNK. No reduction of the interaction of MET Y1365F with SHC1, GRB2, and BLNK was observed compared to wild-type MET, whereas reduced interaction between MET Y1284F with SHC1, GRB2, and BLNK was observed, although MET Y1284F demonstrated reduced expression, as compared to wild-type MET.  $\alpha$ -tubulin was used as a loading control.

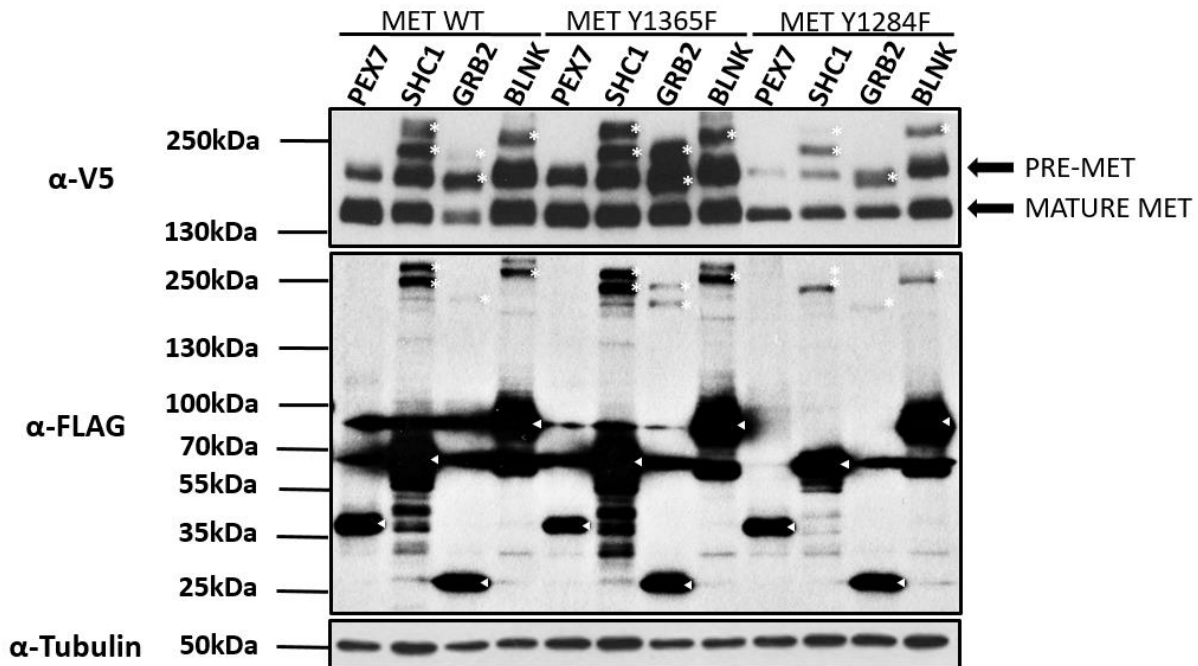


**Figure 23:** The ability of MET Y1365F and MET Y1284F to interact with PEX7, SHC1, GRB2, and BLNK, as compared to wild-type MET, was assessed by Western blot analysis using anti-V5 and anti-FLAG antibodies to detect bait and prey expression, respectively, as well as spliced proteins if the interaction occurred. Precursor MET (PRE-MET) and mature MET are denoted with arrows.  $\alpha$ -tubulin was used as a loading

control. Parental prey proteins are highlighted by triangles, while spliced proteins are highlighted by asterisks. Note that the spliced band of MET-GRB2 is the same size as pre-MET. Sizes of proteins detected by Western blot when performing a SIMPL assay involving MET are summarized in Table S1.

To assess the role of canonical GRB2-binding site on MET, Y<sup>1356</sup>VNV (Ponzetto et al. 1996) as the binding site for BLNK on MET, the interaction of BLNK with wild-type MET, MET Y1356F, and MET Y1356F N1358A was compared by performing the transient SIMPL assay. PEX7 was used as a negative control, whereas SHC1 was used as a positive control. MET-prey combinations were co-transfected into T-REx HEK293 cells. Protein expression was induced by the addition of tetracycline (1 µg/ml) 24 hours after the transfection. Cells were lysed 24 hours after the addition of tetracycline and lysates were subjected to Western blot analysis using anti-V5 and anti-FLAG antibodies to detect bait and prey expression, respectively, as well as spliced proteins if the interaction occurred (Figure 24). No interaction was observed when co-expressing PEX7 and any MET variant. Spliced signals of the appropriate sizes (Table S1) were observed upon co-expressing all MET variants with SHC1, GRB2, and BLNK. Neither MET mutant affected the interaction with SHC1, as compared to wild-type MET. Both MET Y1356F and MET Y1356F N1358A demonstrated reduced interaction with BLNK and GRB2, as compared to wild-type MET. No additive effect between MET Y1356F and MET Y1356F N1358A in the interaction with GRB2 and BLNK was observed.  $\alpha$ -tubulin was used as a loading control.

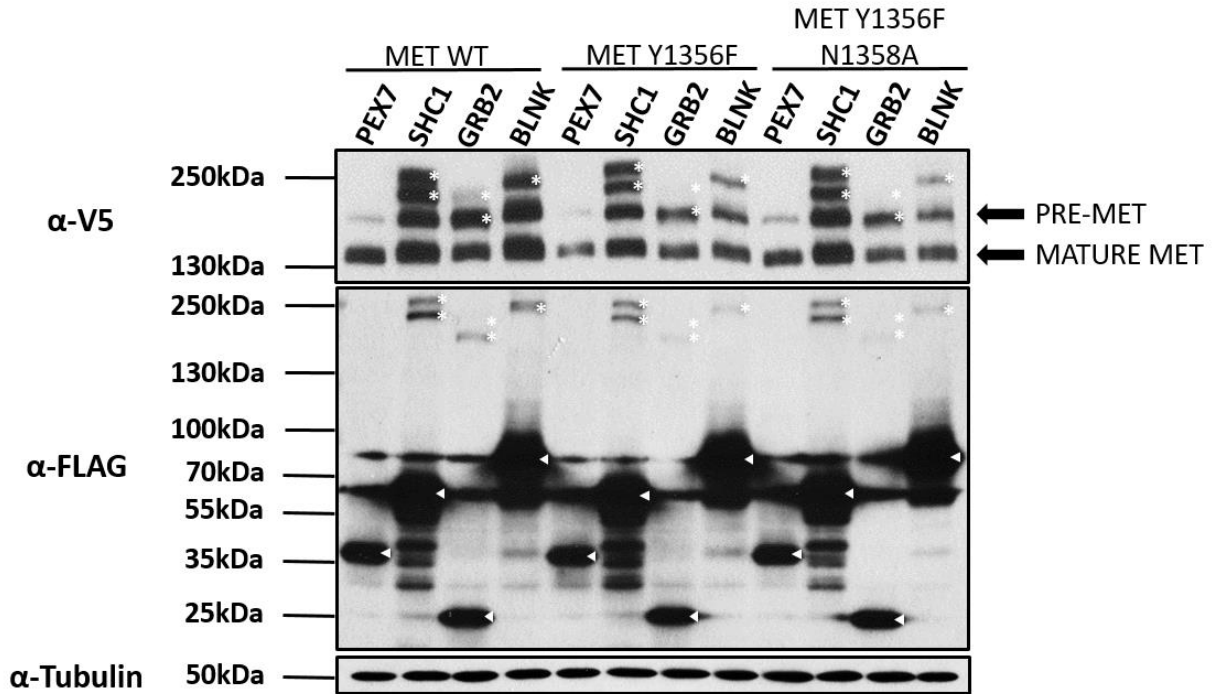


**Figure 24:** The ability of MET Y1356F and MET Y1356F N1358A to interact with PEX7, SHC1, GRB2, and BLNK, as compared to wild-type MET, was assessed by Western blot analysis using anti-V5 and anti-FLAG antibodies to detect bait and prey expression, respectively, as well as spliced proteins if the interaction occurred. Precursor MET (PRE-MET) and mature MET are denoted with arrows.  $\alpha$ -tubulin was used as a loading control. Parental prey proteins are highlighted by triangles, while spliced proteins are highlighted by asterisks. Note that the spliced band of MET-GRB2 is the same size as pre-MET. Sizes of proteins detected by Western blot when performing a SIMPL assay involving MET are summarized in Table S1.

To assess the effect of an asparagine residue in the GRB2-binding site on MET, Y<sup>1356</sup>VNV (Ponzetto et al. 1996), the interaction of MET N1358A with PEX7, GRB2, and BLNK was compared to wild-type MET, MET Y1356F, and MET Y1356F N1358A using the transient SIMPL assay. Bait-prey combinations were co-transfected in T-REx HEK293 cells. Protein expression was induced by the addition of tetracycline (1 µg/ml) 24 hours after the transfection. Cells were lysed 24 hours after the addition of tetracycline and lysates were subjected to Western blot analysis using anti-V5 and anti-FLAG antibodies to detect bait and prey expression, respectively, as well as spliced proteins if the interaction occurred (Figure 25). No interaction was observed when co-expressing PEX7 with any MET variant. MET Y1356F and MET Y1356F N1358A demonstrated reduced interaction with BLNK and GRB2, as compared to wild-type MET. The interaction of GRB2 and BLNK with MET N1358A was unaffected, as compared to wild-type MET. α-tubulin was used as a loading control.

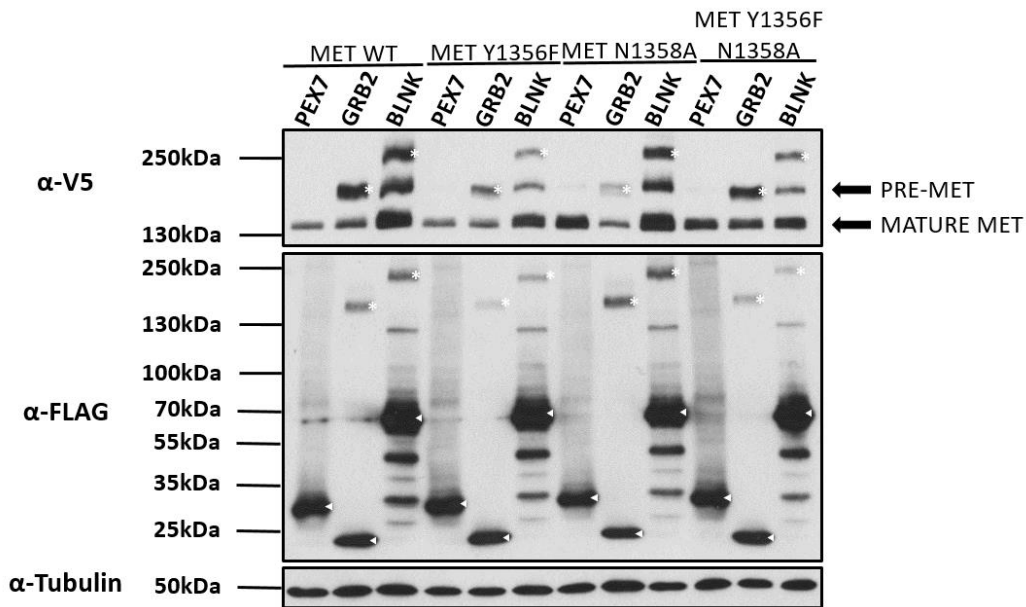


**Figure 25:** The ability of MET Y1356F, MET N1358A and MET Y1356F N1358A to interact with PEX7, GRB2, and BLNK, compared to wild-type MET, was assessed by Western blot analysis using anti-V5 and anti-FLAG antibodies to detect bait and prey expression, respectively, as well as spliced proteins if the interaction occurred. Precursor MET (PRE-MET) and mature MET are denoted with arrows. α-tubulin was used as a loading control. Parental prey proteins are highlighted by triangles, while spliced proteins are highlighted by asterisks. Note that the spliced band of MET-GRB2 is the same size as pre-MET. Sizes of proteins detected by Western blot when performing a SIMPL assay involving MET are summarized in Table S1.

Collectively, these results indicated that tyrosine residues Y1356 and to a lesser extent Y1349 were responsible for creating a binding site for BLNK on MET. To investigate the potential additive effects of mutating more than one tyrosine on MET on the interaction with BLNK, a series of combinatorial MET tyrosine mutants, lacking different combinations of the most C-terminal tyrosine residues, were generated by site-directed mutagenesis, as described above (Page 35). The following MET mutants were generated: MET Y1349F Y1356F, MET Y1349F Y1365F, MET Y1356F Y1365F, and MET Y1349F Y1356F Y1365F. Table 30 summarizes MET double/triple mutants. The generated mutants of the *MET* gene were cloned into SIMPL bait destination vector (Figure S1, A) using Gateway Technology. The generated SIMPL expression clones were verified by Sanger sequencing and are summarized in Table 31.

**Table 30:** List of Gateway entry clones containing *MET* gene with double or triple C-terminal tyrosine residues mutations, generated by site-directed mutagenesis.

<b><i>MET</i> Mutant</b>	<b>Entry Clone</b>
<i>MET</i> Y1349F Y1356F	pDONR223-MET Y1349F Y1356F
<i>MET</i> Y1349F Y1365F	pDONR223-MET Y1349F Y1365F
<i>MET</i> Y1356F Y1365F	pDONR223-MET Y1356F Y1365F
<i>MET</i> Y1349F Y1356F Y1365F	pDONR223-MET Y1349F Y1356F Y1365F

**Table 31:** List of SIMPL expression clones containing *MET* gene with double or triple C-terminal tyrosine residues mutations. All of them were cloned into SIMPL bait destination vector IN4B.

<b><i>MET</i> Mutant</b>	<b>Expression Clone</b>
<i>MET</i> Y1349F Y1356F	IN4B-MET Y1349F Y1356F
<i>MET</i> Y1349F Y1365F	IN4B-MET Y1349F Y1365F
<i>MET</i> Y1356F Y1365F	IN4B-MET Y1356F Y1365F
<i>MET</i> Y1349F Y1356F Y1365F	IN4B-MET Y1349F Y1356F Y1365F

To determine whether the introduction of these mutations affected the expression and phosphorylation of MET, their expression and phosphorylation profiles were compared to wild-type MET by expressing them in T-REx HEK293 cells. To keep the amount of MET transfected in T-REx HEK293 cells the same as in the SIMPL assay, the constructs were co-transfected alongside the empty SIMPL prey vector in a 1:1 ratio. Protein expression was induced by the addition of tetracycline (1 µg/ml) 24 hours after transfection. Cells were lysed 24 hours after the addition of

tetracycline and lysates were subjected to Western blot analysis using anti-V5 and anti-pTyr antibodies to detect MET expression and phosphorylation, respectively (Figure 26). Compared to wild-type MET, MET Y1349F Y1356F and MET Y1356F Y1365F exhibited reduced expression, whereas MET Y1349F Y1365F and MET Y1349F Y1356F Y1365F expression were comparable to wild-type MET. Despite the removal of some phosphorylation sites, none of these MET mutants were completely inactivated, as indicated by their phosphorylation profiles.  $\alpha$ -tubulin was used as a loading control.

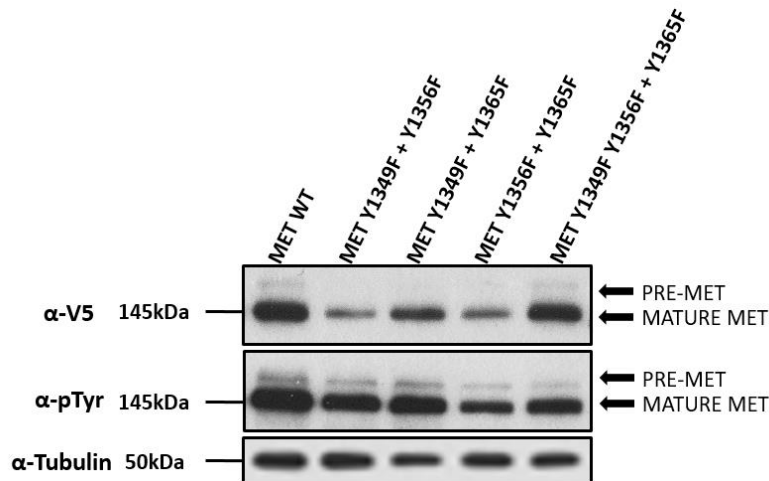


**Figure 26:** Expression and phosphorylation profiles of MET double or triple tyrosine mutants were compared to wild-type MET by Western blot analysis using anti-V5 and anti-pTyr antibodies to detect MET expression and phosphorylation, respectively. The precursor MET (PRE-MET) and mature MET are denoted with arrows.  $\alpha$ -tubulin was used as a loading control.

To assess the effect of removing multiple tyrosine residues of MET on its interaction with BLNK, the SIMPL assay was performed. MET-prey combinations were co-transfected into T-REx HEK293 cells. PEX7 was used as a negative control, whereas SHC1 and GRB2 were used as positive controls. Protein expression was induced by the addition of tetracycline (1  $\mu$ g/ml) 24 hours after transfection. Cells were lysed 24 hours after the addition of tetracycline and lysates were subjected to Western blot analysis using anti-V5 and anti-FLAG antibodies to detect bait and prey expression, respectively, as well as spliced proteins if the interaction occurred (Figure 28). No interaction was observed when co-expressing PEX7 and any MET variant. Compared to wild-type MET, the interaction of BLNK with MET Y1349F Y1356F was reduced, while the interaction of



BLNK with MET Y1349F Y1365F was unaffected (Figure 27, A). The interaction of SHC1 and GRB2 with MET Y1349F Y1365F was also reduced, compared to wild-type MET and MET Y1349F Y1365F. The interaction of BLNK with MET Y1356F Y1365F and MET Y1349F Y1365F Y1365F was reduced, as compared to wild-type MET (Figure 27, B).  $\alpha$ -tubulin was used as a loading control.

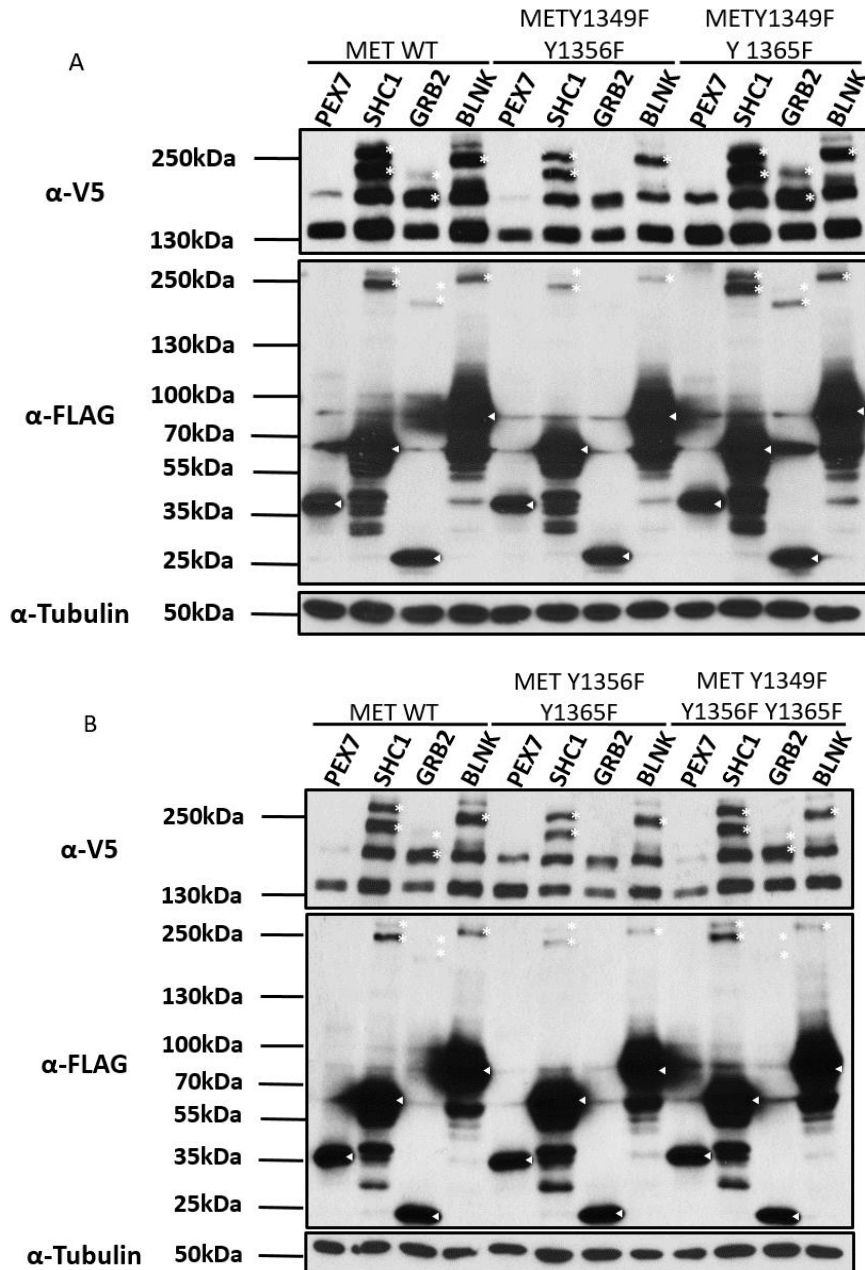


**Figure 27:** The ability of MET mutants MET Y1349F Y1356F and MET Y1349F Y1365F (**A**), and MET Y1356F Y1365F and MET Y1349F Y1356F Y1365F (**B**) to interact with PEX7, SHC1, GRB2, and BLNK was assessed by Western blot analysis using anti-V5 and anti-FLAG antibodies to detect bait and prey expression,

respectively, as well as spliced proteins if the interaction occurred. Precursor MET (PRE-MET) and mature MET are denoted with arrows.  $\alpha$ -tubulin was used as a loading control. Parental prey proteins are highlighted by triangles, while spliced proteins are highlighted by asterisks. Note that the spliced band of MET-GRB2 is the same size as pre-MET. Sizes of proteins detected by Western blot when performing a SIMPL assay involving MET are summarized in Table S1.

#### **4.5. MET Mutants Localize to Cell Surface**

To determine whether the observed reduced interaction of MET mutants with BLNK was not the result of mislocalization of MET due to the introduction of tyrosine mutations, a series of surface biotinylations was performed. Wild-type MET and each of the MET mutants (MET Y1349F, MET Y1356F, and MET Y1356F N1358A) were transfected in T-REx HEK293 cells. Protein expression was induced by the addition of tetracycline (1  $\mu$ g/ml) 24 hours after transfection. Cells were subjected to surface biotinylation 24 hours after the addition of tetracycline. Three different conditions were analyzed: mock (no transfection) with biotin, tetracycline with biotin, and tetracycline with no biotin. The fractions representing input, supernatant (i.e. intracellular proteins), and pull-down (i.e. the surface proteins) were subjected to Western blot analysis using an anti-V5 antibody (Figure 28). Expression of both precursor and mature MET was observed in the input for all MET variants only in the transfected cells. Both precursor and mature MET were observed in the intracellular fraction for all MET variants, regardless of the presence of biotin. The mature form of MET was detected in the pull-down for all MET variants in the presence of biotin. Precursor MET was detected in the pull-down sampled at a markedly lower level than in the supernatant fraction, as well as compared to mature MET. The amount of MET mutants in the pull-down fractions was comparable to wild-type MET.  $\alpha$ -tubulin was used as a loading control. No  $\alpha$ -tubulin was observed in the pull-down.

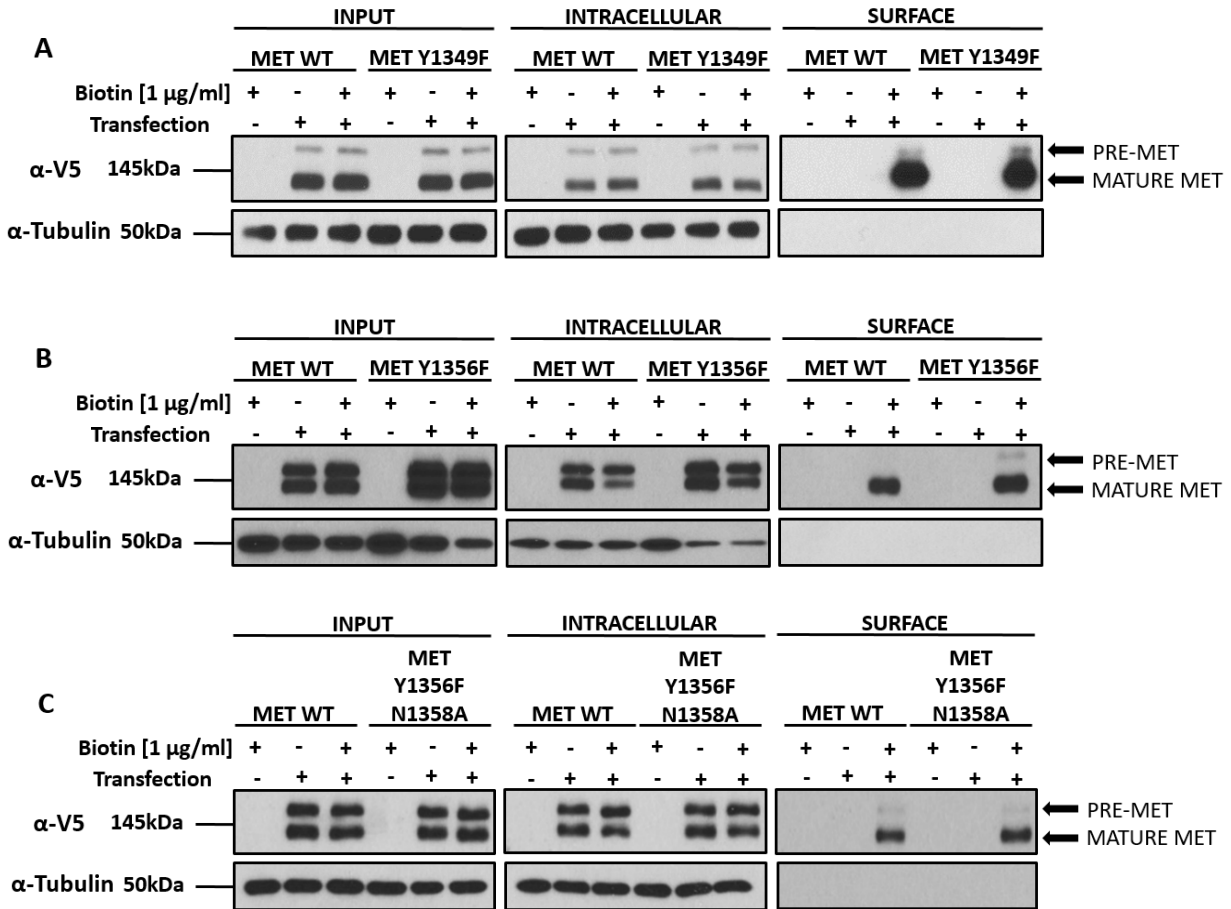


**Figure 28:** The comparison of surface levels of MET mutants MET Y1349F (A), MET Y1356F (B), and MET Y1356F N1358A (C) to wild-type MET was investigated by a combination of surface biotinylation and Western blot analysis using an anti-V5 antibody to detect MET expression. The supernatant represents the intracellular fraction of proteins, whereas the pull-down represents the surface fraction of the proteins. Only the mature MET was detected in the pull-down for all MET variants in the presence of biotin. The amount of MET mutants in the pull-down fractions was comparable to wild-type MET.  $\alpha$ -tubulin was used as a loading control. No  $\alpha$ -tubulin was observed in the pull-down.

#### 4.6. Mapping Residues on BLNK that Participate in MET-BLNK Interaction

To determine the amino acid residues on BLNK responsible for its binding to MET, three series of BLNK mutants were used: BLNK tyrosine mutants, BLNK proline mutants, and BLNK leucine and SH2 domain mutants. The entry clones containing those mutants are summarized in Table 9. Mutants of the *BLNK* gene were cloned into SIMPL prey destination vector (Figure S1, B) using Gateway Technology. The generated SIMPL expression clones were verified by Sanger sequencing and are summarized in Table 32.

**Table 32:** List of generated SIMPL expression clones containing mutants of *BLNK* gene. All of them were cloned into SIMPL prey destination vector IC2.

<b><i>BLNK</i> Mutant</b>	<b>Expression Clone</b>
<i>BLNK</i> Y72F	IC2-BLNK Y72F
<i>BLNK</i> Y84F	IC2-BLNK Y84F
<i>BLNK</i> Y96F	IC2-BLNK Y96F
<i>BLNK</i> Y84F Y96F	IC2-BLNK Y84F Y96F
<i>BLNK</i> Y72F Y84F Y96F	IC2-BLNK Y72F Y84F Y96F
<i>BLNK</i> Y178F	IC2-BLNK Y178F
<i>BLNK</i> Y189F	IC2-BLNK Y189F
<i>BLNK</i> P204A	IC2-BLNK P204A
<i>BLNK</i> P212A	IC2-BLNK P212A
<i>BLNK</i> P204A P212A	IC2-BLNK P204A P212A
<i>BLNK</i> P204A P212A Y72F	IC2-BLNK P204A P212A Y72F
<i>BLNK</i> L18E	IC2-BLNK L18E
<i>BLNK</i> I25E	IC2-BLNK I25E
<i>BLNK</i> SH2Δ	IC2-BLNK SH2Δ
<i>BLNK</i> SH2Δ L18E	IC2-BLNK SH2Δ L18E
<i>BLNK</i> SH2Δ Y72F	IC2-BLNK SH2Δ Y72F
<i>BLNK</i> SH2Δ L18E Y72F	IC2-BLNK SH2Δ L18E Y72F
<i>BLNK</i> R372A	IC2-BLNK R372A
<i>BLNK</i> R372A L18E	IC2-BLNK R372A L18E
<i>BLNK</i> R372A I25E	IC2-BLNK R372A I25E

Firstly, the ability of BLNK tyrosine mutants to bind to MET was assessed (Koretzky et al. 2006). The following BLNK tyrosine mutants were used: BLNK Y72F, BLNK Y84F, BLNK Y96F, BLNK Y84F Y96F, BLNK Y72F Y84F Y96F, BLNK Y178F, and BLNK Y189F (Figure 29, A). The tyrosine residues were mutated to phenylalanine residues to disable phosphorylation at those residues but keep the conformation of BLNK as intact as possible. To determine whether the introduction of these mutations affected BLNK expression, the expression profile of these BLNK mutants was compared to wild-type BLNK in T-REx HEK293 cells. To keep the amount of transfected BLNK the same as in the SIMPL assay, the constructs were co-transfected into T-REx HEK293 cells with the empty SIMPL bait vector in a 1:1 ratio. Protein expression was induced by the addition of tetracycline (1  $\mu\text{g/ml}$ ) 24 hours after transfection. Cells were lysed 24 hours after the addition of tetracycline and lysates were subjected to Western blot analysis using an anti-FLAG antibody to detect BLNK expression (Figure 29, B). All BLNK mutants demonstrated expression comparable to wild-type BLNK, except BLNK Y72F Y84F Y96F, whose expression was not detected.  $\alpha$ -tubulin was used as a loading control.

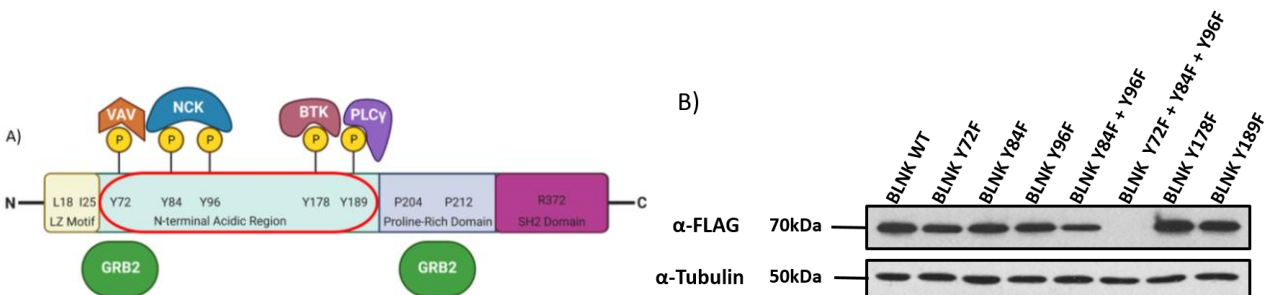


**Figure 29: (A)** Schematic representation of BLNK, showing the locations of mutated tyrosine residues and partners of BLNK that interact via those residues. Created in BioRender.com<sup>15</sup>. **(B)** Expression of BLNK tyrosine mutants was analyzed by Western blot using an anti-FLAG antibody.  $\alpha$ -tubulin was used as a loading control.

The ability of BLNK tyrosine mutants to interact with MET, as compared to wild-type BLNK was assessed by performing the transient SIMPL assay. MET-BLNK combinations were co-transfected in T-REx HEK293 cells. PEX7 was used as a negative control, whereas SHC1 and GRB2 were used as positive controls. Protein expression was induced by the addition of tetracycline (1  $\mu\text{g/ml}$ ) 24 hours after transfection. Cells were lysed 24 hours after the addition of tetracycline, and lysates

were subjected to Western blot analysis using anti-V5 and anti-FLAG antibodies to detect bait and prey expression, respectively, as well as spliced proteins if the interaction occurred (Figure 30). No interaction between MET and PEX7 was detected. Spliced proteins of the appropriate sizes (Table S1) were observed upon co-expressing MET with SHC1, GRB2, and BLNK. Interaction between MET and BLNK Y72F, BLNK Y84F, BLNK Y84F Y96F was reduced, as compared to wild-type BLNK. BLNK Y72F reduced the interaction with MET more than BLNK Y84F and BLNK Y84F Y96F. Interaction between MET and BLNK Y96F was increased, while BLNK Y178F and BLNK Y189F remained unaffected in their interaction with MET, as compared to wild-type BLNK.  $\alpha$ -tubulin was used as a loading control.

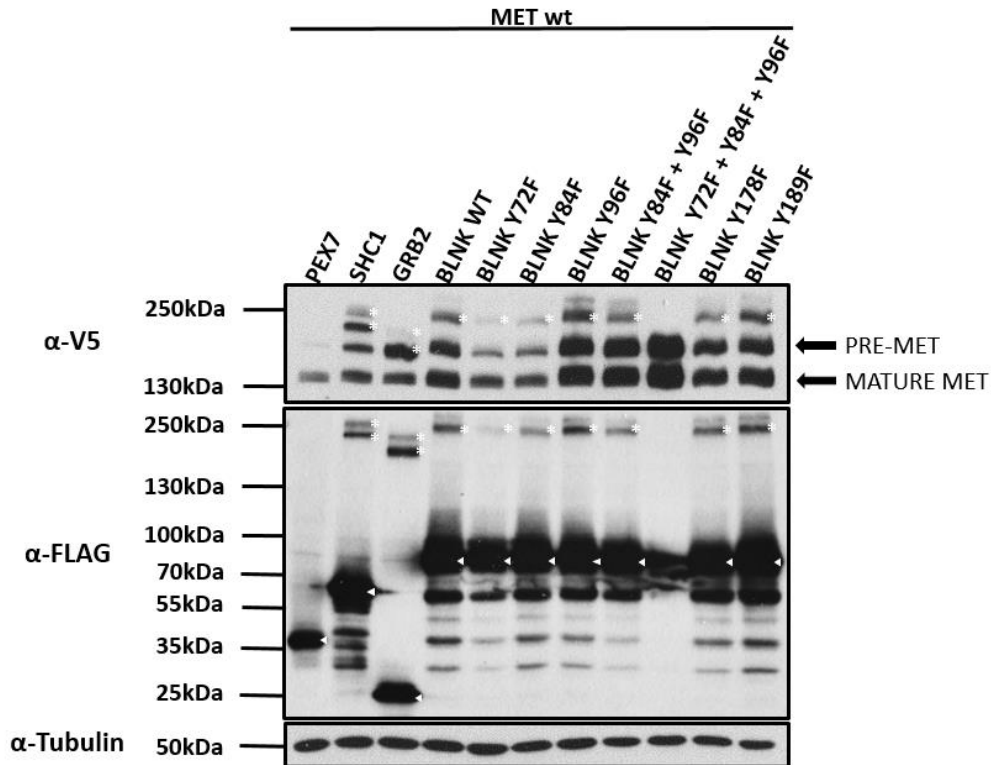


**Figure 30:** The ability of BLNK tyrosine mutants to interact with MET was analyzed by Western blot using anti-V5 and anti-FLAG antibodies to detect bait and prey expression, respectively, as well as spliced proteins if the interaction occurred. Precursor MET (PRE-MET) and mature MET are denoted with arrows.  $\alpha$ -tubulin was used as a loading control. Parental prey proteins are highlighted by triangles, while spliced proteins are highlighted by asterisks. Note that the spliced band of MET-GRB2 is the same size as pre-MET. Sizes of proteins detected by Western blot when performing a SIMPL assay involving MET are summarized in Table S1.

Secondly, the ability of BLNK proline mutants to interact with MET, as compared to wild-type BLNK was assessed. The following BLNK proline mutants were used: BLNK P204A, BLNK P212A, BLNK P204A P212A, and BLNK P204A P212A Y72F (Figure 31, A). The aforementioned proline residues were mutated as they represent a suspected binding site for GRB2 on BLNK (Arya et al. 2017). The suspected SH3 domain binding sites in the proline-rich region of BLNK could indicate a mediator in MET-BLNK interaction. To determine whether the introduction of these mutations affected BLNK expression, the expression profile of these BLNK mutants was compared to wild-type BLNK in T-REx HEK293 cells. To keep the amount of transfected BLNK the same as in the SIMPL assay, the constructs were co-transfected into T-REx HEK293 cells with the empty SIMPL bait vector in a 1:1 ratio. Protein expression was induced by the addition of tetracycline (1 µg/ml) 24 hours after transfection. Cells were lysed 24 hours after the addition of tetracycline and lysates were subjected to Western blot analysis using an anti-FLAG antibody to detect BLNK expression (Figure 31, B). BLNK P212A demonstrated expression comparable to wild-type BLNK. All other BLNK proline mutants demonstrated decreased expression, as compared to wild-type BLNK.  $\alpha$ -tubulin was used as a loading control.

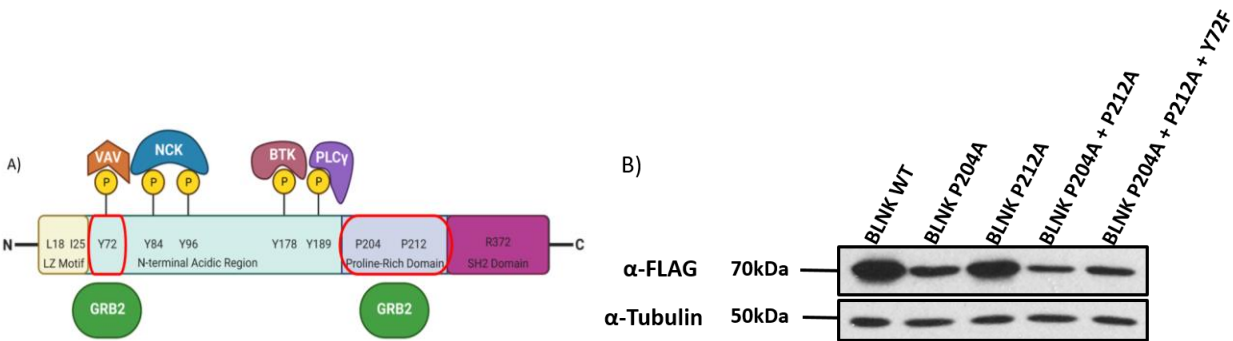


**Figure 31: (A)** Schematic representation of BLNK protein, showing the locations of suspected GRB2-binding sites. Created in Biorender.com. **(B)** Expression of BLNK proline mutants was analyzed by Western blot using an anti-FLAG antibody.  $\alpha$ -tubulin was used as a loading control.

The ability of BLNK proline mutants to interact with MET, as compared to wild-type BLNK was assessed by performing the transient SIMPL assay. MET-BLNK combinations were co-transfected in T-REx HEK293 cells. PEX7 was used as a negative control, whereas SHC1 and GRB2 were used as positive controls. Protein expression was induced by the addition of tetracycline (1 µg/ml) 24 hours after transfection. Cells were lysed 24 hours after the addition of tetracycline, and lysates

were subjected to Western blot analysis using anti-V5 and anti-FLAG antibodies to detect bait and prey expression, respectively, as well as spliced proteins if the interaction occurred (Figure 32). No interaction between MET and PEX7 was detected. Spliced proteins of the appropriate sizes (Table S1) were observed upon co-expressing MET with SHC1, GRB2, and BLNK. The interaction of these BLNK mutants with MET was unaffected, as compared to wild-type BLNK. Expression of BLNK P204A, BLNK P204A P212A, and BLNK P204A P212A Y72F was decreased, as compared to wild-type BLNK and BLNK P212A. MET expression was increased when co-expressed with BLNK mutants containing the mutation of proline P204.  $\alpha$ -tubulin was used as a loading control.

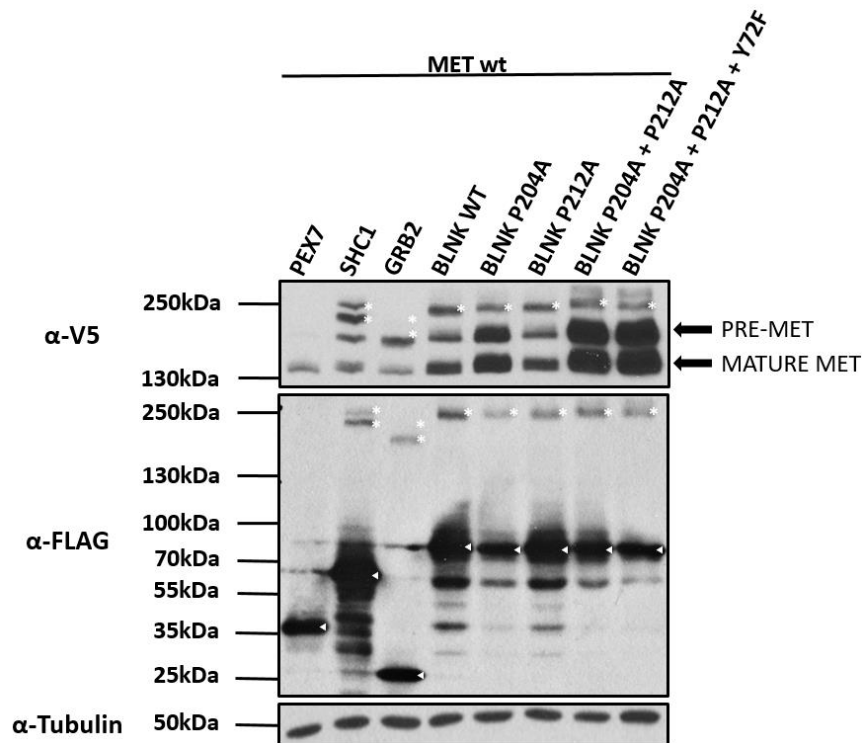


**Figure 32:** The ability of BLNK proline mutants to interact with MET was analyzed by Western blot using anti-V5 and anti-FLAG antibodies to detect bait and prey expression, respectively, as well as spliced proteins if the interaction occurred. Precursor MET (PRE-MET) and mature MET are denoted with arrows.  $\alpha$ -tubulin was used as a loading control. Parental prey proteins are highlighted by triangles, while spliced proteins are highlighted by asterisks. Note that the spliced band of MET-GRB2 is the same size as pre-MET. Sizes of proteins detected by Western blot when performing a SIMPL assay involving MET are summarized in Table S1.



Thirdly, the ability of BLNK leucine-zipper and SH2 domain mutants to interact with MET, as compared to wild-type BLNK was assessed. The following BLNK leucine-zipper and SH2 domain mutants were used: BLNK L18E, BLNK I25E, BLNK SH2Δ, BLNK SH2Δ L18E, BLNK R372A, BLNK R372A L18E, and BLNK R372A I25E (Figure 33, A). The leucine and isoleucine residues were mutated to glutamate according to Kohler et al. (2005). The SH2 domain of BLNK was deleted as the SH2 domain is known to participate in the phosphorylation-dependent interactions (Wagner et al. 2013). The arginine R372 was mutated as it is located in the canonical FLVR motif in the SH2 domain of BLNK, F<sup>369</sup>LVR (Wagner et al. 2013). To determine whether the introduction of these mutations affected BLNK expression, the expression profile of these BLNK mutants was compared to wild-type BLNK in T-REx HEK293 cells. To keep the amount of transfected BLNK the same as in the SIMPL assay, the constructs were co-transfected into T-REx HEK293 cells with the empty SIMPL bait vector in a 1:1 ratio. Protein expression was induced by the addition of tetracycline (1 μg/ml) 24 hours after transfection. Cells were lysed 24 hours after the addition of tetracycline and lysates were subjected to Western blot analysis using an anti-FLAG antibody to detect BLNK expression (Figure 33, B). Compared to wild-type BLNK, expression of BLNK SH2Δ and BLNK SH2Δ L18E was decreased, whereas expression of all other BLNK mutants was unaffected. A size shift of the bands representing BLNK SH2Δ and BLNK SH2Δ L18E was observed compared to wild-type BLNK, indicating the deletions. α-tubulin was used as a loading control.

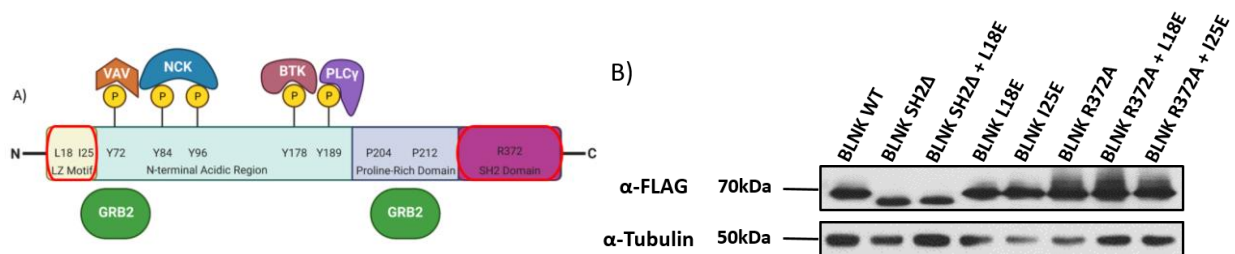


**Figure 33: (A)** Schematic representation of BLNK, showing the locations of mutated leucine residues and SH2 domain. Created in BioRender.com. **(B)** Expression of BLNK leucine and SH2 domain mutants was analyzed by Western blot using an anti-FLAG antibody to detect BLNK expression. α-tubulin was used as a loading control.

The ability of BLNK leucine and SH2 domain mutants to interact with MET was assessed by performing the transient SIMPL assay. MET-BLNK combinations were co-expressed in T-REx HEK293 cells. PEX7 was used as a negative control, whereas SHC1 and GRB2 were used as positive controls. Protein expression was induced by the addition of tetracycline (1 µg/ml) 24 hours after transfection. Cells were lysed 24 hours after the addition of tetracycline and lysates were subjected to Western blot analysis using anti-V5 and anti-FLAG antibodies to detect bait and prey expression, respectively, as well as spliced proteins if the interaction occurred (Figure 34). No interaction between MET and PEX7 was detected, whereas spliced proteins of the appropriate sizes (Table S1) were detected upon co-expressing MET with SHC1, GRB2, and BLNK. The interaction of BLNK SH2Δ with MET was markedly decreased, whereas BLNK SH2Δ L18E abolished the interaction, as compared to wild-type BLNK. Interaction of MET with BLNK L18E was reduced, whereas BLNK I25E did not affect the interaction, as compared to wild-type BLNK, although MET expression was reduced upon co-expression with BLNK L18E. BLNK R372A did not affect the interaction with MET, whereas BLNK R372A L18E and BLNK R372A I25E reduced the interaction with MET, as compared to wild-type BLNK. α-tubulin was used as a loading control.

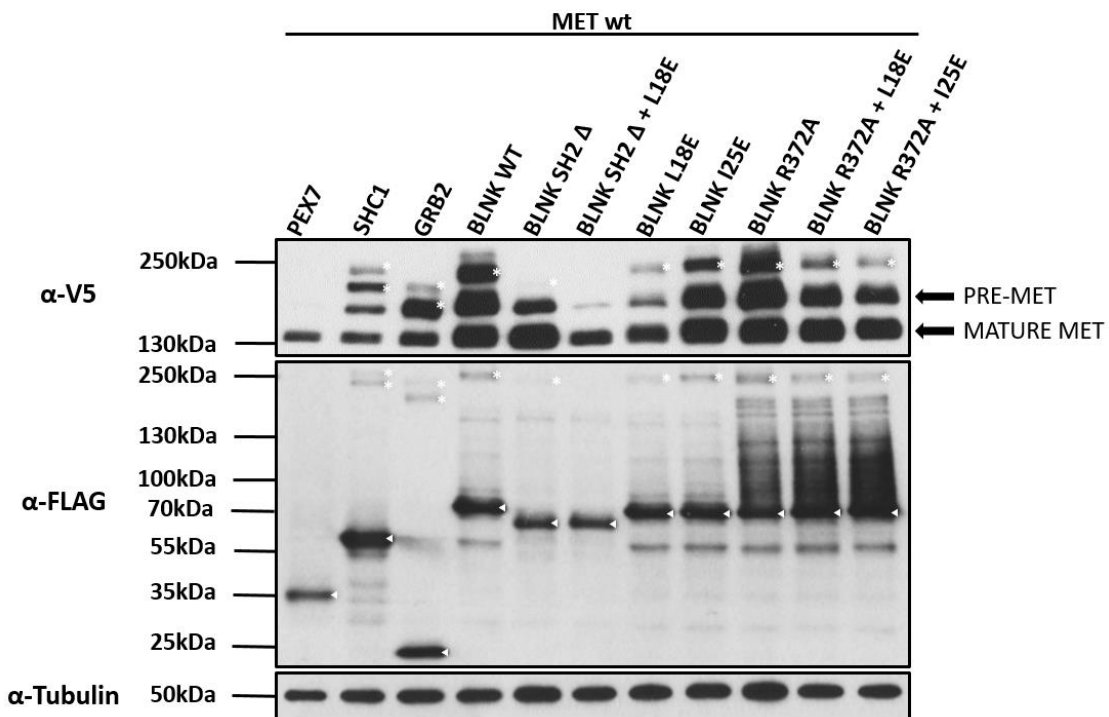


**Figure 34:** The ability of BLNK leucine and SH2 domain mutants to interact with MET was analyzed by Western blot using anti-V5 and anti-FLAG antibodies to detect bait and prey expression, respectively, as

well as spliced proteins if the interaction occurred. Precursor MET (PRE-MET) and mature MET are denoted with arrows.  $\alpha$ -tubulin was used as a loading control. Parental prey proteins are highlighted by triangles, while spliced proteins are highlighted by asterisks. Note that the spliced band of MET-GRB2 is the same size as pre-MET. Sizes of proteins detected by Western blot when performing a SIMPL assay involving MET are summarized in Table S1.

To examine whether all identified residues on BLNK that reduced interaction with MET displayed any additive effects in their ability to interact with MET, the following BLNK mutants were used: BLNK Y72F SH2 $\Delta$  and BLNK SH2 $\Delta$  L18E Y72F. To determine whether the introduction of these mutations affected BLNK expression, the expression profile of these BLNK mutants was compared to wild-type BLNK in T-REx HEK293 cells. To keep the amount of transfected BLNK the same as in the SIMPL assay, the constructs were co-transfected into T-REx HEK293 cells with the empty SIMPL bait vector in a 1:1 ratio. Protein expression was induced by the addition of tetracycline (1  $\mu$ g/ml) 24 hours after transfection. Cells were lysed 24 hours after the addition of tetracycline and lysates were subjected to Western blot analysis using an anti-FLAG antibody to detect BLNK expression (Figure 35). BLNK SH2 $\Delta$  and BLNK SH2 $\Delta$  L18E demonstrated reduced expression, whereas the expression of BLNK Y72F SH2 $\Delta$  and BLNK SH2 $\Delta$  L18E Y72F was unaffected, as compared to wild-type BLNK. A size shift of the bands representing these BLNK mutants was observed compared to wild-type BLNK, indicating the deletions.  $\alpha$ -tubulin was used as a loading control.

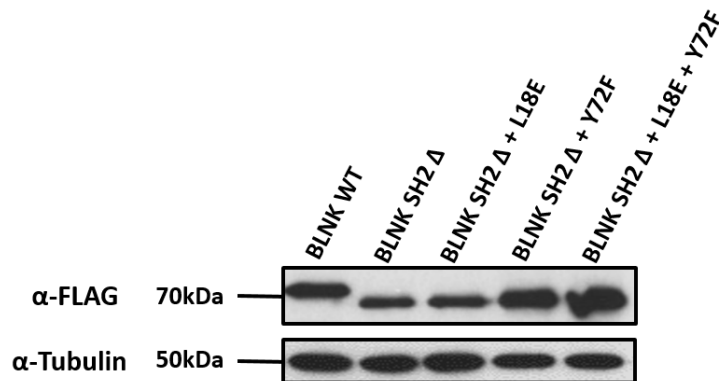


**Figure 35:** Expression profile of BLNK combinatorial mutants containing a deletion of SH2 domain was analyzed by Western blot using an anti-FLAG antibody to detect BLNK expression.  $\alpha$ -tubulin was used as a loading control.

The ability of BLNK combinatorial mutants that harbor an SH2 deletion to interact with MET was assessed by performing the transient SIMPL assay. MET-BLNK combinations were co-transfected in T-REx HEK293 cells. PEX7 was used as a negative control. Protein expression was induced by the addition of tetracycline (1 µg/ml) 24 hours after transfection. Cells were lysed 24 hours after the addition of tetracycline and lysates were subjected to Western blot analysis using anti-V5 and anti-FLAG antibodies to detect bait and prey expression, respectively, as well as spliced proteins if the interaction occurred (Figure 36). No interaction was detected between MET and PEX7, whereas the interaction of MET and wild-type BLNK was detected. Any BLNK mutant that contained the deletion of the SH2 domain abolished the interaction with MET, hence no additive effects on the interaction with MET were observed. α-tubulin was used as a loading control.

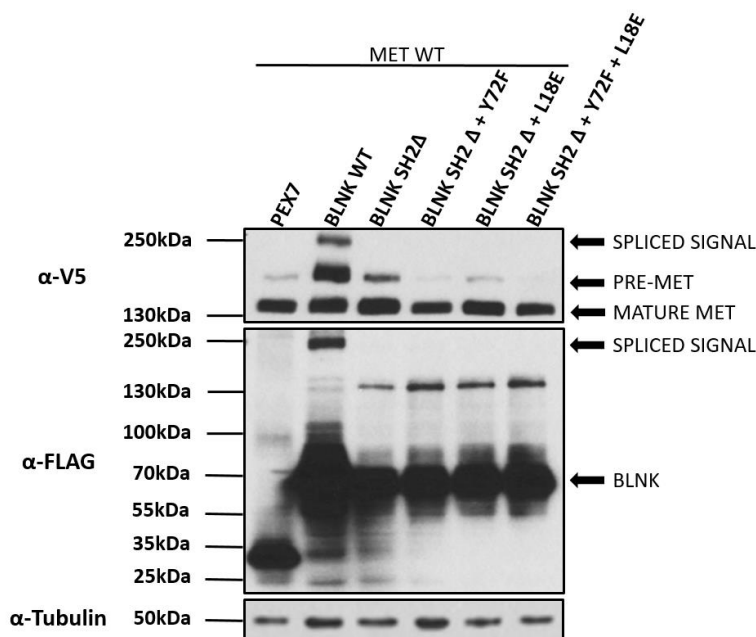


**Figure 36:** The ability of BLNK combinatorial mutants that harbor a deletion of an SH2 domain to interact with MET was analyzed by Western blot using anti-V5 and anti-FLAG antibodies to detect bait and prey expression, respectively, as well as spliced proteins if the interaction occurred. Precursor MET (PRE-MET), mature MET, BLNK, and spliced MET-BLNK are denoted with arrows. α-tubulin was used as a loading control. Parental prey proteins are highlighted by triangles, while spliced proteins are highlighted by asterisks. Note that the spliced band of MET-GRB2 is the same size as pre-MET. Sizes of proteins detected by Western blot when performing a SIMPL assay involving MET are summarized in Table S1.

#### **4.7. A Combination of the Alternative SIMPL Format and SIMPL ELISA Uncovers a Dual GRB2-Binding Site on BLNK**

BLNK and GRB2 are constitutively bound in a complex (Arya et al. 2017). To determine the GRB2 binding site on BLNK, the transient SIMPL assay was performed. *GRB2* gene was cloned into N-terminal SIMPL bait destination vector (Figure S1, D) using Gateway Technology. The generated NIN4-GRB2 expression clone was verified by Sanger sequencing. Several BLNK mutants were tested in their ability to interact with GRB2, according to a suspected binding site for GRB2 on BLNK (Arya et al. 2017). GRB2-BLNK combinations were co-expressed in T-REx HEK293 cells. PEX7 was used as a negative control. Protein expression was induced by the addition of tetracycline (1 µg/ml) 24 hours after transfection. Cells were lysed 24 hours after the addition of tetracycline and lysates were subjected to Western blot analysis using anti-FLAG antibody to detect prey expression and anti-V5 antibody to detect bait expression, as well as the transfer of V5 tag if the interaction occurred (Figure 37). No interaction was detected when GRB2-PEX7 were co-expressed, whereas the interaction of GRB2 with wild-type BLNK was detected. Compared to wild-type BLNK, BLNK Y72F, BLNK Y84F, and BLNK P212A did not affect the interaction with GRB2. BLNK P204A, BLNK P204A P212A, and BLNK P204A P212A Y72F reduced the interaction with GRB2, as compared to wild-type BLNK. BLNK P204A P212A Y72F reduced the interaction with GRB2 more than the other BLNK mutants. BLNK mutants that contained the mutation of P204 also demonstrated reduced expression, as compared to wild-type BLNK.  $\alpha$ -tubulin was used as a loading control.

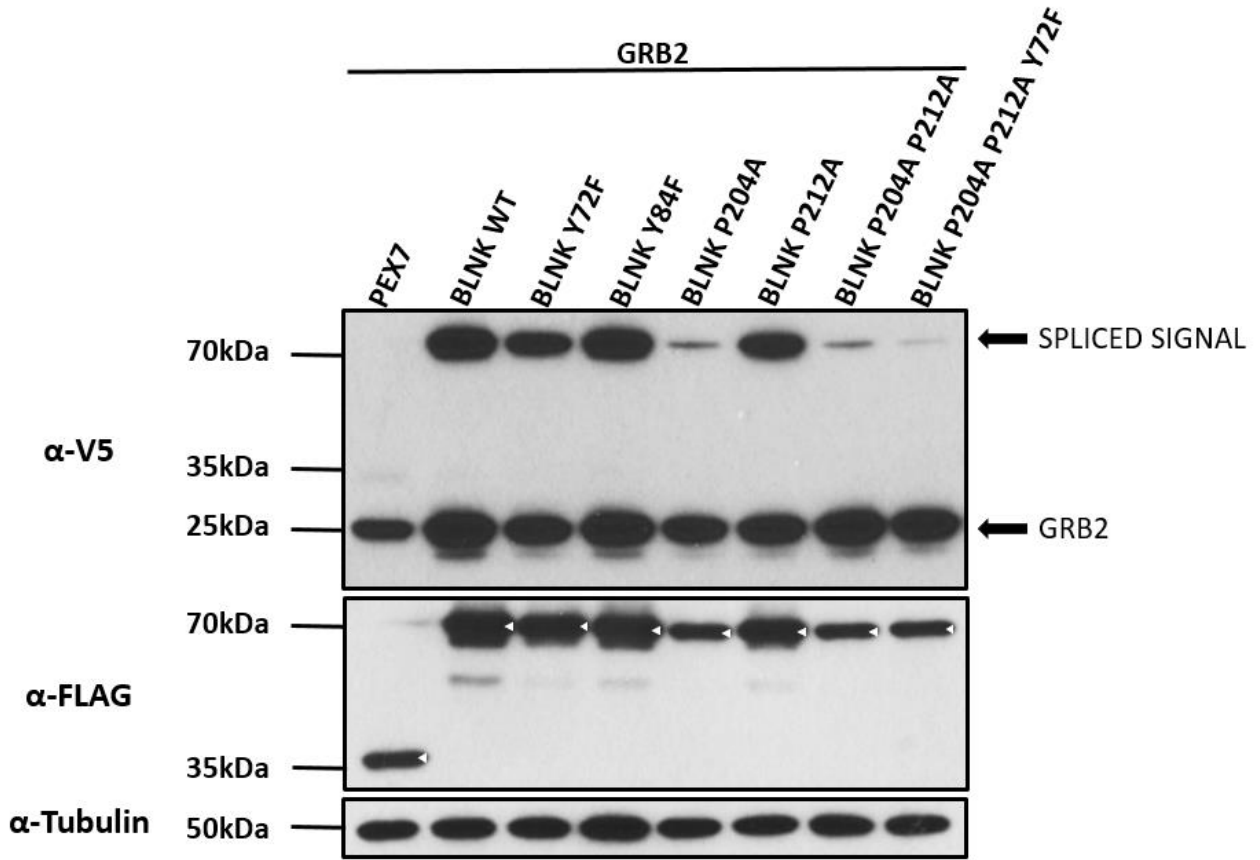


**Figure 37:** The ability of BLNK mutants to interact with GRB2 was assessed by Western blot analysis using anti-FLAG antibody to detect prey expression and anti-V5 antibody to detect bait expression, as well as the transfer of V5 tag if the interaction occurred. GRB2 and spliced GRB2-BLNK signals are denoted with arrows.  $\alpha$ -tubulin was used as a loading control.

To account for the effects of the differential expression of the above BLNK mutants in their interaction with GRB2 in SIMPL assay, the SIMPL-ELISA, where expression of baits and preys can be quantified, was performed. GRB2-BLNK combinations were co-expressed in T-REx HEK293 cells. PEX7 was used as a negative control. Protein expression was induced by the addition of tetracycline (0.5 µg/ml) 24 hours after transfection. Cells were lysed 24 hours after the addition of tetracycline and lysates were subjected to a sandwich ELISA analysis. Bait expression was examined by coating the plate with an anti-V5 antibody and then detected with an HRP-conjugated anti-HA antibody (Figure 38, A). Prey expression was examined by coating the plate with an anti-FLAG antibody and then detected with an HRP-conjugated anti-MYC antibody (Figure 38, B). Spliced signals were examined by coating the plate with an anti-FLAG antibody and then detected with an HRP-conjugated anti-HA antibody (Figure 38, C). A low basal signal was observed in the mock control (no transfection) and transfection with an empty vector for both bait and prey expression. Expression of GRB2 was reduced when co-expressed with PEX7, as compared to when co-expressed with BLNK. (Figure 38, A). BLNK P204A, BLNK P204A P212A, and BLNK P204A P212A Y72F demonstrated reduced expression when co-expressed with GRB2, whereas expression of BLNK Y72F, BLNK Y84F, and BLNK P212A remained unaffected, as compared to wild-type BLNK (Figure 38, B). No interaction was detected when GRB2 and PEX7 were co-expressed (Figure 38, C). Due to the expression differences between various BLNK mutants, the interactions were normalized to respective bait and prey expressions to draw conclusions. (Figure 38, D). A two-tailed student's t-test with  $n = 3$  was used to examine the significance of these results. Therefore, the student t test was used to assess the interaction differences between the interaction of GRB2 with wild-type BLNK (Figure 38, D, second column), PEX7 (Figure 38, D, first column), and several BLNK mutants (Figure 38, D, columns 3-8). PEX7 demonstrated a statistically significant reduction of interaction with GRB2 (Figure 38, D, first column). BLNK Y72F and BLNK Y84F did not affect the interaction with GRB2, compared to wild-type BLNK (Figure 38, D, columns 3 and 4). BLNK P204A, BLNK P212A, BLNK P204A P212A, and BLNK P204A P212A Y72F demonstrated a statistically significant reduction in their interaction with GRB2, compared to wild-type BLNK (Figure 38, D, columns 5-8). BLNK P204A P212A Y72F reduced the interaction with GRB2 more than other BLNK mutants (Figure 38, D, column 8).

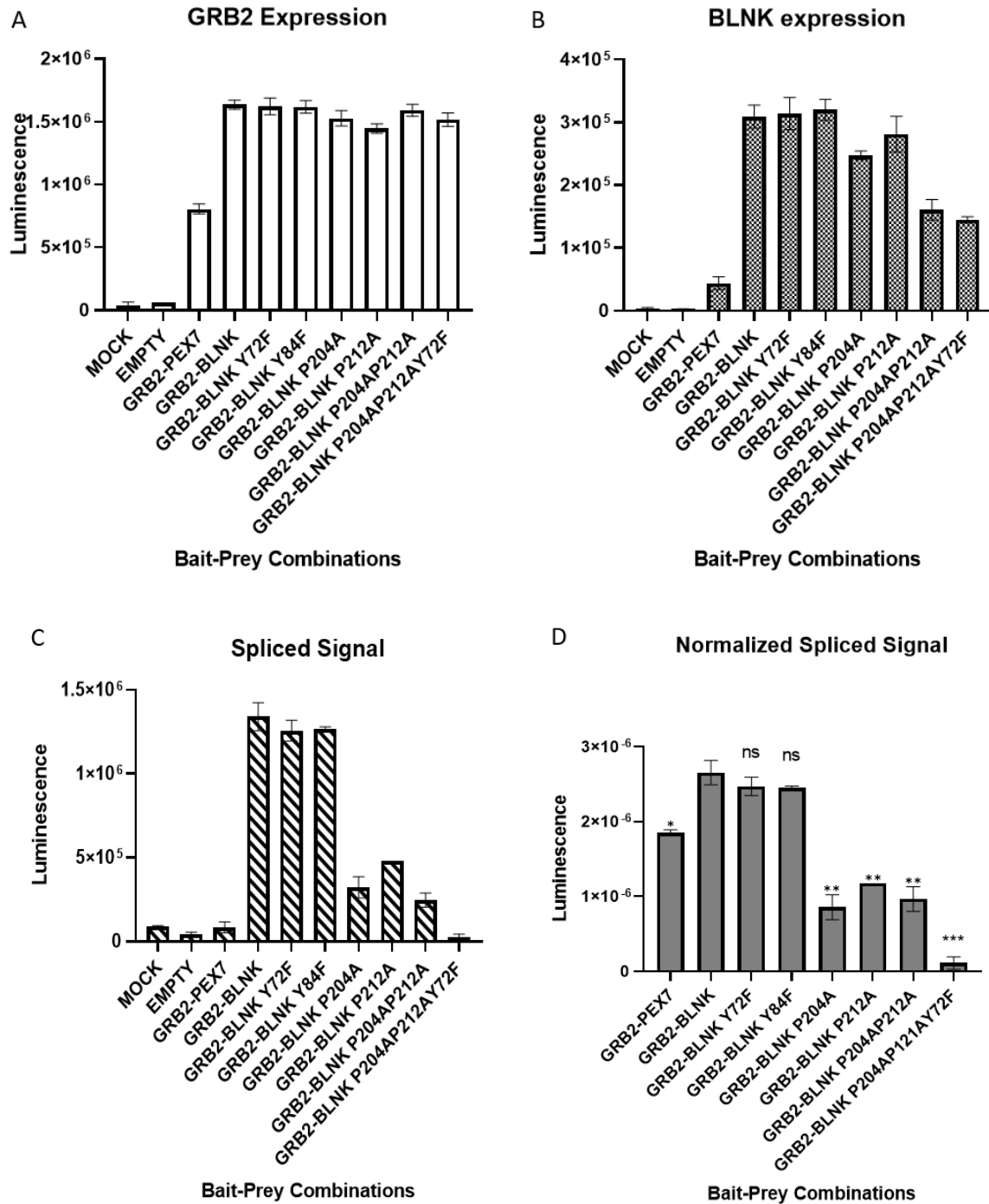


**Figure 38:** A SIMPL ELISA to determine GRB2-binding site on BLNK. **(A)** Bait expression. **(B)** Prey expression. **(C)** Raw spliced signals. **(D)** Spliced signals, normalized to bait and prey expression. A two-tailed student's t-test (n = 3) was used to assess the significance of interaction differences between the interaction of GRB2 with wild-type BLNK (second column), PEX7 (first column), and several BLNK mutants (columns 3-8). N.S. – non-significant, \* p < 0.05, \*\* p < 0.01, \*\*\* p < 0.001.



#### 4.8. Creation of Stable Doxycycline-Inducible BLNK shRNA Knock-Down System

BLNK shRNA cassettes were created by PCR reaction, using the pBS-tH1 construct as a template (Figure S5), cloned into Gateway donor vector pDONR223 using Gateway BP reaction, and verified by Sanger sequencing (Table 33).

**Table 33:** List of generated Gateway entry clones containing BLNK shRNA constructs. All the constructs were cloned into Gateway donor vector pDONR223.

<b>BLNK shRNA</b>	<b>Entry Clone</b>
BLNK shRNA 1	pDONR223-BLNK shRNA 1
BLNK shRNA 2	pDONR223-BLNK shRNA 2
BLNK shRNA 3	pDONR223-BLNK shRNA 3
BLNK shRNA 4	pDONR223-BLNK shRNA 4
BLNK shRNA 5	pDONR223-BLNK shRNA 5
BLNK shRNA 6	pDONR223-BLNK shRNA 6
BLNK shRNA 7	pDONR223-BLNK shRNA 7
BLNK shRNA 8	pDONR223-BLNK shRNA 8

The generated BLNK shRNA constructs were transferred in a Gateway lentivirus transfer vector pLV709G (Figure S4) using Gateway Technology and verified by Sanger sequencing (Table 34).

**Table 34:** List of generated Gateway expression clones containing BLNK shRNA constructs. All the constructs were cloned into Gateway destination lentivirus transfer vector pLV709G.

<b>BLNK shRNA</b>	<b>Expression Clone</b>
BLNK shRNA 1	pLV709G-BLNK shRNA 1
BLNK shRNA 2	pLV709G-BLNK shRNA 2
BLNK shRNA 3	pLV709G-BLNK shRNA 3
BLNK shRNA 4	pLV709G-BLNK shRNA 4
BLNK shRNA 5	pLV709G-BLNK shRNA 5
BLNK shRNA 6	pLV709G-BLNK shRNA 6
BLNK shRNA 7	pLV709G-BLNK shRNA 7
BLNK shRNA 8	pLV709G-BLNK shRNA 8

The generated constructs will be used to create cancer cell lines with the ability to induce knock-down of BLNK by adding doxycycline to cells to investigate the effect of knocking down BLNK in those cell lines on cancer cell signaling.

## 5. DISCUSSION

### 5.1. The Validation of MET-BLNK Interaction Using SIMPL Assay

BLNK is a newly discovered interacting partner of MET RTK, identified by screening a library of 100 out of 121 SH2/PTB domain-containing proteins against MET using the MaMTH assay (unpublished data, Štagljar lab). MET-BLNK interaction was orthogonally confirmed by co-immunoprecipitation assay. To further validate MET-BLNK interaction, a SIMPL assay was performed in T-REx HEK293 cells. PEX7 protein was chosen as a negative control prey because it is localized in the peroxisomes (Mukai et al. 2002), whereas mature MET is localized on the cell surface (Koch et al. 2020). Therefore, PEX7 is an appropriate negative control to use with MET in SIMPL assay. SHC1 and GRB2 proteins were chosen as positive controls because they are both previously reported as known interactors of MET (Koch et al. 2020). The results demonstrated that SHC1 and GRB2 interact with both precursor and mature MET, whereas BLNK interacts with only one form of MET in the transient SIMPL system. Therefore, MET-BLNK interaction was successfully recapitulated by SIMPL. To investigate whether BLNK interacts with precursor or mature form of MET, the site where precursor MET is cleaved in the maturation of MET can be mutated and then the interaction of the only precursor MET with BLNK can be investigated using SIMPL assay. Bait and prey proteins were expressed, and spliced proteins were detected regardless of tetracycline addition, indicating the leakiness of CMV promoters that control the expression of bait and prey proteins, as previously reported (Gossen & Bujard 1992) and demonstrated by Mateševac (2019). T-REx HEK293 cells stably express Tet repressor, indicating that transient transfection of bait and prey constructs using PEI is very efficient and that the level of Tet repressor in cells was not sufficient for proper repression of bait and prey expression. This issue could be circumvented by generating stable cell lines, wherein bait and/or prey expression can be controlled. Nonetheless, tetracycline was added to cells when performing the subsequent SIMPL assays.

## 5.2. MET Kinase Activity is Required for MET-BLNK Interaction

Since MET is a receptor tyrosine-kinase, its kinase activity is required for the majority of its protein-protein interactions (Koch et al. 2020). Therefore, two MET mutants were used to test if MET phosphorylation is a prerequisite for the interaction of MET with BLNK. According to UniProt, MET K1110A is a kinase-dead mutant because of its inability to bind ATP, whereas MET D1204A is a kinase-dead because of mutating an essential aspartate residue in the active site that serves as the proton acceptor. MET K1110A point mutation reduced the accumulation of both precursor and mature MET compared to wild-type MET, indicating that this mutation affects MET expression. Expression of MET D1204A was not detected, indicating that the active site of MET did not tolerate mutations. The phosphorylation profile of MET K1110A demonstrated that this mutant was not detectably phosphorylated, hence was largely inactive. MET K1110A was used to assess whether the interaction of BLNK with MET is phosphorylation-dependent. Compared to wild-type MET, MET K1110A reduced the interaction with BLNK, although it remains to be investigated how much of the interaction reduction can be ascribed to reduced MET expression. Furthermore, BLNK demonstrated behavior equivalent to SHC1, a known phosphorylation-dependent interaction partner of MET (Koch et al. 2020) when co-expressed with MET K1110A. These results indicated that MET-BLNK interaction could be phosphorylation-dependent.

## 5.3. The Generation and Characterization of the Stable MET-SIMPL System

The transient SIMPL assay performed in T-REx HEK293 cells exhibited no tetracycline-inducible control over bait and prey expression. Therefore, a stable MET-SIMPL system was generated by integrating the MET-V5-IN construct into the genome of T-REx HEK293 cells using Flp-In Technology. Characterization of this system began with the examination of tetracycline-inducible MET expression. MET expression was detected only with the addition of tetracycline. Therefore, the MET-SIMPL system exhibited control over bait expression unmatched by the transient system.

Localization of precursor and mature MET in the MET-SIMPL system was assessed. Precursor MET localizes in the vesicles of the Golgi apparatus, whereas mature MET localizes to the cell surface (Koch et al. 2020). Surface biotinylation was performed to confirm the proper localization

of both. MET expression was detected in the input only in presence of tetracycline. No MET was detected in the input without the addition of tetracycline, as well as in the pull-down samples without the addition of tetracycline and biotin, demonstrating there is no endogenous protein in the system labeled with V5 tag, as well as demonstrating the specificity of streptavidin-conjugated beads towards biotinylated proteins. In other words, no non-specific pull-down was observed. The presence of precursor MET predominantly in the supernatant fraction confirmed that precursor MET was localized within cells. The pull-down of samples incubated with biotin demonstrated that mature MET was localized at the surface. Mature MET was also detected in the intracellular fraction of cells. There were three potential explanations for this observation: MET was overexpressed in the MET-SIMPL system (indicating that more mature MET was present in cells than the cell surface can accommodate), the overexpression of MET led to its activation and subsequent internalization by the process of endocytosis as a part of a negative feedback loop to regulate MET activity (Koch et al. 2020) or one of the two main reagents in the experiment (biotin, streptavidin agarose beads) was added in the limited quantity compared to another. If the amount of biotin used in the experiment was not sufficient to tag all surface proteins, some of the untagged MET that was localized at the surface would not be pulled down with streptavidin beads. If the amount of streptavidin agarose beads was not sufficient, the beads were saturated and not all biotinylated MET molecules were pulled down. No loading control was detected in the pull-down samples, indicating that no biotin was internalized by cells during the experiment. Collectively, these results were consistent with the localization of MET in the MET-MaMTH system (Štagljar lab, unpublished data).

Next, the ability of MET in the MET-SIMPL system to interact with known partners was assessed. PEX7 was chosen as a negative control, whereas SHC1, GRB2, and BLNK were chosen as positive controls. The interaction of MET with all positive controls was successfully recapitulated in the MET-SIMPL system. One difference was observed compared to transient SIMPL assay: only one spliced band was detected upon co-expressing MET with SHC1 and GRB2. This result could be explained by differential processing of MET in transient and stable systems.

The repression capacity of a single Tet repressor locus, stably integrated into the genome of the system was assessed, using a mock control (no transfection)  $\pm$  tetracycline, empty SIMPL prey

vector transfection  $\pm$  tetracycline, and BLNK transfection with different concentrations of tetracycline. MET expression was detected in mock control only with the addition of tetracycline. The expression of MET in cells transfected with empty SIMPL prey vector was detected only in the presence of tetracycline, indicating that the CMV promoter located on the empty SIMPL prey vector did not take Tet repressor away from repressing the CMV promoter that controls MET expression. When co-expressing MET stably and BLNK transiently in this system without the addition of tetracycline, MET expression was completely repressed, whereas BLNK expression only displayed basal leaky expression and was otherwise repressed, indicating a notable improvement over prey expression control compared to expressing both proteins transiently. The absence of spliced proteins without the addition of tetracycline further confirmed the expression control over the MET-SIMPL system. Both the expression of MET and BLNK, as well as MET-BLNK interaction demonstrated a dose-dependent increase with the addition of tetracycline in increasing concentrations. The saturation of both expression and interaction was observed at the concentration of tetracycline of 0.5  $\mu\text{g/ml}$ . Collectively, the MET-SIMPL system demonstrated markedly increased control over bait and prey expression and the ability to temporally induce the expression of both.

Lastly, the responsiveness of the MET-SIMPL system to crizotinib, a known MET inhibitor (Rodig & Shapiro 2010) was investigated. Crizotinib is a competitive tyrosine-kinase inhibitor that inhibits MET by binding to its ATP-binding site (Rodig & Shapiro 2010). The effect of crizotinib on MET expression and phosphorylation was tested first. DMSO was used as solvent control and it did not affect MET expression and phosphorylation. Therefore, any effect on MET was ascribed to crizotinib only. A dose-dependent reduction of MET expression upon administration of increasing doses of crizotinib was observed. There were three potential explanations for this observation. First, MET is a proto-oncogene that enhances protein synthesis in the cells via the AKT-mTOR axis (Koch et al. 2020). Therefore, inhibition of MET could hinder protein synthesis, including MET itself. Second, phosphorylation could be a prerequisite for maintaining the stability of MET. MET K1110A exhibited a similar expression decrease, as compared to wild-type MET upon the addition of crizotinib in a sufficient dose. That observation was ascribed to the introduction of a mutation that potentially affected the stability of MET. On the contrary, there

was no mutation of wild-type MET that could affect its stability. Therefore, phosphorylation could confer stability to MET. Third, crizotinib is known to decrease the expression of MET, as reported by the clinical studies on patients with lung (Bang 2011) and breast cancers (Ayoub et al. 2017). A steep dose-dependent reduction of MET phosphorylation upon the administration of increasing doses of crizotinib was observed. Therefore, the addition of a sufficient dose of crizotinib was phenotypically equivalent to MET kinase-dead mutant. The advantage of using crizotinib over MET kinase-dead mutants lies in the ability to add different concentrations of crizotinib to cells and observe the gradual effect on MET expression and phosphorylation, as well as interaction with its partners. Next, the effect of crizotinib on the interaction of MET with SHC1 was tested. MET-SHC1 interaction diminished with increasing crizotinib concentrations. The concentration of crizotinib of 5 nM reduced the interaction, which correlates with results previously yielded by the MET-MaMTH system (Saraon et al. 2020). Crizotinib in higher concentrations (> 5 nM) affected the expression of MET and SHC1, which also correlates with findings obtained from MET-MaMTH drug screening studies (Saraon et al. 2020). Finally, the effect of crizotinib on MET-BLNK interaction was assessed. Like MET-SHC1, MET-BLNK interaction diminished with increasing crizotinib concentrations, further demonstrating phosphorylation-dependency of MET-BLNK interaction.

Collectively, these results demonstrated two important features of the MET-SIMPL system: the MET-SIMPL system expressed a fully functional MET receptor tyrosine-kinase with proper signaling and the applicability of the MET-SIMPL system as a drug-screening platform that can detect new potential inhibitors of MET. Also, the generation of a stable system that expresses full-length wild-type MET represents an improvement in the field of MET research, compared to the traditional use of MET-TPR fusion protein (Ponzetto et al. 1996).

#### **5.4. Mapping Residues on MET that Participate in MET-BLNK Interaction**

The phosphorylation-dependency of MET-BLNK interaction and the fact that BLNK is an SH2 domain-containing protein led to the hypothesis that one or multiple phosphorylated tyrosine residues on MET participated in MET-BLNK interaction. To uncover the identity of the tyrosine residue(s), a series of MET tyrosine mutants were tested against BLNK using a SIMPL screening

approach. The following MET phospho-null mutants were used: MET Y1349F, MET Y1356F, MET Y1356F N1358A, MET N1358A, MET Y1365F, MET Y1284F, MET Y1003F, and MET exon 14 skipping mutant. The tyrosine residues were mutated to phenylalanine to disable the phosphorylation of MET at those residues. Expression and phosphorylation profile of MET mutants indicated that mutations Y1349F, Y1356F, and Y1356F N1358A did not affect MET expression or phosphorylation, mutation Y1284F reduced MET expression and phosphorylation, and mutations Y1365F and Y1003F, as well as deleting exon 14 increased expression of MET. Exon 14 of MET contains amino acids S985 and Y1003, essential for downregulation of MET through ubiquitin-proteasome system (Koch et al. 2020). Therefore, the upregulation of MET expression and activity upon removing Y1003 or exon 14 was consistent with previous findings (Koch et al. 2020). The expression and phosphorylation profile of MET Y1365F indicated that this tyrosine could also have a potential role in the downregulation of MET since its mutation upregulated MET expression, which remains to be investigated.

The screening to uncover the binding site for BLNK on MET demonstrated that phenotypically equivalent MET Y1003F and MET exon 14 skipping mutant did not reduce the interaction with BLNK, thus eliminating the juxtamembrane domain of MET as the potential binding site for BLNK. MET Y1349F exhibited reduced interaction with BLNK, compared to wild-type MET. MET Y1356F further reduced the interaction with BLNK, compared to MET Y1349F. Tyrosine Y1356 of MET is one of two critical C-terminal docking site tyrosine residues of MET that recruits many of its downstream effectors, such as GRB2 (Ponzetto et al. 1996). Therefore, Y1356 could be a major residue participating in MET-BLNK interaction. MET Y1365F did not reduce the interaction with BLNK and was eliminated as a potential BLNK-binding site. MET Y1284F reduced the interaction with BLNK, but it was due to a lesser expression of this MET mutant, compared to wild-type MET.

Since BLNK and GRB2 are known to be constitutively bound in a complex regardless of upstream activation (Arya et al. 2017), and amino acid residues Y1356 and N1358 constitute the GRB2 binding motif Y<sup>1356</sup>VNV (Ponzetto et al. 1996), to determine whether GRB2 could modulate MET-BLNK interaction, the interaction of BLNK and GRB2 was then compared between wild-type MET, MET Y1356F, and MET Y1356F N1358A. Both MET mutants reduced the interaction with BLNK and GRB2, with no additive effects observed between MET Y1356F and MET Y1356F

N1358A. Interaction of BLNK with both MET Y1356F and MET Y1356F N1358A was reduced in the same manner as GRB2, a known binding partner of tyrosine Y1356 (Ponzetto et al. 1996), which provided additional evidence that tyrosine Y1356 was the tyrosine BLNK binds to. Mutation of amino acid N1358 is reported to specifically uncouple GRB2 from MET (Ponzetto et al. 1996). Therefore, to further investigate the role of the Y<sup>1356</sup>VNV motif on MET in the binding of BLNK and whether GRB2 acts as a mediator in MET-BLNK interaction, the ability of an additional MET mutant, MET N1358A to bind to BLNK and GRB2 was compared to wild-type MET, MET Y1356F and MET Y1356F N1358A. Only MET mutants that harbor mutation of Y1356 decreased the interaction with BLNK and GRB2. MET N1358A did not reduce the interaction with BLNK, as compared to wild-type MET. Interestingly, MET N1358A did not uncouple the interaction of MET with GRB2, as reported by Ponzetto et al. (1996).

To investigate the potential additive effects of mutating more than one of the most C-terminal tyrosine residues of MET on the interaction with BLNK, a series of MET combinatorial mutants were generated. The following MET mutants were generated: MET Y1349F Y1356F, MET Y1349F Y1365F, MET Y1356F Y1365F, and MET Y1349F Y1356F Y1365F. Their expression profiles demonstrated that MET Y1349F Y1356F and MET Y1356F Y1365F exhibited reduced expression, whereas MET Y1349F Y1365F and MET Y1349F Y1356F Y1365F expressed comparably to wild-type MET. The phosphorylation profiles of these MET mutants indicated that none of these mutants are inactive. MET Y1349F Y1356F, MET Y1356F Y1365F, and MET Y1349F Y1356F Y1365F reduced the interaction with BLNK, whereas MET Y1349F Y1365F did not affect the interaction with BLNK, compared to wild-type MET, which provided additional insight into the importance of tyrosine Y1356 in the binding of BLNK to MET. MET mutants that harbor mutation of tyrosine Y1356 all reduced the interaction with BLNK, and those without the mutation of tyrosine Y1356 do not reduce the interaction with BLNK. Collectively, these results indicated that BLNK binds to MET to phosphorylated tyrosine Y1356. MET mutant MET Y1349F demonstrated reduced interaction with BLNK, but to a lesser extent than MET Y1356F. That tyrosine also plays a major role when phosphorylated (Ponzetto et al. 1996; Koch et al. 2020). Therefore, that tyrosine residue could potentially confer stability to MET-BLNK interaction, which remains to be further investigated.



## **5.5. MET Mutants Localize to the Cell Surface**

MET mutants MET Y1349F, MET Y1356F, and MET Y1356F N1358A reduced the interaction with BLNK. Proper localization of these MET mutants needed to be determined to validate those findings. Phosphorylation of tyrosine residues in receptor tyrosine-kinases was reported to regulate the maturation of RTKs (Schmidt-Arras et al. 2005). Therefore, mutating tyrosine residues in MET could alter its processing and ultimately its localization, although no such findings have thus far been reported. To determine whether the reduction of interaction between the aforementioned MET mutants and BLNK is not the result of mislocalization of MET due to introduced tyrosine residue mutations, a series of surface biotinylation experiments were performed. Surface levels of MET Y1349F, MET Y1356F, and MET Y1356F N1358A were compared to wild-type MET. The results indicated that all three MET mutants localized to the cell surface comparably to wild-type MET. Therefore, reduced interaction of the MET mutants with BLNK was not due to mislocalization of MET mutants, rather due to reduced binding of MET and BLNK.

## **5.6. Mapping Residues on BLNK that Participate in MET-BLNK Interaction**

To determine the amino acid residues on BLNK responsible for its binding on MET, three series of BLNK mutants were used. The first set of BLNK mutants were tyrosine mutants. Five of all tyrosine residues on BLNK have been well studied for their capacity to bind to different interaction partners of BLNK, once phosphorylated (Koretzky et al. 2006). Once phosphorylated, the tyrosine residues in the N-terminal acidic domain create the binding sites for various interaction partners of BLNK (Koretzky et al. 2006). Proteins of the VAV family bind to BLNK via a phosphorylated tyrosine residue Y72, NCK protein binds to BLNK via phosphorylated tyrosine residues Y84 and Y96, BTK protein binds to BLNK via its phosphorylated tyrosine residue Y178, and PLC $\gamma$  interacts with BLNK via its phosphorylated tyrosine residue Y189 (Koretzky et al. 2006). These tyrosine residues were mutated to phenylalanine residues to disable phosphorylation of BLNK at those residues. The following BLNK tyrosine mutants were used: BLNK Y72F, BLNK Y84F, BLNK Y96F, BLNK Y84F Y96F, BLNK Y72F Y84F Y96F, BLNK Y178F, and BLNK Y189F. Their expression profiles demonstrated that all of them expressed comparably to wild-type BLNK, except BLNK Y72F Y84F Y96F, whose expression was not detected, indicating that mutating three different tyrosine residues destabilized BLNK, possibly because those residues mediate BLNK

folding. BLNK Y72F markedly reduced the interaction with MET, BLNK Y84F and BLNK Y84F Y96F reduced the interaction with MET, BLNK Y96F increased interaction with MET although that increase was not notable, and BLNK mutants BLNK Y178F and BLNK Y189F did not affect the interaction with MET. These results indicated a potential role of tyrosine Y72 of BLNK in its binding on MET. Tyrosine Y84 of BLNK could contribute to MET-BLNK interaction, whereas tyrosine Y96 could be a negative regulator of MET-BLNK interaction. It is unlikely that BLNK binds to tyrosine Y1356 of MET via its tyrosine residues directly due to the repulsion of two negatively charged phosphorylated tyrosine residues. Tyrosine residue Y72 of BLNK is a predicted binding site for the SH2 domain of GRB2 on BLNK, as indicated by HPRD and Songyang et al. (1994). Therefore, there was an indication for GRB2 to be a mediator in MET-BLNK interaction.

The second set of BLNK mutants were the proline mutants. The central proline-rich region of BLNK contains several proline residues that create a potential binding site for the SH3 domains of GRB2 (Arya et al. 2017). The following BLNK proline mutants were used: BLNK P204A, BLNK P212A, BLNK P204A P212A, and BLNK P204A P212A Y72F. Their expression profiles indicated that BLNK P212A expressed comparably to wild-type BLNK, whereas the other mutants exhibited reduced expression compared to wild-type BLNK, indicating that P204 was necessary for the stability of BLNK. None of these BLNK mutants affected the interaction with MET, suggesting that BLNK did not bind to MET through its proline-rich domain. MET expression was increased upon co-expression with BLNK mutants BLNK P204A, BLNK P204A P212A, and BLNK P204A P212A Y72F, indicating that those BLNK mutants stabilized MET or prevented MET degradation.

The third set of mutants were of BLNK leucine-zipper region and BLNK SH2 domain mutants. The N-terminal leucine zipper motif of BLNK confers the recruitment of BLNK to the cell membrane (Kohler et al. 2005), whereas an SH2 domain usually participates in the phosphorylation-dependent binding of the interaction partners of receptor tyrosine-kinases (Wagner et al. 2013). The following BLNK mutants were created: BLNK L18E, BLNK I25E, BLNK SH2 $\Delta$ , BLNK SH2 $\Delta$  L18E, BLNK R372A, BLNK R372A L18E, and BLNK R372A I25E. Their expression profiles indicated that BLNK SH2 $\Delta$  and BLNK SH2 $\Delta$  L18E expressed less than wild-type BLNK, whereas the remaining BLNK mutants expressed comparably to wild-type BLNK. BLNK SH2 $\Delta$  markedly reduced the interaction with MET, whereas BLNK SH2 $\Delta$  L18E abolished the interaction.

BLNK L18E decreased the interaction with MET, whereas BLNK I25E did not affect the interaction with MET. BLNK R372A did not affect the interaction with MET, whereas BLNK R372A L18E and BLNK R372A I25E decreased the interaction with MET. These results indicated that the SH2 domain is critical in the binding of BLNK to phosphorylated (active) MET, as is previously reported for other proteins containing an SH2 domain (Wagner et al. 2013). The importance of an SH2 domain in the binding of BLNK to MET was further demonstrated by using BLNK mutants BLNK SH2Δ Y72F and BLNK SH2Δ L18E Y72F. These BLNK mutants expressed comparably to wild-type BLNK. Any BLNK mutant that harbored the deletion of an SH2 domain abolished the interaction with MET. These results led to the conclusion that BLNK binds to MET through its SH2 domain, similarly to other SH2 domain-containing proteins (Wagner et al. 2013).

### **5.7. GRB2 Has a Dual Binding Site on BLNK**

GRB2 and BLNK are constitutively bound in a complex regardless of upstream activation of receptors (Arya et al. 2017). To uncover the binding site for GRB2 on BLNK and to assess the potential role of GRB2 as a mediator in MET-BLNK interaction, a BLNK mutant deficient in the binding of GRB2 was necessary. To determine the binding site of GRB2 on BLNK, a series of BLNK mutants were tested for their interaction with GRB2 using the SIMPL screening approach. GRB2 was tagged N-terminally with the intein fragment IN since the *GRB2* gene from the ORFeome (Štagljar lab) has a STOP-codon at its 3' end. The following BLNK mutants were tested to uncover the binding site for GRB2: BLNK Y72F, BLNK Y84F, BLNK P204A, BLNK P212A, BLNK P204A P212A, and BLNK P204A P212A Y72F. BLNK mutants BLNK Y72F, BLNK Y84F, and BLNK P212A did not affect the interaction with GRB2, whereas BLNK mutants BLNK P204A, BLNK P204A P212A, and BLNK P204A P212A Y72F reduced the interaction with GRB2, with BLNK mutant BLNK P204A P212A Y72F demonstrating an additive effect on reducing the interaction with GRB2, as compared to BLNK P204A alone. Since these BLNK mutants demonstrated differential expression, their expression needed to be quantified to normalize BLNK-GRB2 interaction to prey expression. Therefore, a SIMPL ELISA was performed. When the spliced signals were normalized to respective bait and prey expression values, it was demonstrated that BLNK mutants BLNK P204A, BLNK P212A, BLNK P204A P212A, and BLNK P204A P212A Y72F all significantly reduced the interaction with GRB2, with a noticeable additive effect of BLNK mutant BLNK P204A P212A Y72F that nearly

abolished the interaction with GRB2. Interestingly, the interaction of BLNK P212A with GRB2 was inconsistent when comparing Western blot and ELISA analyses. BLNK P212A did not reduce the interaction with GRB2 in Western blot analysis. These results led to a hypothesis that GRB2 binds BLNK on two sites: an SH2 domain of GRB2 binds to the phosphorylated tyrosine Y72 of BLNK and an SH3 domain of GRB2 binds to the central proline-rich domain of BLNK. Interestingly, mutation Y72F did not affect the interaction with GRB2 but demonstrated an additive effect on interaction when mutated alongside residues P204A and P212A.

When these ELISA results of BLNK-GRB2 interaction were compared with the effect of BLNK proline mutations on MET-BLNK interaction, two important observations were made. First, GRB2 did not mediate MET-BLNK interaction since BLNK P204A P212A Y72F uncoupled the interaction with GRB2 but did not affect the interaction with MET. Notably, T-REx HEK293 cells used in the SIMPL assay express endogenous GRB2, as indicated by Protein Atlas. Therefore, the reduced interaction of MET with BLNK mutant BLNK Y72F remains unclear. There could be another mediator of MET-BLNK interaction, other than GRB2, which remains to be investigated. Second, BLNK might be a positive regulator of MET, as per previous data (Štagljar lab), whereas GRB2 bound to BLNK might be a negative regulator of MET. BLNK mutants BLNK P204A and BLNK P204A P212A partially uncoupled the interaction with GRB2. MET expression increased upon co-expression with these BLNK mutants. BLNK P204A P212A Y72F almost completely uncoupled the interaction with GRB2; MET expression was also notably increased upon co-expression with this BLNK mutant. These observations indicated that the more BLNK is uncoupled from GRB2, the more MET expression was increased. This observation would need further research to uncover if BLNK confers more stability of MET when uncoupled with GRB2. To study the effect of the relationship of BLNK and GRB2 on MET expression and activity, a MET-BLNK double stable construct was created using Gibson Assembly (Figure S6). This construct will be used with Flp-In Technology to create the double stable MET-BLNK SIMPL system. T-REx HEK293 cells that will be used to create this system express endogenous GRB2. Therefore, GRB2 can be either knocked down or overexpressed in this system to assess the effect of the amount of GRB2 on MET. Furthermore, MET and BLNK mutants that uncoupled the binding with GRB2 will be co-expressed outside of the SIMPL assay to investigate if increased MET expression can be recapitulated.

## 6. CONCLUSION

MET-BLNK interaction was successfully confirmed and its phosphorylation-dependency was uncovered using the SIMPL assay. A stable MET-SIMPL system was generated, characterized, and used to demonstrate the phosphorylation-dependency of MET-BLNK interaction, as well as the feasibility of the MET-SIMPL system as a drug-screening platform for MET inhibitors. MET Y1356 was identified as the probable primary binding site for BLNK. An SH2 domain of BLNK was identified as the domain responsible for the binding of BLNK to MET. The role of tyrosine Y72 on BLNK in the binding of MET remained unclear. BLNK mutants that contained the mutation of proline residue P204 increased MET expression. Tyrosine residue Y72 and proline residues P204 and P212 on BLNK were identified as binding sites for GRB2. GRB2 was dismissed as a mediator of MET-BLNK interaction. BLNK was identified as a potential positive regulator of MET, whereas GRB2 was identified as a potential negative regulator of MET.

## 7. REFERENCES

- Aranko A. S. et al. (2014): Nature's recipe for splitting inteins, *Protein Engineering, Design & Selection*, **27(8)**:263-271.
- Arya R. et al. (2017): Grb2 carboxyl-terminal SH3 domain can bivalently associate with two ligands, in an SH3 dependent manner, *Nature Scientific Reports*, **7**: 1284.
- Ayoub M. N. et al. (2017): Crizotinib, a MET inhibitor, inhibits growth, migration, and invasion of breast cancer cells in vitro and synergizes with chemotherapeutic agents, *OncoTargets and Therapy*, **10**: 4869–4883.
- Bang Y-J. (2011): The potential for crizotinib in non-small cell lung cancer: a perspective review, *Therapeutic Advances in Medical Oncology*, **3(6)**: 279-291.
- Bean J. et al. (2007): MET amplification occurs with or without T790M mutations in EGFR mutant lung tumors with acquired resistance to gefitinib or erlotinib, *Proceedings of the National Academy of Sciences of the United States of America*, **104**: 20932-20937.
- Birchmeier C. et al. (2003): MET, metastasis, motility and more, *Nature Reviews Molecular Cellular Biology*, **4**: 915-925.
- Brindel J. L. et al. (2013): EGF receptor activated MET through MAPK to enhance non-small cell lung cancer lung carcinoma invasion and brain metastasis, *Cancer Research*, **73**: 5053-5065.
- Clark S. G. et al. (1992): *C. Elegans* cell-signaling gene *sem-5* encodes a protein with SH2 and SH3 domains, *Nature*, **356**: 340-344.
- Di Renzo M. F. et al. (1995): Overexpression and amplification of MET during the progression of colorectal cancer, *Clinical Cancer Research*, **1**: 147-154.
- Di Renzo M. F. et al. (2000): Somatic mutations of the MET oncogene are selected during metastatic spread of human HNSC carcinomas, *Oncogene*, **19**: 1547-1555.
- Du Z. & Lovly C. M. (2018): Mechanisms of receptor tyrosine-kinase activation in cancer, *Molecular Cancer*, **17**: 58-71.
- Fan S. et al. (2005): Role of NF- $\kappa$ B signaling in hepatocyte growth factor/scatter factor-mediated cell protection, *Oncogene*, **24**: 1749-1766.
- Flemming A. et al. (2002): The adaptor protein SLP-65 acts as a tumor suppressor that limits pre-B cell leukemia, *Nature Immunology*, **4(1)**: 38-43.

- Frampton G. M. et al. (2015): Activation of MET via diverse exon 14 splicing alterations occurs in multiple tumor types and confers clinical sensitivity to MET inhibitors, *Cancer Discovery*, **5**: 850-859.
- Fu C. et al. (1998): BLNK: central linker protein in B cell activation, *Immunity*, **9**: 93-103.
- Gherardi E. et al. (2003): Functional map and domain structure of MET, the product of the c-MET proto-oncogene and receptor for hepatocyte growth factor/scatter factor, *Proceedings of the National Academy of Sciences of the United States of America*, **100(21)**: 12039-12044.
- Gossen M. & Bujard H. (1992): Tight control of gene expression in mammalian cells by tetracycline-responsive promoters, *Proceedings of the National Academy of Sciences of the United States of America*, **89(12)**: 5547-5551.
- Hanahan D. & Weinberg R. A. (2011): Hallmarks of cancer: the next generation, *Cell*, **144(5)**: 646-674.
- Heist R. S. et al. (2016): MET exon 14 skipping in non-small cell lung cancer, *The Oncologist*, **21**: 481-486.
- Houldsworth J. et al. (1990): Gene amplification in gastric and esophageal adenocarcinomas, *Cancer Research*, **50**: 6417-6422.
- Hubbard S. R. (1999): Structural analysis of receptor tyrosine-kinases, *Progress in Biophysics & Molecular Biology*, **71**: 343-358.
- Hui A. Y. et al. (2009): Src and FAK mediate cell-matrix adhesion-dependent activation of MET during transformation of breast epithelial cells, *Journal of Cellular Biochemistry*, **107**: 1168-1181.
- Jeffers M. et al. (1997): Degradation of MET tyrosine-kinase receptor by the ubiquitin-proteasome system, *Cellular and Molecular Biology*, **17(2)**: 799-808.
- Johnson G. L. et al. (2002): Mitogen-activated protein kinase pathways mediated by ERK, JNK and p38 protein kinases, *Science*, **298**: 1911-1912.
- Koch J. P. et al. (2020): MET targeting: time for a rematch, *Oncogene*, **39**: 2845-2862.
- Kohler F. et al. (2005): A leucine zipper in the N-terminus confers membrane association to SLP-65, *Nature Immunology*, **6**: 204-210.
- Kong-Beltran M. et al. (2004): The Sema domain of MET is necessary for receptor dimerization and activation, *Cancer Cell*, **6**: 75-84.

- Kong-Beltran M. et al. (2006): Somatic mutations lead to an oncogenic deletion of MET in lung cancer, *Cancer Research*, **66**: 283-289.
- Koretzky G. A. et al. (2006): SLP76 and SLP65: complex regulation of signaling in lymphocytes and beyond, *Nature Reviews, Immunology*, **6(1)**: 67-78.
- Kotlyar M. et al. (2015): In silico prediction of physical protein interactions and characterization of interactome orphans, *Nature Methods*, **12(1)**: 79-84.
- Lemmon M. A. & Schlessinger J. (2010): Cell signaling by receptor tyrosine-kinases, *Cell*, 141(7): 1117-1134.
- Luo L. Y & Hahn W. C. (2015): Oncogenic signaling adaptor proteins, *Journal of Genetics and Genomics*, **42**: 521-529.
- Mateševac J. (2020): Mapping of small GTPase proteins HRAS, NRAS and MRAS using the Split Intein-Mediated Protein Ligation assay, Master Thesis, Faculty of Science, University of Zagreb
- Matsumoto K. & Nakamura T. (2006): Hepatocyte growth factor and the MET system as a mediator of tumor-stromal interaction, *International Journal of Cancer*, **119**: 477-483.
- McDonnell L. M. et al. (2015): Receptor tyrosine-kinase mutations in developmental syndromes and cancer: two sides of the same coin, *Human Molecular Genetics*, **24**: R60-R66.
- Mukai S. et al. (2002): Intracellular localization, function, and dysfunction of the peroxisome-targeting signal type 2 receptor, PEX7p, in mammalian cells, *The Journal of Biological Chemistry*, **277(11)**: 9548–9561.
- Organ S. L. & Tsao M. S. (2011): An overview of the c-MET signaling pathway, *Therapeutic Advances in Medical Oncology*, **3**: S7-S19.
- Park M. et al. (2005). Presence of autocrine hepatocyte growth factor-MET signaling and its role in proliferation and migration of SNU-484 gastric cancer cell line, *Experimental & Molecular Medicine*, **37**: 213-219.
- Petschnigg J. et al. (2011): Interactive proteomics research technologies: recent applications and advances, *Current Opinion in Biotechnology*, **22**: 50-58.
- Petschnigg J. et al. (2014): The mammalian-membrane two-hybrid assay (MaMTH) for probing membrane-protein interactions in human cells, *Nature Methods*, **11**: 585-592.



- Petrini I. (2015): Biology of MET: a double life between normal tissue repair and tumor progression, *Annals of Translational Medicine*, **3(6)**: 82-98.
- Ponzetto C. et al. (1994): A multifunctional docking site mediates signaling and transformation by the hepatocyte growth factor receptor family, *Cell*, **77**: 261-271.
- Ponzetto C. et al. (1996): Specific Uncoupling of GRB2 from the MET Receptor, *The Journal of Biological Chemistry*, **271(24)**: 14119–14123.
- Reis H. et al. (2018): MET expression in advanced non-small-cell lung cancer: effect on clinical outcomes of chemotherapy, targeted therapy, and immunotherapy, *Clinical Lung Cancer*, **19(4)**: e441-e463.
- Robertson S. C. et al. (2000): RTK mutations and human syndromes: when good receptors turn bad, *Trends in Genetics*, **16(6)**: 265-271.
- Robinson R. et al. (2000): The protein tyrosine-kinase family of the human genome, *Oncogene*, **19**: 5548-5557.
- Rodig S. J. & Shapiro G. I. (2010): Crizotinib, a small-molecule dual inhibitor of the c-MET and ALK receptor tyrosine-kinases, *Current opinion in investigational drugs*, **11(12)**: 1477-90.
- Saraon P. et al. (2020): A drug discovery platform to identify compounds that inhibit EGFR triple mutants, *Nature Chemical Biology*, **16**: 577–586.
- Schmidt-Arras D. E. et al. (2005): Tyrosine Phosphorylation Regulates Maturation of Receptor Tyrosine-Kinases, *Molecular and Cellular Biology*, **25(9)**: 3690–3703
- Segaliny A. et al. (2015): Receptor tyrosine-kinases: characterization, mechanism of action and therapeutic interests for bone cancers, *Journal of Bone Oncology*, **4(1)**: 1-12.
- Shah H. N. & Muir T. W. (2014): Inteins: nature's gift to protein chemists, *Chemical Science*, **5**: 446-461.
- Snider J. et al. (2015): Fundamentals of protein interaction network mapping, *Molecular Systems Biology*, **11**: 848-869.
- Snider J. & Štagljar I. (2016): Membrane yeast two-hybrid (MYTH) mapping of full-length membrane protein interactions, *Cold Spring Harbor Protocols*.
- Songyang Z. et al. (1994): Specific Motifs Recognized by the SH2 Domains of Csk, 3BP2, fps/fes, GRB2, HCP, SHC, Syk, and Vav, *Molecular and Cellular Biology*, **14(4)**: 2777-2785.

- Stelzl U. et al. (2005): A human protein-protein interaction network: a resource for annotating the proteome, *Cell*, **122(6)**: 957-968.
- Trusolino L. et al. (2010): MET signaling: principles and functions in development, organ regeneration, and cancer, *Nature Reviews Molecular Cell Biology*, **11**: 834-848.
- Valla, R. (2018): Posttranslational modifications of proteins, Seminar Paper, University of Zagreb, Faculty of Science, downloaded from <https://urn.nsk.hr/urn:nbn:hr:217:092203>.
- Wagner M. et al. (2013): Molecular mechanisms of SH2-and PTB-domain-containing proteins in receptor tyrosine-kinase signaling, *Cold Spring Harbor Perspectives in Biology*, **5(12)**: a008987.
- Yao Z. et al. (2020): Split intein-mediated protein ligation, a method for detecting protein-protein interactions and their inhibition, *Nature Communications*, **11**: 2440-2453.

#### Web Resources:

- 1) Biorender, <https://app.biorender.com/>, retrieved on May 18, 2021.
- 2) Human Protein Reference Database, [http://hprd.org/PhosphoMotif\\_finder](http://hprd.org/PhosphoMotif_finder), retrieved on June 1, 2021.
- 3) Methods: Flp-In™ System for Generating Stable Mammalian Expression Cell Lines, Invitrogen, <https://www.thermofisher.com/hr/en/home/references/protocols/proteins-expression-isolation-and-analysis/protein-expression-protocol/flp-in-system-for-generating-constitutive-expression-cell-lines>, retrieved on June 1, 2021.
- 4) Methods: Gateway Cloning, Thermo Fisher Scientific, <https://tools.thermofisher.com/content/sfs/manuals/gatewayman.pdf>, retrieved on December 30, 2020.
- 5) Methods: Gibson Assembly<sup>R</sup> Cloning Kit, New England Biolabs, <https://international.neb.com/protocols/2012/12/11/gibson-assembly-protocol-e5510>, retrieved on December 31, 2020.
- 6) Methods: Growth and Maintenance of T-REx™ Cell Lines, Thermo Fisher Scientific, <https://www.thermofisher.com/order/catalog/product/R71007#/R71007>, retrieved on December 30, 2020.

- 7) Methods: Monarch PCR and DNA Cleanup Kit, <https://international.neb.com/protocols/2015/11/23/monarch-dna-gel-extraction-kit-protocol-t1020>, retrieved on January 16, 2021.
- 8) Methods: Pierce BCA Protein Assay kit, Thermo Fisher Scientific, <https://www.thermofisher.com/order/catalog/product/23227#/23227>, retrieved on December 31, 2020.
- 9) Methods: Polyacrylamide Gel Electrophoresis, ROTH, <https://www.carlroth.com/medias/Info-Brochure-PAGEInstructions-EN.pdf?context=bWFzdGVyfHRIY2huaWNhbERvY3VtZW50c3w2OTY0Mdd8YXBwbGljYXRpb24vcGRmfHRIY2huaWNhbERvY3VtZW50cy9oY2QvaGFjLzg5ODAzODc5ODc0ODYucGRmfGVkYjM5ZiU3OTA5Y2ZiYzU2OTkxNjEwM2UwOGU1YmJjNDM2MjRmNTZiYzkyZiQ2ZiA1NzI5ZTNiNGE5Mjk5ZGM>, retrieved on December 31, 2020.
- 10) Methods: Presto Mini Plasmid Kit Quick Protocol, Geneaid, <https://www.geneaid.com/data/files/1608174169791710574.pdf>, retrieved on December 30, 2020.
- 11) Protein Atlas, <https://www.proteinatlas.org/ENSG00000177885-GRB2>, retrieved on June 1, 2021.
- 12) UniProtKB - P08581 (MET\_HUMAN), <https://www.uniprot.org/uniprot/P08581>, retrieved on June 1, 2021.

## 8. SUPPLEMENTARY FIGURES & TABLES

Supplementary figures and tables contain vector maps of vectors used in this research (Figure S1, Figure S2, Figure S4, Figure S6), the optimization of Western blot analysis for the SIMPL assay involving MET (Figure S3), approximate sizes of spliced protein involving MET in the SIMPL assay (Table S1), and schematic representation of the cassette for the design of stable doxycycline-inducible BLNK shRNA knock-down system (Figure S5).

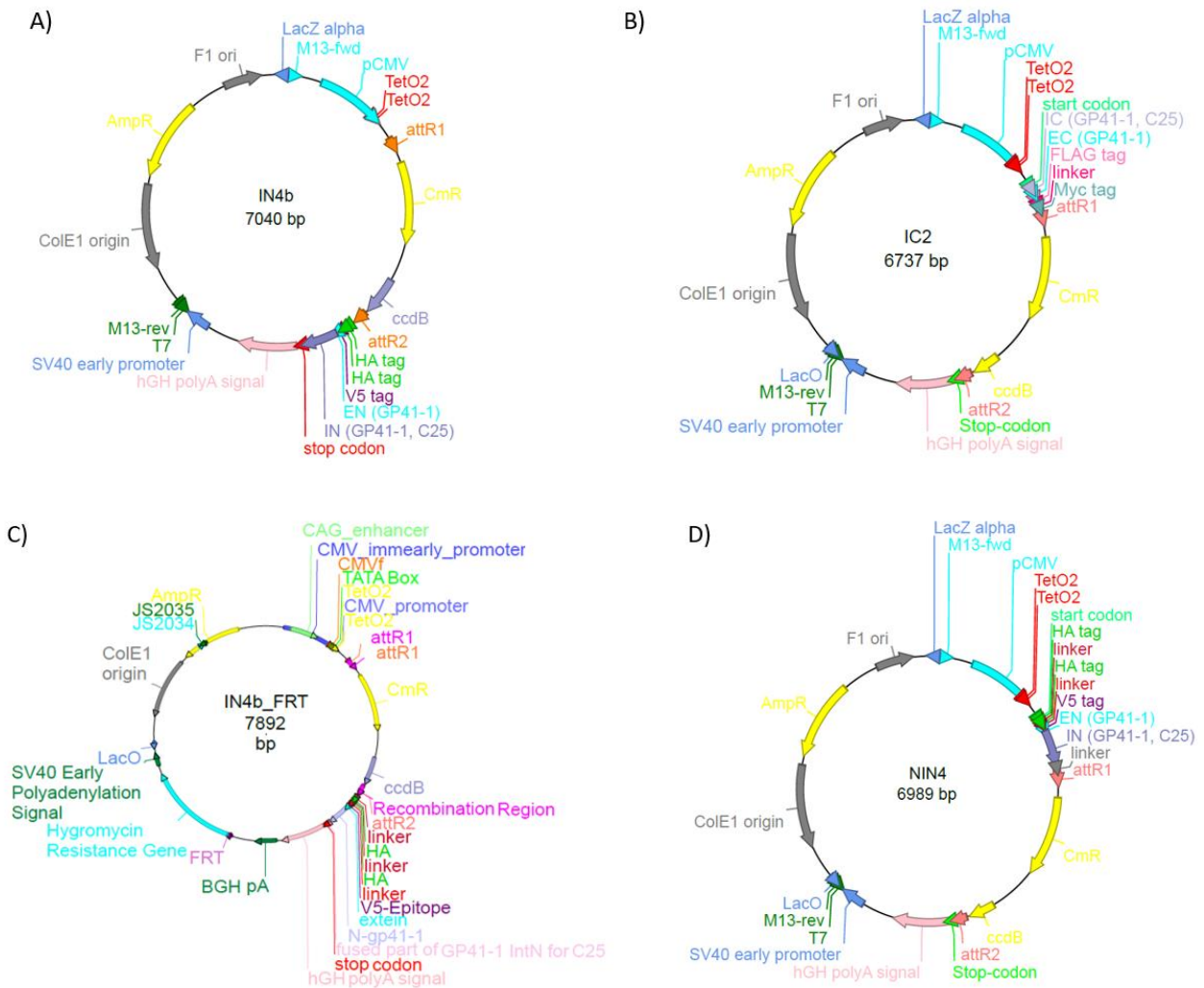


**Figure S1:** Gateway destination vectors used in the SIMPL assay. **(A)** Map of C-terminal SIMPL bait destination vector (IN4B). **(B)** Map of N-terminal SIMPL prey destination vector (IC2). **(C)** Map of C-terminal SIMPL bait destination vector that also contains an FRT site and hygromycin resistance gene. **(D)** Map of N-terminal SIMPL bait destination vector (NIN4).

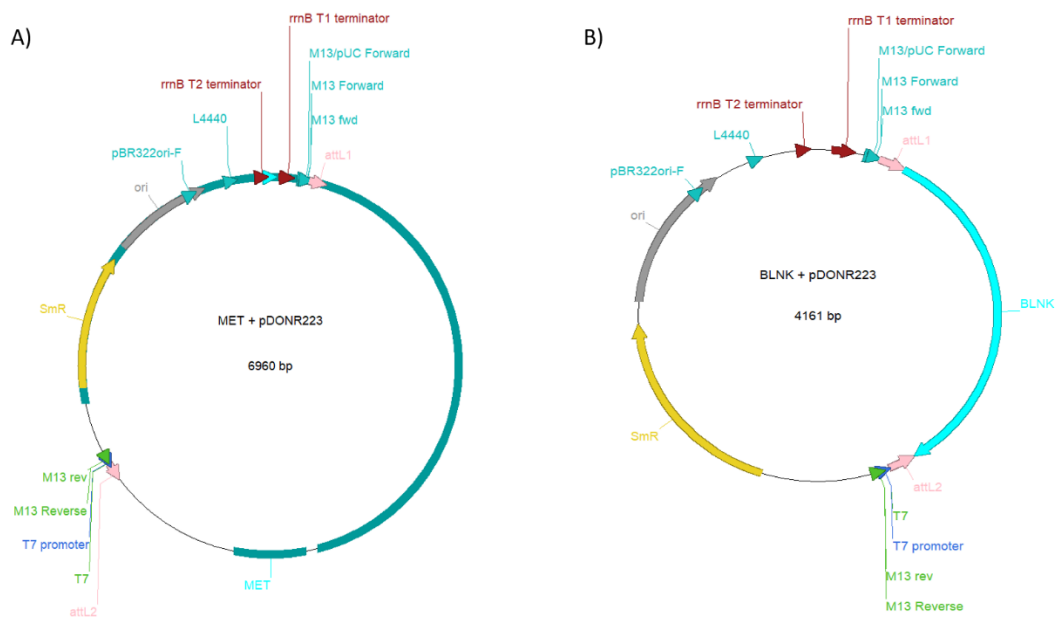


**Figure S2:** Vector maps of entry clones used in site-directed mutagenesis. **(A)** Map of MET entry clone. **(B)** Map of BLNK entry clone.

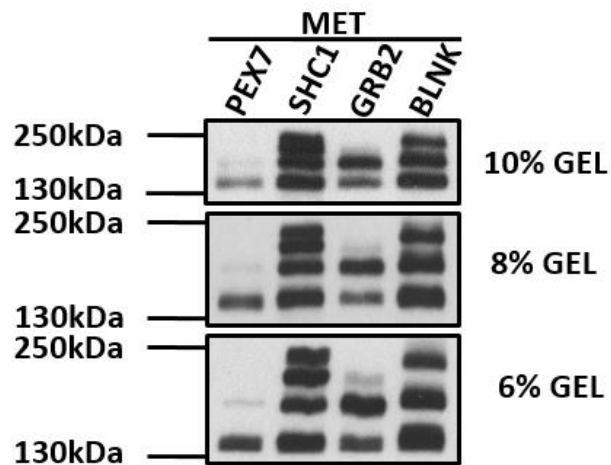


**Figure S3:** Optimization of Western blot when using an anti-V5 antibody in the SIMPL assay involving MET. Due to similar sizes of mature MET, precursor MET, and spliced proteins involving MET, gel electrophoresis using 10 % or 8 % polyacrylamide gel did not provide sufficient separation to distinguish the bands representing the aforementioned proteins in the blot, whereas the use of 6 % polyacrylamide gel provided the necessary separation.

**Table S1:** Sizes of proteins detected by Western blot when performing a SIMPL assay involving MET.

Protein	Size (kDa)	Protein	Size (kDa)
MATURE MET	145	PRE-MET	170
MET-PEX7	180	PRE-MET-PEX7	205
MET-SHC1	197	PRE-MET-SHC1	222
MET-GRB2	170	PRE-MET-GRB2	195
MET-BLNK	215	PRE-MET-BLNK	240

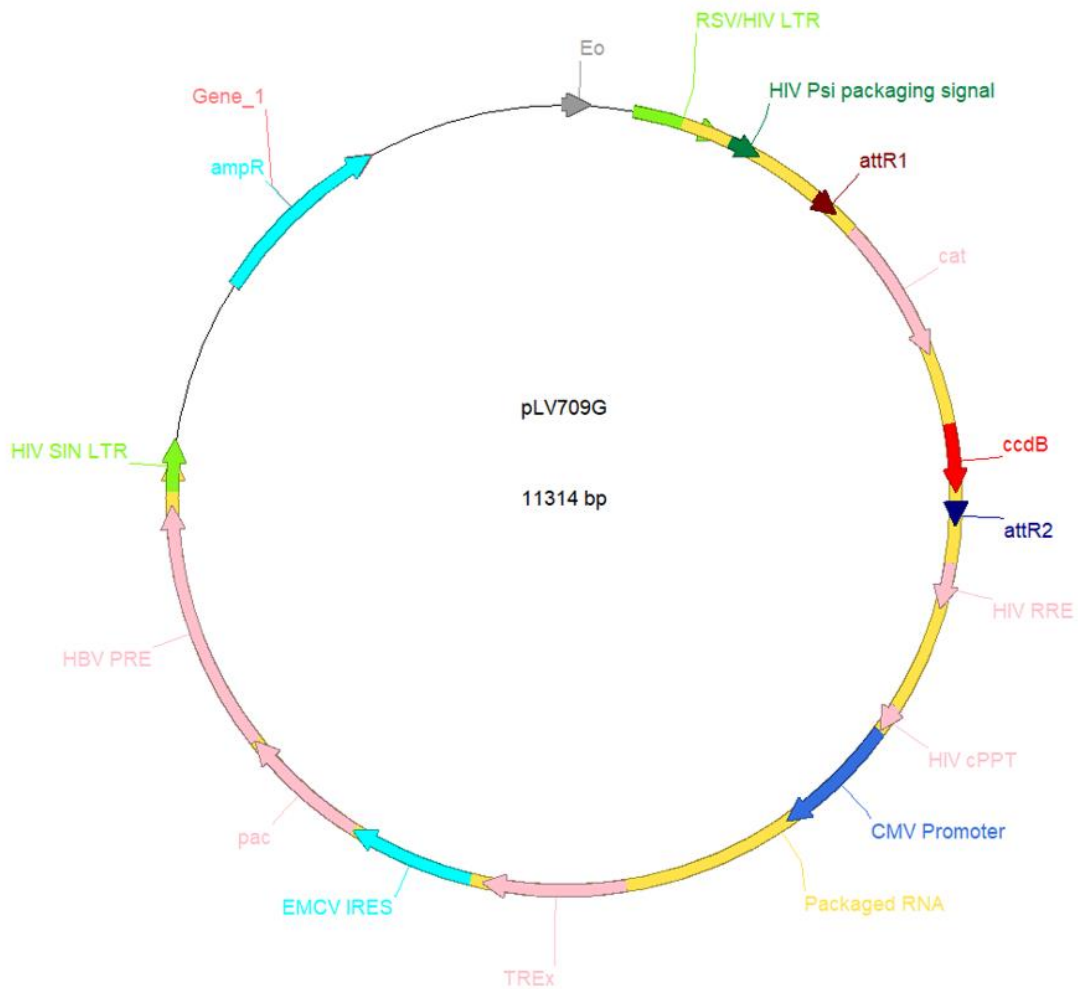


**Figure S4:** Vector map of lentiviral destination vector pLV709G used to clone BLNK shRNA constructs.

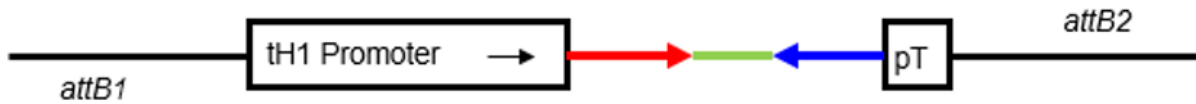


**Figure S5:** Schematic representation of an shRNA cassette generated for the creation of a stable doxycycline-inducible BLNK knock-down system. Black lines represent the template (pBS-tH1 construct), while the red arrow, green line, and blue arrow represent the shRNA sense strand, loop, and shRNA antisense strand, respectively.

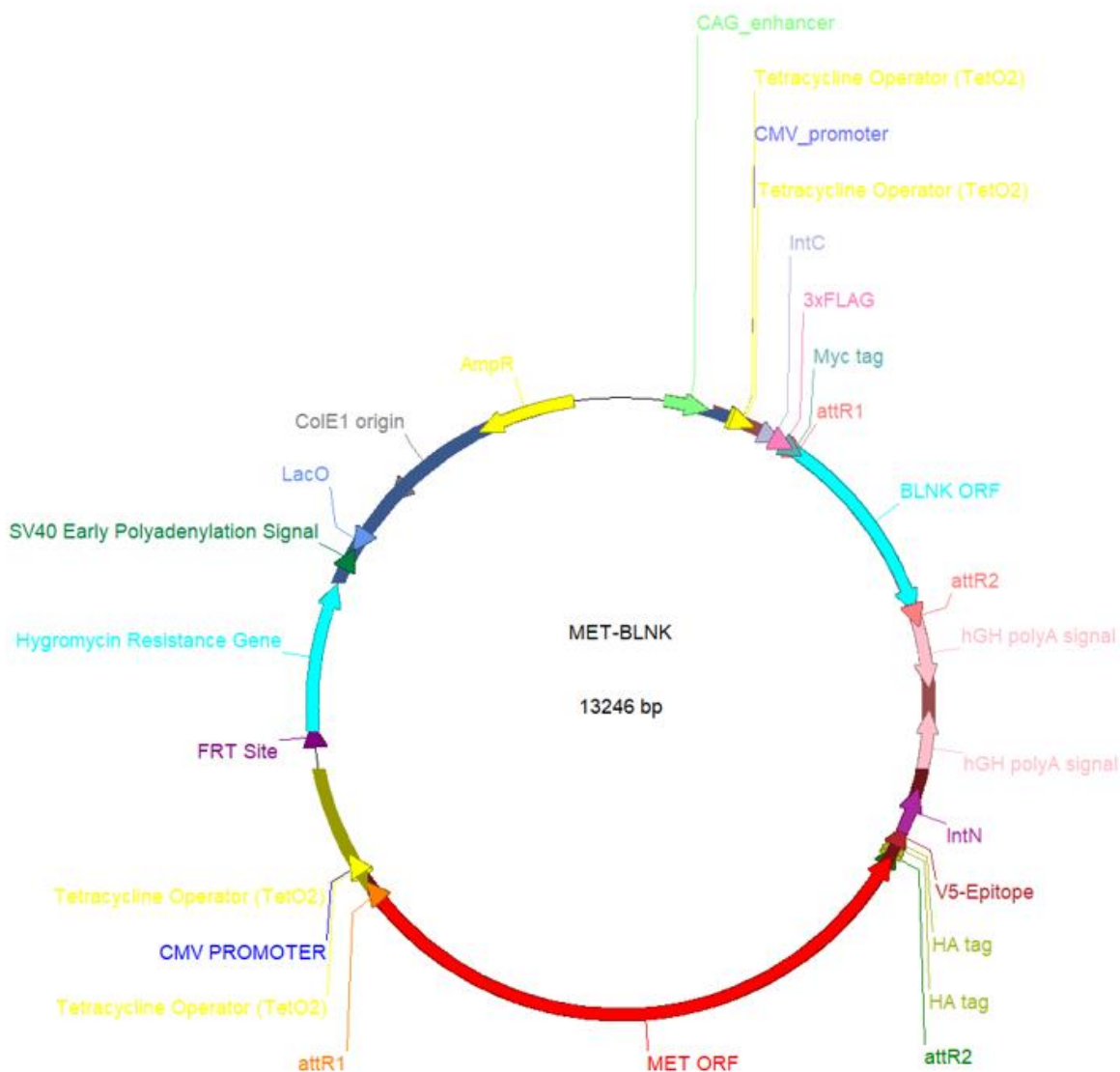


**Figure S6:** Vector map of MET-BLNK IN4B\_FRT construct.

## 9. CURRICULUM VITAE

Robert Valla was born on April 30, 1996. He attended Grammar School in Sisak, Croatia, from 2011 to 2015. He enrolled in the undergraduate program in molecular biology at the Faculty of Science, University of Zagreb, Zagreb, Croatia in the year 2015. He earned the title of univ. bacc. biol. mol. in the year 2018, cum laude. In the same year, he enrolled the graduate program of molecular biology at the Faculty of Science, University of Zagreb, Zagreb, Croatia. He was temporarily enrolled as an IVGS student at the University of Toronto, Toronto, Canada from September 2020 to May 2021 at the Faculty of Medicine to perform this master thesis in the Igor Štagljar research laboratory, Terrence Donnelly Centre for Cellular and Biomolecular Research.

As a student, Robert was a demonstrator in executing the practical part of the courses Cell Biology, Biochemistry 1, and Biochemistry 2. As a graduate student, Robert improved his laboratory skills through skill training performed in the Clinic for Tumors, Clinical Hospital Sestre Milosrdnice in Zagreb under the supervision of Dr. Sc. Snježana Ramić and in the Laboratory for Plant Molecular Biology at the Faculty of Science, the University of Zagreb under the supervision of Dr. Sc. Nataša Bauer, Assoc. Prof.

Robert was a recipient of a STEM scholarship for excellence during his third year as an undergraduate student. He was also a recipient of a prestigious Igor Štagljar Scholarship Fund, which enabled his departure to Toronto, Canada to perform this master thesis.

Notably, during his graduate program in molecular biology, Robert was the recipient of a Dean's Award for the best student at the program.

Robert was an active participant in the manifestation Night of Biology at the Faculty of Science, University of Zagreb.

Croatian is Robert's native language. He also speaks English at full professional proficiency and German at average proficiency. Robert has a driver's license (B category). He skillfully uses MS Office Package, Internet, and Bioinformatics tools.